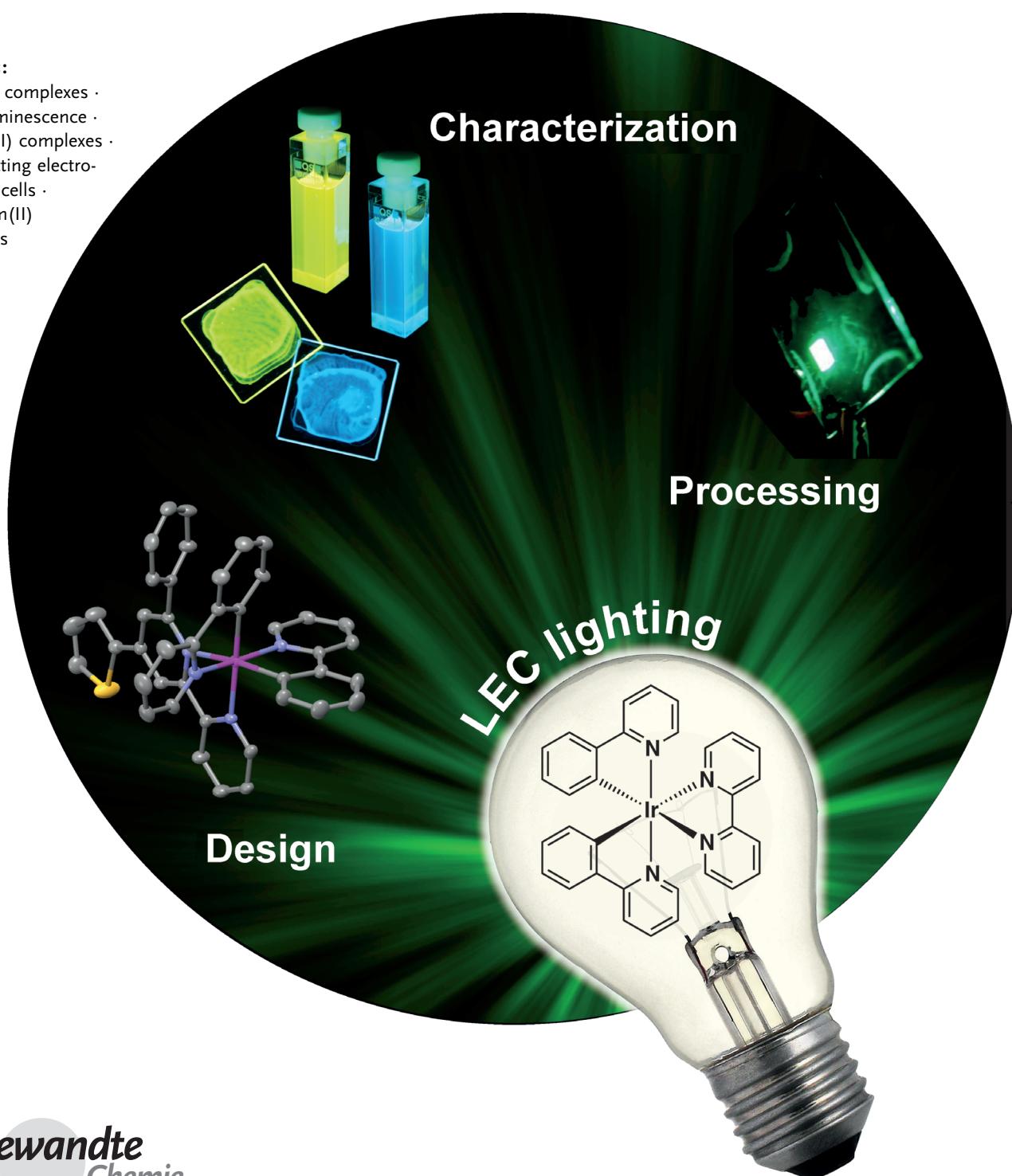


Luminescent Ionic Transition-Metal Complexes for Light-Emitting Electrochemical Cells

Rubén D. Costa, Enrique Ortí, Henk J. Bolink,* Filippo Monti, Gianluca Accorsi, and Nicola Armaroli*

Keywords:

copper(I) complexes ·
electroluminescence ·
iridium(III) complexes ·
light-emitting electro-
chemical cells ·
ruthenium(II)
complexes



Higher efficiency in the end-use of energy requires substantial progress in lighting concepts. All the technologies under development are based on solid-state electroluminescent materials and belong to the general area of solid-state lighting (SSL). The two main technologies being developed in SSL are light-emitting diodes (LEDs) and organic light-emitting diodes (OLEDs), but in recent years, light-emitting electrochemical cells (LECs) have emerged as an alternative option. The luminescent materials in LECs are either luminescent polymers together with ionic salts or ionic species, such as ionic transition-metal complexes (*iTMCs*). Cyclometalated complexes of Ir^{III} are by far the most utilized class of *iTMCs* in LECs. Herein, we show how these complexes can be prepared and discuss their unique electronic, photophysical, and photochemical properties. Finally, the progress in the performance of *iTMCs* based LECs, in terms of turn-on time, stability, efficiency, and color is presented.

From the Contents

1. Introduction: Lighting the World	8179
2. Flat Lighting Devices	8191
3. Ionic Transition-Metal Complexes for LECs: The Rise of Iridium	8185
4. <i>iTMCs</i> -Based LECs	8193
5. Conclusion and Outlook	8206

1. Introduction: Lighting the World

The diffusion of artificial lighting is one of the greatest achievements of the past century, but even today, in many poor regions of the world, the rhythm of everyday life is beaten by the daily light-dark cycle: at sunset virtually all of human activities are stopped. For millennia artificial lighting was generated by the open fire, which was eventually tamed through the use of lamps, as testified by archaeological findings all around the world. Until the second half of the 19th century, rural dwellings worldwide utilized fuels of animal or vegetal origin, such as whale oil or beeswax. In 1879, taking advantage of the work of many other inventors and after having tested hundreds of different materials as filaments, Thomas Edison patented the incandescent carbon filament lamp, a milestone of modern lighting, whose diffusion took advantage of the almost concomitant spreading of electric grids. Edison's device converted just 0.2% of electricity into light, but it was 20-times more efficient than a candle in converting chemical energy into useful photons.^[1]

In the following decades, electric lighting devices underwent substantial progress in terms of efficiency and all the systems that are still used nowadays were introduced: the tungsten lamp (1906), that dominated residential lighting for one century, the sodium vapor lamp (1930s), now utilized for street illumination in its modern high-pressure variant, the fluorescent tubes (1940s), very popular in large internal environments, such as offices and factories.^[2] The evolutions of these three fundamental designs were introduced in relatively recent times: the halogen lamp, an advanced filament system, entered the market in the 1960s and the compact fluorescence lamp, a sort of hybrid between bulbs and fluorescent tubes, appeared in the 1980s. Initially, the latter was unenthusiastically received by consumers because of high price, long dimming times, and poor white quality, a set of issues now largely solved. Figure 1 shows the historical trend of the efficiency of some lighting systems in converting

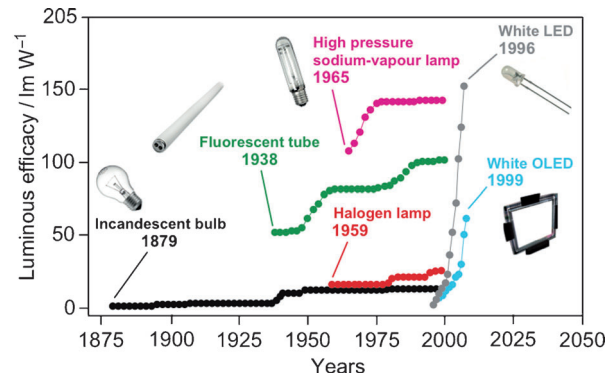


Figure 1. Historical trend of luminous efficacy of the most common light sources.

electricity into visible (Vis) electromagnetic radiation that can be sensed by the receptors of the human eye.

Nowadays, artificial lighting is an over 70 billion Euro market worldwide. The lighting industry provides 150 000 jobs in Europe alone and produces items not only for stationary applications but also for the transportation sector, particularly automotive. The electricity consumption for lighting amounts to approximately 3 PWh, that is, 20% of the world total, with an estimated CO₂ production of 2 Gt, about 7% of the global

[*] Dr. R. D. Costa, Prof. Dr. E. Ortí, Dr. H. J. Bolink
Instituto de Ciencia Molecular (ICMol), Universidad de Valencia
Catedrático J. Beltrán 2, 46980 Paterna, Valencia (Spain)
E-mail: henk.bolink@uv.es
F. Monti, Dr. G. Accorsi, Dr. N. Armaroli
Molecular Photoscience Group
Istituto per la Sintesi Organica e la Fotoreattività
Consiglio Nazionale delle Ricerche
Via P. Gobetti 101, 40129 Bologna (Italy)
E-mail: nicola.armaroli@cnr.it

emissions and equivalent to 70 % of the emissions produced by transportation.^[3,4] Thus, efficiency gains in this sector would significantly contribute to the energy transition that we must carry out in the present century.^[5,6]

Compared to two centuries ago, the per capita average availability of artificial photons for lighting in Europe has increased by about 12000 times, with the price almost unchanged.^[4] However, it has to be emphasized that about 1.5 billion people around the world still lack access to electricity and obtain illumination by burning fuels. It is estimated that about one million barrels of oil (1.2 % of production) is still burnt daily for lighting purposes.^[7] This poses high safety and health risks through accidental fires and indoor air pollution.^[8]

The few data summarized above show that there is an urgent need for further improvements in lighting, so as to make it more widespread, sustainable, and affordable. The tremendous progress made during the 20th century in improving the quality and availability of artificial lighting was accomplished through the use of two main technologies: incandescent- and discharge-based lamps.^[4] Incandescent lamps consist of a bulb containing a wire filament that emits light upon heating in a vacuum. They emit up to 95 % of the energy as infrared photons (i.e., heat) hence their efficiency is intrinsically low. Discharge lamps generate light by means of an internal electrical discharge between electrodes that produces ultraviolet (UV) radiation, which is then down-converted into visible light by solid or gaseous compounds; they can be substantially more efficient than the incandescent counterpart but often at the expense of color quality. There is a variety of both type of lamps but these two traditional lighting concepts have been exploited near to their limit; thus,

new lighting approaches have emerged in the last two decades (Figure 1).^[9]

The emerging concept for illumination is solid-state lighting (SSL),^[10] in which selected semiconductor materials are stimulated to produce visible light under the action of an electrical field (electroluminescence) in suitably engineered devices where the transport of charge occurs in one specific direction (diodes). Through this approach, the primary product of these lighting devices is the photon itself, unlike traditional sources where visible light is essentially a by-product of other processes, such as heating or discharging. As a result, SSL creates visible light with reduced heat generation or parasitic energy dissipation, while its solid-state nature provides for greater resistance, increasing significantly the lifespan of appliances.

There are two main families of SSL devices, namely light-emitting diodes (LEDs)^[11] and organic light-emitting diodes (OLEDs).^[12–14] LED technology is based on inorganic semiconductors made from combination of several elements (e.g., In, Ga, P, N) and provides highly efficient and convenient light point sources of different colors; LEDs are now standard for screen backlighting, automotive applications, traffic signaling, advertising, and decoration.^[10] Notably, they are acquiring an increasing market share in ambient illumination thanks to the consolidation of white LED concepts.^[15]

OLEDs are flat light sources where the photon output is generated through electroluminescence within a multilayer stack a few hundred nanometers thick.^[14,16] They are used extensively as displays in small handheld applications and in prototype TVs. The core of the device is the layer containing the luminescent material, typically a polymer, a small fluorescent molecule, or a phosphorescent transition-metal complex embedded in a charge transporting matrix.^[17] State-of-



Rubén D. Costa got his B.S. in Chemistry from the University of Valencia in 2006. His Ph.D. work was performed at the Institute for Molecular Science where he graduated in 2010. He focused on how the design of ionic transition-metal complexes enhances the performance in lighting devices. Currently, he has a Humboldt Fellowship at the University of Erlangen in the group of Prof. Dirk M. Guldi. His current research interests concern the theoretical and photophysical study of organic/inorganic hybrid materials and their utilization in lighting and photovoltaic devices.



Henk Bolink is a full time researcher at the University of Valencia, Spain. He obtained his Ph.D. in Materials Science at the University of Groningen, The Netherlands in 1997. In 2001 he joined Philips, to lead the materials development activity of Philips's PolyLED project. His current research interests encompass: inorganic/organic hybrid materials and mixed electronic/ionic charge-transporting materials and their integration in opto-electronic applications.



Enrique Ortí obtained his Ph.D. in chemistry from the University of Valencia (Spain) in 1985. Then he moved to the University of Namur (Belgium) where he worked as postdoctoral fellow under the supervision of Prof. J.-L. Brédas (1987). He returned to the University of Valencia as associated professor and now as a full professor. His research interests concern the application of quantum chemistry to the theoretical calculation of electroactive/photoactive molecular systems involved in organic/molecular electronics.



Filippo Monti graduated in 2009 (M.Sc.) from the University of Bologna in Industrial Chemistry, working on copper(I) complexes for light-emitting electrochemical cells (LECs). He is now completing his Ph.D. in Chemical Sciences at ISOF-CNR, under the guidance of Nicola Armaroli. At present, he is involved in a European project for developing flexible and large-area lighting sources based on LEC that rely on phosphorescent ionic transition-metal complexes as the single active component.

the-art white OLEDs are based on multilayer stacks sometimes consisting of more than 15 individual layers.^[18] Such a multilayer stack can only be prepared by vacuum sublimation that implies the use of thermally stable non-ionic materials. Therefore, the choice of suitable compounds within the huge family of luminescent transition-metal complexes, which are normally ionic species,^[19–22] is dramatically narrowed. The high manufacturing cost of OLEDs, associated with the multi-layer evaporation process and the need for rigorous encapsulation of the devices, are two of the main obstacles that have prevented significant penetration of this technology in the lighting market to date.

The above limitations of OLED technology have stimulated the exploitation of new concepts for flat electroluminescent lighting devices;^[23] among these, LECs (light-emitting electrochemical cells) are the most popular.^[24–30] LECs have a much simpler architecture than OLEDs, are processed from solution, do not rely on air-sensitive charge-injection layers or metals for electron injection and hence require less-stringent packaging procedures. LECs consist of an ionic luminescent material in an ionic environment sandwiched between two electrodes. The luminescent material is either a conjugated light-emitting polymer or an ionic transition-metal complex (iTMC). The first type is referred to as polymer-LECs (PLECs).^[26,30] The second type is even simpler as it uses an ionic emitter that enables single-component devices; this type of LECs is referred to as iTMC-LECs.^[24,27–29,31–34] This Review illustrates the fundamentals of LEC technology, focuses on the most promising luminescent materials for iTMC-LECs, particularly ionic Ir^{III} complexes, and highlights the latest achievements and remaining challenges of iTMC-LECs in the frame of the rapidly developing area of lighting technologies.



Gianluca Accorsi obtained his M.Sc. in Chemistry (1999) and Ph.D. in Chemical Sciences (2006) at the University of Bologna. Currently, he is a researcher at ISOF-CNR. His scientific interests are in photo-induced energy- and electron-transfer processes in supramolecular systems and nanostructures containing fullerenes, transition-metal complexes, aromatic conjugated oligomers, and porphyrins for light energy conversion and lighting technology. Since 2000, he has published nearly 80 research papers and book chapters.



Nicola Armaroli obtained his Ph.D. in chemistry in 1994 from the University of Bologna. After post-doctoral work in the U.S. and Italy, in 1997 he joined the Italian National Research Council (CNR), where he became research director in 2007. His activity is concerned with the photochemistry and photophysics of molecules and materials targeted at lighting devices and solar energy conversion. He has published three books and over 150 papers and since 2010 he has chaired the Working Party on Chemistry and Energy of EUChemS.

2. Flat Lighting Devices

2.1. Light-Emitting Electrochemical Cells: Motivation and Definition

State-of-the-art organic light-emitting diodes are typically made of multiple layers of organic materials, sandwiched in between an anode, typically a transparent oxide film, such as indium-tin oxide (ITO), and an air-unstable cathode (Ca, Ba) often coupled with an electron-injection layer (Figure 2, left). Such complex architectures are necessary to provide a balanced injection of positive and negative charges across the device, which must precisely recombine in the light-emitting layer, to grant the physical integrity of the whole device under the applied bias for hundreds of hours.^[14,16] Nowadays, OLEDs can be utilized for display and illumination but their manufacturing still needs costly and complex procedures in an inert environment that must be followed by a rigorous encapsulation of the final device, particularly because of the presence of low work-function metals or doped injection layers which are extremely sensitive to ambient oxygen and moisture.^[14,16] The multilayer structure, additionally, makes large-area processing extremely difficult, and ultimately imposes a production cost of OLEDs still incompatible with widespread applications in the general lighting market.

Light-emitting electrochemical cells (LECs) have a much simpler architecture, are processed from solution, and do not rely on air-sensitive charge-injection layers or metals for electron injection (Figure 2, right). The concept of LEC was introduced in 1995 by Pei et al., who mixed an inorganic salt to a mixture of a conjugated luminescent polymer and an ionic conductive polymer (Figure 3, left).^[26,35] Soon after this seminal contribution, an alternative approach was proposed by Maness et al., who utilized a Ru^{II} ionic transition-metal

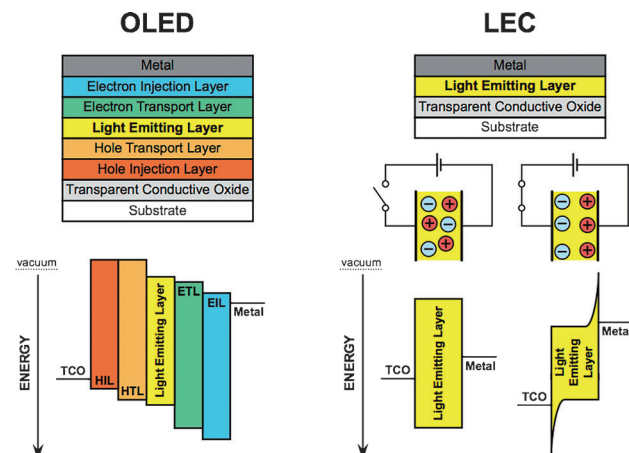


Figure 2. Schematic representations of a typical OLED (left) and LEC (right). An OLED consists of multiple layers that are in most cases deposited stepwise by thermal vacuum evaporation. The injection of electrons is achieved by the use of 1) a low work function metal or 2) chemically n-doped electron injection layer, both of which are unstable in air and require rigorous encapsulation. In contrast, a LEC consists of only one opto-electronically active layer whose negative counterions are displaced when an external bias is applied. This set up enables an efficient hole and electron injection from air-stable metals.

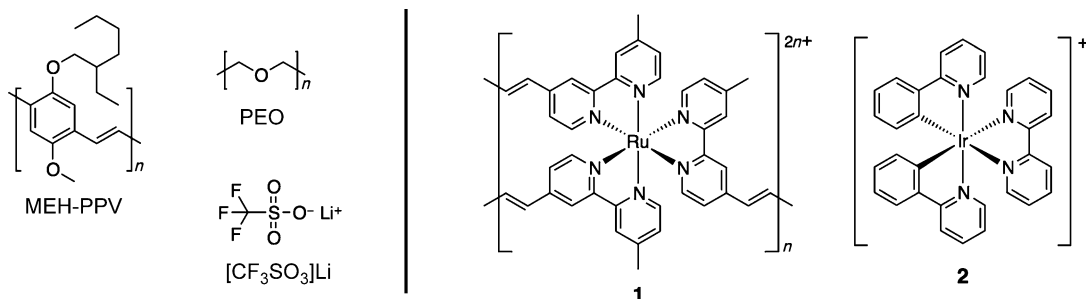


Figure 3. Materials used in the first polymer-based LECs: MEH-PPV = poly[5-(2'-ethylhexyloxy)-2-methoxy-1,4-phenylene vinylene], PEO = poly(ethylene oxide) and $[\text{CF}_3\text{SO}_3]^{-}\text{Li}^{+}$ = lithium trifluoromethanesulfonate. Compound **1** is the first iTMC used for LECs: poly-[Ru(vbpy)₃]²⁺, vbpy = 4-vinyl-4'-methyl-2,2'-bipyridine. Compound **2** is the archetypal complex of the largest class of Ir^{III}-iTMCs used in LECs: [Ir(ppy)₂(bpy)]⁺ in which ppy = 2-phenylpyridinate and bpy = 2,2'-bipyridine.

complex as the single active component in the light-emitting layer (**1**, Figure 3).^[27]

In this approach, the Ru^{II} complex and its counterion $[\text{PF}_6]^{-}$ play several key roles: promotion of charge injection from the electrodes, electron and hole transport through the device and, thanks to the intrinsic orange emission, luminescence. Nowadays, iTMC-LECs are mostly based on luminescent ionic biscyclometalated Ir^{III} complexes^[36] (the archetypal complex of this large family of complexes is **2**, Figure 3),^[37] which, like the original Ru^{II} complex, may sustain charge injection and transport while affording, at the same time, light emission. A crucial benefit in the use of ionic compounds is processability: iTMCs dissolve in polar benign solvents, allowing the devices to be prepared by facile coating or printing processes. In addition, the use of iTMCs allows novel device fabrication processes, such as soft-contact lamination,^[38] as well as the development of large-area illumination panels^[39,40] that do not require any patterning (see Section 4.1). Finally, the insensitivity of LEC devices to the work function of the electrode material allows air-stable metals to be used as anode and cathodes, greatly decreasing the severe technical requirements for the encapsulation of devices. Taken in concert, these characteristics facilitate large-area processing and might give entry to flat electroluminescent devices at more affordable costs.

2.2. LECs: Mechanism of Work

LEC materials can be either conjugated light-emitting polymers or ionic transition-metal complexes, the related devices are termed polymer-LECs (PLECs)^[26,30] or iTMC-LECs,^[27–29,31–34] respectively. Both types of LECs have been studied for over 15 years,^[26,27] throughout which many materials, device concepts, and driving schemes have been tested. This research has led to notable achievements in color, efficiency, turn-on time, and stability, which will be commented in Section 4. Now we describe the peculiar operational mechanism of LECs, which has been generally described by two rationales, the electrodynamic (ED)^[41–43] and the electrochemical doping (ECD)^[26,35,44] models (Figure 4). Both models agree in that the injection barrier for electrons and holes is reduced by the separation of the ions in the light-emitting layer upon application of a bias.

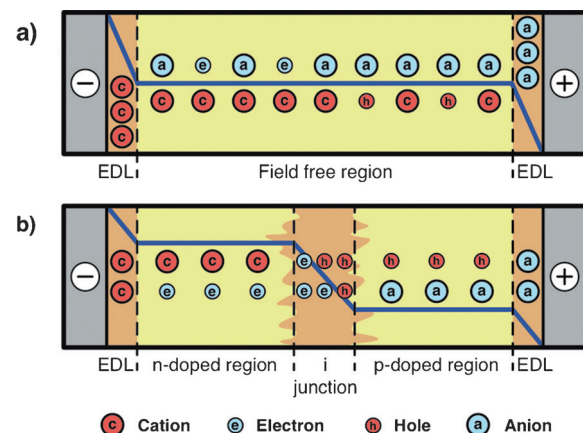


Figure 4. Illustration of the potential profile as well as the electronic and ionic charge distribution in a LEC during steady-state operation. Potential profiles and charge distributions as predicted by the a) ED and the b) ECD models. The thick blue line represents the potential profile; the electronic and ionic charge carriers are illustrated by the cyan (negatively charged) and red (positively charged) symbols, respectively. Furthermore, the high- and low-field regions in the bulk are highlighted in orange and yellow, respectively. In the low-field regions, negative and positive centers are mutually compensated. Adapted from Ref. [51].

The ED model assumes that the accumulation of ions leads to the formation of electric double layers (EDLs) at the electrodes which brings about a sharp drop of the electric potential near the electrode interfaces and promotes charge injection from the electrodes. In the bulk of the material the anions and cations are still joined and light emission occurs from the so-called field-free region in the bulk of the device.

The ECD model, on the other hand, assumes that the accumulation of ions at the anode and cathode leads to the formation of highly conductive p- and n-doped regions, respectively (Figure 4, n-doping: negative doping, i.e. addition of an electron; p-doping: positive doping, i.e. removal of an electron). The doped regions widen over time, until a p-i-n junction (i = intrinsic, undoped) between them is formed. Across the intrinsic region formed, the applied potential drops substantially and favors charge recombination and light emission.

Several papers describing modeling studies that support one or both of these models have appeared.^[41,42,44–48] Both models are corroborated by experimental data that, in most cases, were obtained from PLECs; they are described below.

The best performances of LECs are obtained when the active material is sandwiched in between two electrodes, that is, one electrode is below and one electrode is on top of the active layer. In these sandwiched devices the active layer has a thickness in between 100 and 200 nm. Although this layout leads to best performances, the active layer is thin and inaccessible and therefore it cannot be used to directly probe its potential profile. This can be done, however, by using another configuration in which the anode and cathode are placed side by side at a given distance (i.e., interdigitated) on a non-conductive substrate with the active layer on top of them (alternatively the active layer can be deposited on the bare substrate and then both contacts deposited on top). In this configuration, referred to as a “planar” configuration, the active material can be accessed by scanning probes (e.g., Kelvin probe) as there is nothing on top of it. To get meaningful information, the electrode spacing in the planar configuration must be at least one order of magnitude larger than in the sandwiched configuration (several micrometers). The performances in the planar configuration are much worse when compared with the sandwiched layout, primarily because of the very small light-generating areas on the total substrate, resulting in a small aperture of these devices. Also some care must be taken when the observations obtained from planar cells are used to explain operations in sandwiched devices, as the electrode spacing is quite different.

An example of a planar device using interdigitated electrodes, where the emission zone was probed with a microscope, is shown in Figure 5, left. It was revealed that, at moderate operation voltage, light emission is concentrated within a narrow zone (1–3 μm) of the larger interelectrode gap (15 μm), which was taken as evidence for the creation of a p-i-n junction (Figure 5, left). The planar device also allowed monitoring the photoluminescence as a function of interelectrode distance and time, under UV illumination. This information is of interest as the conjugated materials employed as the active materials in LECs are fluorescent or phosphorescent with reasonably high efficiencies, and it is known that the photoluminescence is quenched when the material is electrochemically doped. Accordingly, the absence of photoluminescence in certain areas can be indicative of the formation of doped regions. Hence, when the photoluminescence is monitored versus time it is possible to identify the formation

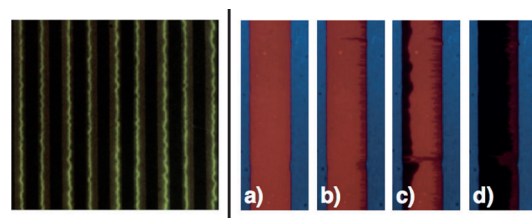


Figure 5. Left: Photograph of a planar PLEC with interdigitated gold electrodes (dark lines); the spacing between electrodes is 15 μm. With 4 V applied across each pair of electrodes, the yellow-green emission is observed from the dynamically formed p–n junction; the width of the junction is about 1–3 μm; adapted from Ref. [26]. Right: Selected photographs of the doping progression in a planar Al/MEHPPV + PEO + CF₃SO₃Li/Al LEC with a 1 mm interelectrode gap with the interdigitated Al electrodes on top of the polymer blend. The Al electrode to the left is the positive anode, and the device was operated at $T = 360\text{ K}$ and 5 V. The photographs were taken at $t = 0\text{ s}$ (a), $t = 546\text{ s}$ (b), $t = 978\text{ s}$ (c), and $t = 2750\text{ s}$ (d) after the voltage was applied. Adapted from Ref. [52].

of doped zones in planar LECs. Under this condition, doped regions resulted to be dark, as monitored by photographs or videos (Figure 5, right).^[49–52]

It is possible to directly measure the electrostatic potential from planar LECs by using Kelvin probe techniques, which is particularly useful as the two proposed models require very distinct potential profiles.^[53] Slinker et al. measured the electrostatic potential of planar iTMC-LECs, which were fabricated by carefully avoiding having active material on top of the electrodes using serial soft lithography.^[54] The profile obtained showed strong potential drops at the electrode interface, without sharp drops at the center of the device (Figure 6, left), providing support for the ED model. Shortly after, a similar experiment was performed on a planar PLEC by Matyba et al., who obtained a profile showing a distinct drop in the center of the device in line with the prediction of the ECD model (Figure 6, right).^[55] The latter observation was confirmed by recent studies performing simultaneous emission and Kelvin probe studies on the same device.^[56]

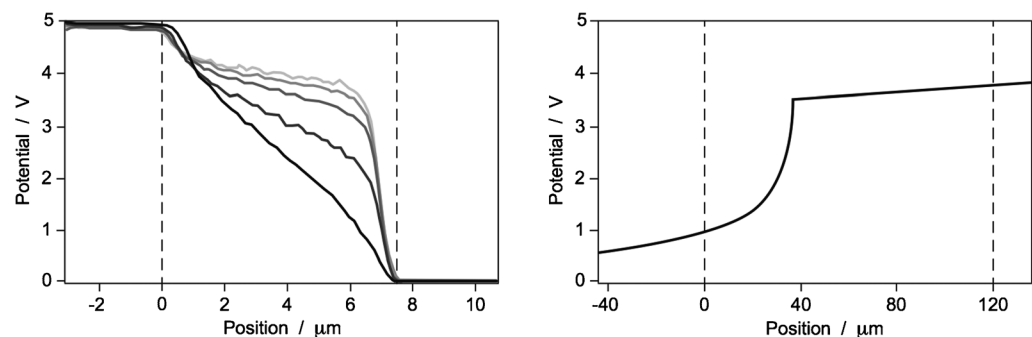


Figure 6. Left: Time dependence of the in situ potential profiles of planar iTMC-LECs for Au/[Ru(bpy)₃]PF₆/Au devices under 5 V operation, in which the [Ru(bpy)₃]PF₆ layer has been patterned to be restricted between the electrodes; first scan is black, the following ones are lines with increasingly lighter gray (the curves are spaced by equal increments of 15 min in time). The inter-electrode region is between the dashed lines; adapted from Ref. [54]. Right: Steady-state potential profile of a planar PLEC during operating at 5 V using Au electrodes. Adapted from Ref. [55].

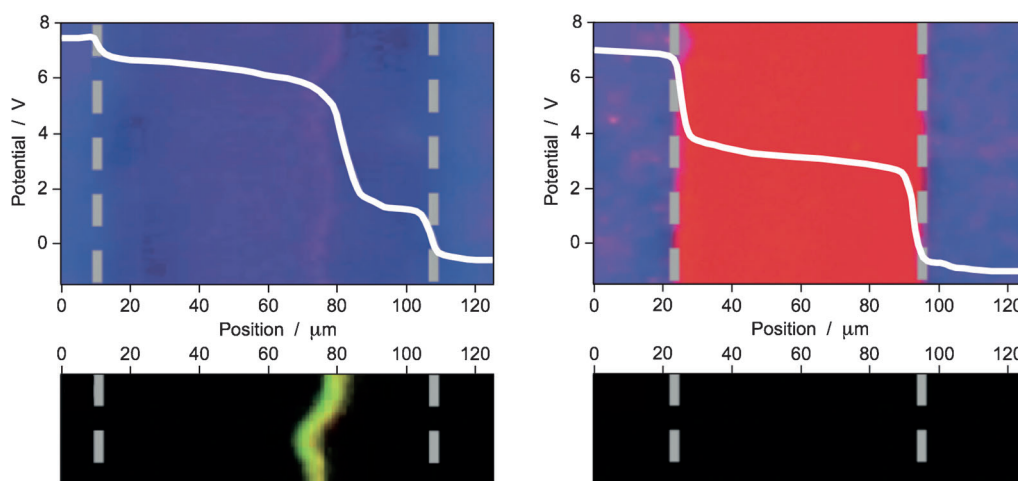


Figure 7. Steady-state potential profiles of a planar PLEC during operation at 8 V. Left: non-injection limited regime (using Al-capped Au electrodes). Right: injection-limited regime (using slightly oxidized Al electrodes). The panels below each potential profile are steady-state photoluminescence images of the devices. The white dashed lines in all micrographs indicate the electrode interfaces; adapted from Ref. [51].

The above data show evidences supporting both models, which sparked debate and increased the uncertainty concerning the actual operational mechanism in planar devices. Recent findings by van Reenen et al. shed new light on the matter.^[51] They obtained two different potential profiles using good (Al-capped Au; Figure 7, left) and poorly injecting contacts (slightly oxidized Al; Figure 7, right). With the Al-capped Au non-injection limited contacts, the profile is in accordance with the ECD model, because a dramatic potential drop is observed in an intermediate region between the two electrodes, where electroluminescence is generated. Additionally, small potential drops are observed at the electrode interface, attributable to the formation of the electric double layers. The potential profile of the planar PLEC with oxidized Al contacts is very different. In that case, the potential drastically drops only at the electrode interfaces with no relevant changes across the bulk of the device, as predicted by the ED model. Therefore, depending on the type of contacts, the potential profile of LECs can be rationalized with either the ECD or the ED model.

Tests described so far try to elucidate the mechanism of LECs functioning in planar devices. However, LECs are typically sandwich-type, which differ substantially in the distance between electrodes (around 0.2 μm) compared to their planar counterparts (8 to 120 μm) and are characterized by a much higher luminance. Hence, it is of great interest to elucidate the specific operation mechanism of sandwiched LECs. First attempts were made using impedance spectroscopy, a technique that applies a small AC perturbation on a DC voltage to get information on the resistance and capacitance of the active material, and supported the ECD model.^[57,58] In fact, the standard tools for studying conventional light-emitting devices, which entail the measurement of luminance (L) and current density (J) as a function of voltage (V) $JL-V$ measurements, are difficult to use in LECs because the application of a voltage triggers the movement of ionic charges and physically modifies the device itself. Therefore, to

obtain reliable operative parameters of a LEC for a given ionic distribution, it is crucial to avoid ionic movement during the $JL-V$ scans.^[59–62] These experiments have shown that $JL-V$ s of fresh LECs are featureless, whereas after poling and fixing of the ions they resemble those of standard OLEDs. A thorough investigation of how LECs evolve from the initial state to the highly luminescent state was recently reported using $JL-V$ analysis on dynamic LECs. In an attempt to perform $JL-V$ analysis on dynamic

LECs as well, a method was developed that applies a fixed voltage and monitors the current density and luminescence over time, while performing rapid $JL-V$ scans at set intervals. Even in this case it is crucial that there is no ionic movement during the $JL-V$ scans, as the electronic characteristics of the device for a given ionic distribution are needed. This was achieved for a sandwiched iTMC-LEC with a scan rate of 2.5 Vs⁻¹ and voltage never below 2 V.^[63] By this method it was shown that, at the start of the operation, the current density is limited by the injection barriers for holes and electrons. With prolonged biasing the injection barriers decrease and the current density becomes limited by the transport through the active material, this is referred to as “bulk-limited” condition. In bulk-limited OLEDs, the double carrier current density is space-charge limited and can be described using Equation (1).

$$J = \alpha \frac{V^2}{x_n^2} \quad (1)$$

Where, x_n is the effective layer thickness and α is a prefactor depending on the dielectric constant, electron and hole mobility, and bimolecular recombination rate.^[64] In Figure 8, the current density versus the effective applied voltage at different operation times is depicted.^[65] At driving times of 85 min and beyond, the current follows the typical quadratic dependence on voltage, indicating that it is space-charge limited. According to Equation (1), the one order of magnitude increase of device current (observed at 3.5 V driving voltage for over 85 min) is due to a decrease of the effective layer thickness by approximately a factor of two. The physical layer thickness of the active material did not change, thus the increase of J after the device had been operating for 85 min was attributed to the continued growth of the n- and p-doped regions adjacent to the electrodes, that reduces the thickness of the undoped (intrinsic, i) light-emitting layer. Additionally, it implies that the charge transport in the intrinsic region is rather similar to OLEDs and governed by space-charge. In

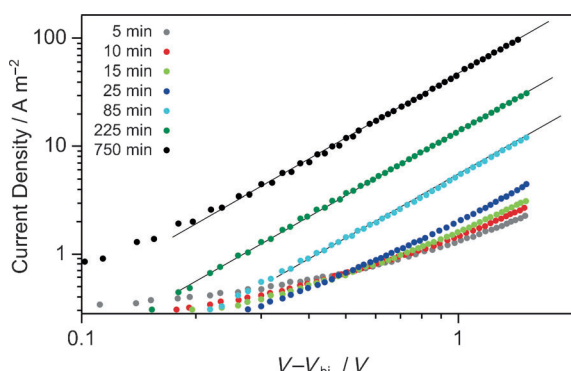


Figure 8. Current density (J) versus effective applied voltage ($V_{\text{eff}} = V - V_{\text{bi}}$, where V_{bi} is taken as the point where the current deviates from an exponential dependence) at different times during constant voltage (3.5 V) operation of a sandwiched LEC based on complex **2**. The parallel black lines indicate the quadratic dependence.

the same work it was also shown that, for a driving voltage of 1.5 V, current transients are in line with the predictions of the ED model.^[63]

The above observation corroborates the results obtained by van Reenen et al. on planar PLEC-based devices, who demonstrated that the electrostatic potential can be in accordance with both the ECD and the ED model, depending on the specific type of contact employed (see above).^[51] Therefore, it appears that the situation described by the ED model occurs when there is only a limited electron injection into the organic film. On the other hand, when substantial electron injection occurs, the formation of doped zones takes place. The speed of the formation of the EDLs and the widening of the doped zones is directly related to the ionic motion and is in general much faster in PLECs than in iTMC-LECs. Initially, the active layer of a LEC device is neutral since charges are randomly distributed. Upon application of a voltage above the band gap of the emitting material, the electric double layers are formed next to both electrodes, whereas the p- and n-doped regions (Figure 4b) start to grow at the expense of the neutral undoped emitting layer (Figure 5, right). In the specific case of iTMC-based LECs, light emission occurs by phosphorescence originating from long-living triplet excitons. Since they are quenched^[66] by electrochemical doping (see above) and the p- and n-doped regions adjacent to the neutral emitting layer continue to grow, the LEC luminance will inexorably decrease over time. Hence, the time-dependent decline of LEC luminance can be caused not only by chemical degradation of the emitting material in the operating device, but also by the increasing amount of excitons being quenched, as the neutral emitting layer thickness is reduced.^[67] Accordingly, switching a device off for several minutes once the maximum luminance level is reached and then re-applying the same voltage, leads to full restoration of light emission.^[63] The correlation between the formation of EDLs and the expansion of the doped zones is probably the reason why a relation between the turn-on time and the lifetime is often found in iTMC-LECs (see Section 4).

3. Ionic Transition-Metal Complexes for LECs: The Rise of Iridium

This Review focuses on iTMC-LECs and, for recent advances on PLECs, the reader can refer to a Review by Sun et al.^[30] and, for doped conjugated polymers, to a Review by Inganäs.^[68] iTMC-LECs differ from PLECs in that the iTMCs are intrinsically ionic and do not need auxiliary charged species to drive the device. Additionally, iTMCs are typically phosphorescent triplet emitters, which allows for higher electroluminescence efficiencies compared to singlet emitters.^[69] iTMCs also allow for easy solubilization in benign solvents and environmentally friendly wet device-preparation processes.^[70]

Early works on iTMC-LECs focused on differently substituted ruthenium(II) complexes, such as the archetype $[\text{Ru}(\text{bpy})_3][\text{PF}_6]_2$ (**3**, Figure 9); these devices achieved external quantum efficiencies up to 5.5%.^[71,72] However, LECs based on ruthenium chromophores offer limited color tuning because the emission band is placed across the orange-red part of the visible spectrum and this restriction strongly limits the applicative potential for lighting and display technologies, which require wider color tunability.

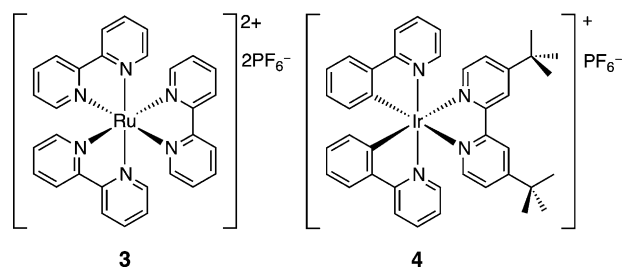


Figure 9. Structural formula of two examples of iTMCs used in LECs: $[\text{Ru}(\text{bpy})_3][\text{PF}_6]_2$ (**3**) and $[\text{Ir}(\text{ppy})_2(\text{dtb-bpy})][\text{PF}_6]$ (**4**).

Using luminescent iTMCs based on different metal centers opened the route to the whole color scale^[20] and, in this regard, the by far most versatile family of iTMCs is that of Ir^{III} (Ir-iTMCs).^[73] These compounds, thanks to a unique combination of physical and chemical properties, provide a huge variety of stable complexes, covering the whole visible spectrum all the way from blue to red.^[36] In particular, changing the metal center from a second-row (e.g., Ru) to a third-row (Ir) transition element, the stability of the related complexes is generally improved by 1) increasing the metal-ligand bond strength and 2) by raising the ligand-field splitting energy (LFSE) and making dissociative metal-centered (MC) excited states less thermally accessible compared to Ru^{II} analogues.^[74] LFSE is further increased, relative to Ru^{II} complexes, thanks to the higher electric charge of the iridium ion and by the presence of anionic cyclometalating ligands (C^N), typically used with Ir^{III} centers. All these combined features of Ir-iTMCs can lead to very high emission quantum efficiencies of virtually any color and impart good photochemical stability.^[29,36,73,75]

The first example of a LEC based on an ionic iridium(III) transition-metal complex was reported by Slinker et al. in

2004.^[76] It was a single-layer device emitting yellow light and based on **4**, a complex that exhibits a photoluminescence quantum yield (PLQY) in oxygen-free acetonitrile solution of 23.5 %.

3.1. Synthesis of Cationic Iridium(III) Cyclometalated Complexes for LECs

Most Ir-iTMCs are synthesized in two steps according to the strategy depicted in Figure 10. First, commercially available $\text{IrCl}_3 \cdot n\text{H}_2\text{O}$ reacts with a slight excess of the desired cyclometalating (often termed also *ortho*-metalating) ligand

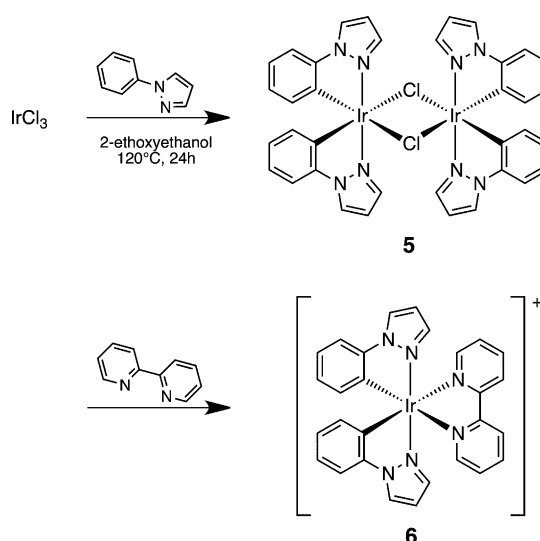


Figure 10. Typical two-step synthesis of a heteroleptic bis-cyclometalated iridium(III) complex. The μ -dichloro-bridged dimer (**5**) involving the desired cyclometalating C^{N} ligands (e.g., 1-phenylpyrazole, Hppz) is isolated and subsequently cleaved using neutral ancillary ligands to obtain the corresponding mononuclear iridium(III) complex (e.g., $[\text{Ir}(\text{ppz})_2(\text{bpy})]\text{Cl}$). Subsequently, counterion exchange of chlorides with, for instance, PF_6^- or BF_4^- affords the final product (**6**).

(C^{N}), the most popular of which are substituted 2-phenylpyridines (Hppy) or 1-phenylpyrazoles (Hppz; Figure 11). The reaction is usually carried out in 2-ethoxyethanol at around 120°C under argon atmosphere for 24 h.^[77,78] The product of this reaction is the cyclometalated Ir^{III} μ -dichloro-bridged dimer $[(\text{C}^{\text{N}})_2\text{Ir}(\mu\text{-Cl})_2]$ (**5**). In iridium dimer complexes such as **5**, the $\text{Ir}-\text{C}/\text{Ir}-\text{C}'$ bonds are stereochemically *cis* to each other, whereas the $\text{Ir}-\text{N}/\text{Ir}-\text{N}'$ are mutually in *trans* position.^[73,79] Tris-cyclometalated iridium(III) complexes are minor byproducts that can be easily separated from the main dichloro-bridged dimer.^[80]

The $[(\text{C}^{\text{N}})_2\text{Ir}(\mu\text{-Cl})_2]$ dimers undergo facile reactions with a variety of monodentate and bidentate neutral imine-type chelating ligands (Figure 12) to yield a plethora of different cationic mononuclear complexes (e.g. **6** in Figure 10) in high yields^[81,82] as chloride salts. Subsequently, these can undergo an ion exchange reactions with less-coordinative and less-reactive anions (e.g., PF_6^- or BF_4^-) to improve the

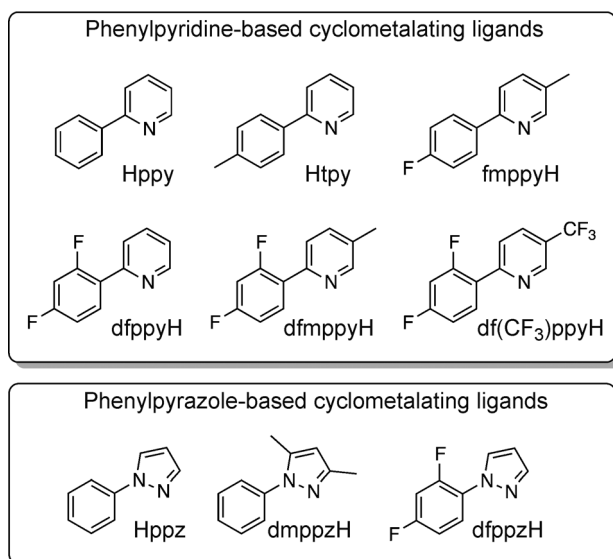


Figure 11. Some examples of cyclometalating (C^{N}) ligands commonly used in the synthesis of Ir-iTMCs.

performance of the complex under the electric field in operating devices (see Section 4).

When the direct addition of the neutral ligands to the dimer affords low yields, an alternative synthetic route can be utilized, carrying out removal of chlorides by treating the μ -dichloro-bridged dimer with silver triflate or other silver-based chloride-abSTRACTING agents.^[83] The chloride-free intermediate, for example, $[(\text{C}^{\text{N}})_2\text{Ir}(\text{H}_2\text{O})_2][\text{CF}_3\text{SO}_3]$, can then be treated with the desired neutral ligand under mild reaction conditions.^[84] It is even possible to avoid this two-step procedure by directly treating the $[(\text{C}^{\text{N}})_2\text{Ir}(\mu\text{-Cl})_2]$ dimer with a stoichiometric amount of neutral ligands in the presence of Ag_2O , to promote the removal of chloride during the reaction.^[85]

3.2. Photophysics of Cationic Ir-iTMCs

The wide availability of robust cationic iridium(III) complexes with tunable luminescence was the fundamental prerequisite for the development of studies on LECs. In this Review, we focus primarily on Ir-iTMCs that have been utilized in LECs, as well as on related complexes that allow the comparison and rationalization of physical properties. Of course, they are only a fraction of the innumerable ionic Ir^{III} complexes that have been synthesized in the last decade.^[29,36,73,75] In this Section, the basic electronic and photophysical properties of Ir-iTMCs will be described, focusing on the main strategies to design a complex with the desired emission color.

3.2.1. The Iridium(III) Metal Center in Octahedral Coordination

Ir^{III} is a 5d^6 metal center and its d orbitals are split by the interaction with the octahedral ligand field into three stabilized t_{2g} (d_{xy} , d_{xz} , d_{yz}) and two destabilized e_g orbitals

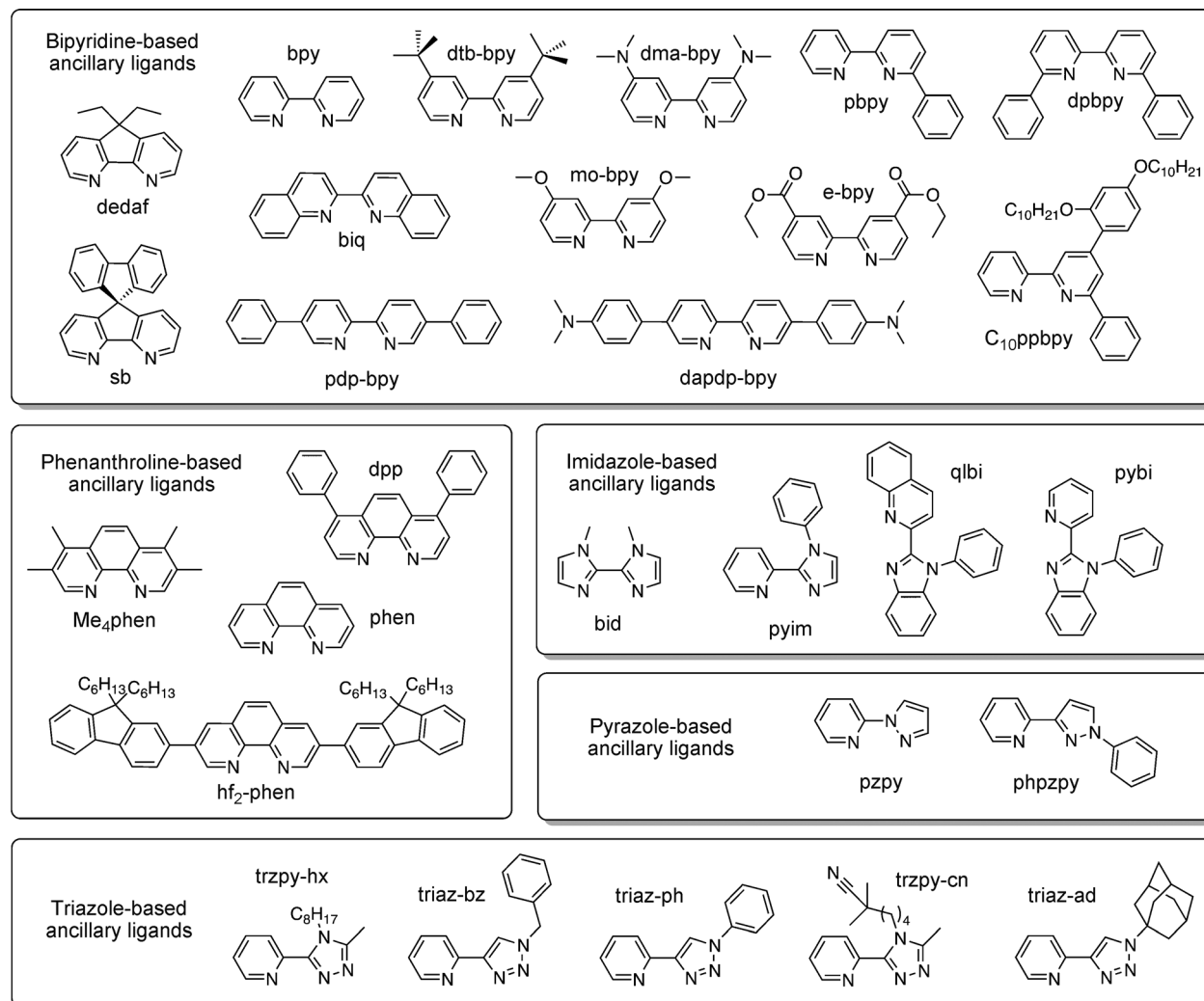


Figure 12. Some of the most widely utilized neutral ancillary ligands used in Ir-iTMCs.

(d_{z²}, d_{x^{2-y²}}), Figure 13a. The energy difference between these two levels (Δ_o) depends on 1) the oxidation state of the metal center: the higher the oxidation state, the higher the Δ_o splitting; 2) the size of the d orbitals: Δ_o is smallest for 3d metals and progressively increases with 4d and 5d metals; 3) the field strength exerted by the ligands, following the so-called spectrochemical series.

Ir-iTMCs exhibit a high Δ_o splitting because of the presence of a highly charged ion belonging to the third row of the d-block of the periodic table, bound to very strong-field ligands (i.e., the anionic cyclometalating ligands). As a result, the electronic configuration of the metal center is always in a low-spin state (t_{2g}⁶e_g⁰, Figure 13a) and the ligand-field stabilization energy is maximized, which means that Ir^{III} complexes are generally stable and rather inert toward substitution. Accordingly, the configuration of the metal orbitals is closed-shell (A_{1g}) and, since the ligand orbitals are fully occupied, the ground-state of the complexes is a singlet (S₀).

Other transition-metal ions have the same d⁶ low-spin configuration of Ir^{III} (e.g., Os^{II}, Ru^{II} and, in the presence of

particular ligands, even Fe^{II}), however their complexes do not exhibit such remarkable photophysical properties (e.g., emission color tunability, high PLQYs, good photostability, etc.) because the scenario in the excited states is very different (Figure 13b). The reasons are as follows:

- Fe^{II}, 3d⁶ configuration: the Δ_o splitting is very small, hence the lowest-lying excited state is ¹MC in nature (i.e., centered on e_g metal orbitals) and, therefore, not emissive.^[74]
- Ru^{II}, 4d⁶ configuration: the Δ_o splitting is increased and the lowest (emissive) excited state is a metal-to-ligand charge transfer triplet (³MLCT), relatively close to ³MC states that can be thermally populated and open a competitive radiationless deactivation pathway to either the ground state or to degradation products; accordingly, the PLQY of Ru^{II} complexes increase substantially with decreasing temperature.^[86]
- Os^{II}, 5d⁶ configuration: the Δ_o splitting is considerable and the ³MC states are usually too high to affect emission properties, but the emissive ³MLCT excited state has lower energy compared to Ru^{II} analogues (emission bands

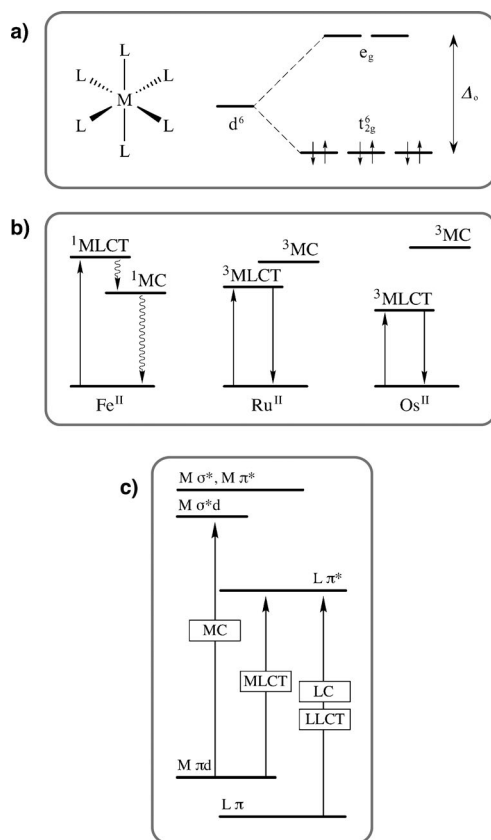


Figure 13. a) Low-spin d⁶ orbital configuration in octahedral field. b) Qualitative electronic excited states description for Fe^{II}, Ru^{II}, and Os^{II} metal complexes. c) Electronic energy-level diagram for a generic Ir-iTMC. MC is metal-centered, LC is ligand-centered, LLCT and MLCT are ligand-to-ligand and metal-to-ligand charge transfer, respectively.

typically peaking in the red/infrared edge of the spectrum) and this favors radiationless pathways thanks to the “energy gap law”,^[87] accordingly, PLQYs of these complexes are typically low, often below 1–2 %.^[88,89]

3.2.2. Spectroscopic Properties of Ir-iTMCs

Since UV or visible light absorption is mostly associated with spin-allowed electronic transitions from the ground state, which is of singlet nature in the case of Ir-iTMCs, the strongest absorption bands in Ir^{III} complexes are ascribable to singlet ligand-centered (^1LC), metal-to-ligand (^1MLCT), and ligand-to-ligand (^1LLCT) charge-transfer transitions.

The absorption spectrum of the archetypal Ir-iTMC complex **2** is depicted in Figure 14 as an example. The UV region is dominated by intense spin-allowed ^1π-π* (^1LC) transitions involving the organic ligands. At longer wavelength (350–450 nm), less-intense ^1MLCT and ^1LLCT bands are present: the ^1LLCT transitions correspond to electron promotions from the phenyl groups of the cyclometalating ligands to the ancillary ligand (e.g., 2,2'-bipyridine, in **2**). Additionally, the weak and long tails observed above 450 nm are due to direct spin-forbidden population of the triplet excited states (^3MLCT, ^3LLCT, and ^3LC (^3π-π*)) transitions enabled by the high spin-orbit coupling of the iridium metal

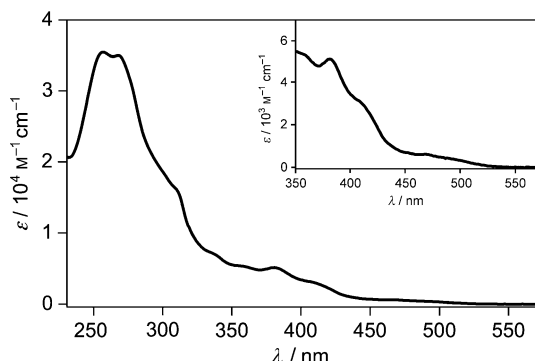


Figure 14. Electronic absorption spectrum of [Ir(ppy)₂(bpy)][PF₆] (**2**) in dichloromethane; MLCT transitions are expanded in the inset.

core (spin-orbit coupling constant ξ = 3909 cm⁻¹)^[90] that allows the mixing of triplet states with the higher-lying ^1MLCT levels. All these transition are schematically summarized in Figure 13c.

The high spin-orbit coupling of Ir^{III} yields almost unitary intersystem crossing efficiency from singlet to triplet excited states, therefore iridium(III) complexes always exhibit efficient spin-forbidden phosphorescence emissions. The emitting state is the lowest-energy triplet (T₁) which normally arises from “mixed” triplet levels, due to the contributions of ^3MLCT, ^3LC, and sometimes also ^3LLCT states (Figure 13c).^[73] Depending on the extent of contribution of the charge-transfer (CT) states, the emission profile is substantially affected: the presence of vibrational features suggests a low charge-transfer (CT) character, whereas broader and less structured shapes are indicative of a high charge-transfer character. As an example, in Figure 15 the room-temperature (RT) photoluminescence (PL) spectra of **2** and of [Ir(ppy)₂(pzpy)][PF₆] (**7**, Figure 19) are depicted. These two complexes have the same ppy cyclometalating ligand, but different ancillary (N⁺N⁻) ligands. On passing from bpy to pzpy (Figure 15) an hypsochromic shift of about 100 nm is observed, which is due to the change of the nature of the T₁ state from a more ^3MLCT/^3LLCT transition (**2**) to a more vibronically structured ^3LC one (**7**). The use of the electron-rich pyrazole ring pushes up the LUMO of the ancillary

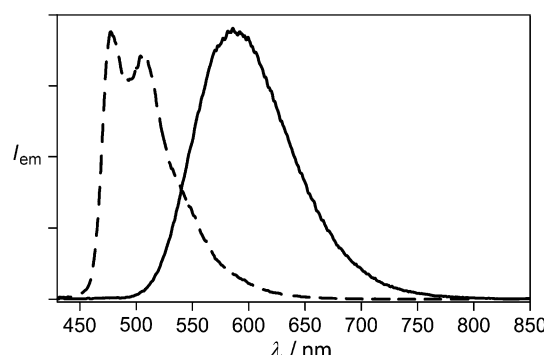


Figure 15. Room temperature emission spectra of [Ir(ppy)₂(pzpy)][PF₆] (**7**, dashed line) and [Ir(ppy)₂(bpy)][PF₆] (**2**, solid line) in solution. The more structured emission profile of **7** is a strong evidence of a predominantly ligand-centered (^3π-π*) emitting state.

(N⁺N) ligand and this orbital becomes closer in energy to the LUMOs of the cyclometalating (C⁺N) ligands. As a consequence, the electronic π–π* excitation of theppy ligands emerges as competitive in energy and the T₁ state increases its ³LC character.

Further evidence of the predominant ligand-centered character of the T₁ excited state could be derived by evaluating the radiative decay rate constant k_r of the complex, using the experimental values of PLQY (Φ) and excited-state lifetime (τ), according to Equation (2).

$$k_r = \Phi \tau^{-1} \quad (2)$$

A smaller k_r value usually indicates a stronger LC character in the “mixed” triplet excited state. For instance, in the case of **4** and **7**, although both complexes have the same PLQY ($\Phi \approx 23\%$) in deoxygenated acetonitrile solution, **7** shows an emission lifetime almost three-times longer than **4** (1.56 μs vs. 0.56 μs).^[82] Therefore **7** exhibits a smaller k_r ($1.5 \times 10^5 \text{ s}^{-1}$) relative to **4** ($4.2 \times 10^5 \text{ s}^{-1}$), confirming a less-pronounced ³MLCT character of its emissive excited state.

It must be pointed out that Ir-iTMCs having a T₁ excited state with pronounced ³MLCT character (e.g., **2** and **4**) generally exhibit shorter emission lifetimes (i.e., 0.43 μs and 0.56 μs, respectively) compared to related ruthenium(II) complexes, which invariably emit from ³MLCT levels (e.g., 0.81 μs for **3**), despite their intrinsically superior PLQYs. This behavior is due to the increased spin-orbit coupling that, in third-row transition-metal complexes, accelerates both radiative and non-radiative singlet-triplet transitions, thereby decreasing the duration of excited-state lifetimes. Having typically higher Φ and shorter τ , Ir-iTMCs exhibit radiative decay rates as much as five-times higher than Ru^{II} analogues.

3.2.3. Molecular-Orbital Features of Ir-iTMCs

To rationalize the photophysical properties of Ir-iTMCs, it is useful to determine the energy and atomic orbital composition of the highest-occupied and the lowest-unoccupied molecular orbitals (HOMO and LUMO, respectively). As already known for neutral iridium(III) complexes, also in the case of charged systems^[91] the HOMO is an admixture of Ir dπ orbitals (t_{2g}) and phenyl π orbitals of the cyclometalated (C⁺N) ligands, whereas the LUMO is usually located on the neutral (N⁺N) ancillary ligand (Figure 16a).^[37] Therefore, the emitting T₁ triplet usually has a mixed ³MLCT/³LLCT character.

To investigate the nature of higher energy LUMOs (LUMO + 1, LUMO + 2, etc.) is useful to understand the non-radiative deactivation pathways of the T₁ emitting state and to assess to which extent the LUMO orbital is located on the neutral ligand. In fact, by changing or chemically modifying the ancillary ligand, it is possible to destabilize the LUMO, while keeping the HOMO relatively unperturbed. This procedure is useful for blue-shifting the emission spectra of cationic iridium complexes, but it has an intrinsic limit: if the LUMO of the neutral ancillary ligand lies too high in energy, the LUMO + 1 or the LUMO + 2, usually located on the cyclometalating ligands, becomes the new LUMO of

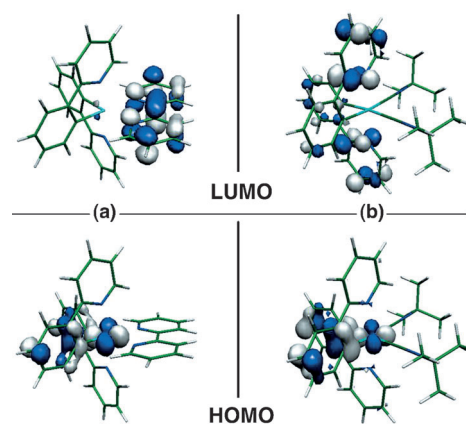


Figure 16. Schematic representation of the electronic density contours calculated for the frontier molecular orbitals of a) $[\text{Ir}(\text{ppy})_2(\text{bpy})]\text{[PF}_6]$ (2) and of b) $[\text{Ir}(\text{ppy})_2(\text{CNtBu})_2]\text{[PF}_6]$ (8), a complex with higher ligand field.

the complex (Figure 16b). If this is the case, as expected from the larger electronegativity of the N atom, the new LUMO is mainly located on the heterocyclic moiety of the (C⁺N) ligand (e.g., the pyridine ring for ppy-based ligands). In this way, the use of ancillary ligands with relatively inaccessible π* orbitals (e.g., carbenes^[85] or isocyanides^[92,93]) leads to low-lying emitting excited states centered on the cyclometalated ligands and the emitting T₁ state exhibits a more ligand-centered character. In such cases, highly structured emissions and strongly increased radiative lifetimes (i.e., small values of k_r) are found. Practically, the ancillary ligand plays a passive role in determining the nature of the excited state as it only influences the Δ_o splitting of the iridium d orbitals by inductive effects through σ bonds.^[36,92]

As the simple description of the HOMO and LUMO is not always exhaustive in describing the emitting triplet state of Ir^{III} complexes, theoretical calculations performed with the time-dependent version of the density functional theory (TD-DFT)^[94,95] result to be very useful in establishing the electronic nature and relative energy ordering of the low-lying triplet states and, in particular, of the emitting excited state T₁. The combination of TD-DFT and DFT calculations are especially helpful in determining the energy position and the electronic and molecular structures of ³MC states.^[37,96,97] As mentioned above, the thermal population of these states might be one of the possible non-radiative deactivation processes that could take place in Ir-iTMCs and, likewise ruthenium(II) metal complexes,^[98] might cause complex instability and degradation both in solution and in LECs. ³MC states formally involve the transfer of one electron from the HOMO dπ orbitals (t_{2g}) to the antibonding dσ* orbitals (e_g) of the iridium ion. The e_g orbital is characterized by a strong σ-antibonding interaction between the iridium atom and the nitrogen atoms of the C⁺N ligands (Figure 17).^[37] Therefore, population of the ³MC states leads to elongation of Ir–N_{C⁺N} bonds and to the opening of the molecular structure of the complex, prompting the entrance of small nucleophilic molecules and leading to degradation of the complex. Despite the fact that the ligand-field stabilization energy is strongly

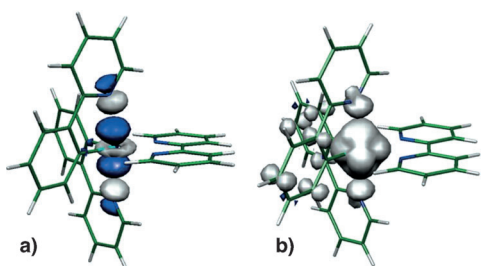


Figure 17. a) Electron density contour (0.05 ebohr^{-3}) calculated for the unoccupied e_g orbital of complex **2** showing the σ -antibonding interactions along the vertical $N(\text{ppy})-\text{Ir}-N(\text{ppy})$ axis. b) Spin density calculated for the optimized structure of the ${}^3\text{MC}$ state of complex **2**.

enhanced by cyclometalation and hence antibonding e_g orbitals are very high in energy,^[36] in some cases ${}^3\text{MC}$ thermal population has been observed for Ir-iTMCs (see Section 3.2.4).^[99]

Because HOMO and LUMO orbitals are usually located on different ligands (except in the case of high-field-strength ancillary ligands, for which the HOMO and the LUMO are located on different moieties of the same cyclometalated ligand), the HOMO–LUMO energy gap can be fine-tuned by playing independently on the cyclometalated (HOMO) or on the ancillary ligands (LUMO), or even on both of them. As a rule of thumb, it can be said that 1) electron-withdrawing substituents on the C^{N} ligands reduce the σ donation to the metal, decrease the electron density on the iridium ion, and lead to a stabilization of the HOMO; and 2) electron-donating substituents on the ancillary ligand or use of intrinsically electron-rich ligands bring about a destabilization of the LUMO. Some examples of how it is possible to influence these levels to tune the emission color in cationic iridium(III) complexes are reported in Section 3.3.

Although it has become feasible to estimate the emission energy of Ir-iTMCs, it remains quite difficult, on the other hand, to predict other emission properties, such as radiative constants (k_r) and emission quantum yields (Φ), only by means of DFT calculations or electrochemical data. Accordingly, in-depth experimental studies remain essential to fully characterize the photophysical properties of luminescent Ir^{III} complexes.

3.2.4. Deactivation Pathways through ${}^3\text{MC}$ Levels

The lowest-lying T_1 excited state of iridium(III) complexes has a mixed ${}^3\text{MLCT}$, ${}^3\text{LLCT}$, and ${}^3\text{LC}$ character that deactivates radiatively to the ground state (Figure 13), typically in the microsecond time scale, with high PLQYs. As pointed out earlier and similarly to Ru^{II} complexes,^[98] non-emissive ${}^3\text{MC}$ levels could offer effective radiationless pathways to the T_1 emitting state; such transitions often entail photodegradation of the complex by nucleophilic-assisted ligand-exchange reactions. In the case of ionic cyclometalated iridium(III) complexes, the energy gap (ΔE) between the T_1 and the ${}^3\text{MC}$ states is usually around 5000 cm^{-1} ,^[100] namely higher than for luminescent Ru^{II} compounds (below 4000 cm^{-1}).^[98] This situation is due to the strong ligand-field

stabilization energy provided by cyclometalating C^{N} ligands and because Ir is a third-row d element. Therefore, the thermal population of ${}^3\text{MC}$ levels of Ir-iTMCs is negligible in most cases but, under particular circumstances, it must be thoroughly considered. This is the case, for instance, when the complex is geometrical distorted or when emission comes from very high (i.e., blue emitting) T_1 states.^[100,101] Moreover, when Ir-iTMCs are used as active materials in LEC devices, the thermal accessibility of metal-centered states might become an issue under the operative conditions. Unfortunately, the experimental determination of ΔE by solid-state electroluminescence measurements cannot be accomplished, unlike photoluminescent liquid samples.^[98]

Key information about the population of thermally accessible non-radiative excited states can be obtained in solution by studying the temperature dependence of the intrinsic deactivation rate constant of the complex $k_{\text{in}} = \tau^{-1}$, where τ is the measured excited-state lifetime. Overall, the deactivation of the emitting excited states in d^6 transition-metal complexes is governed by three main processes (Figure 18a):^[22,100]

- 1) an almost temperature-independent non-radiative pathway, characterized by a rate constant k_{nr1} , that occurs through direct potential energy surface crossing and/or vibrational coupling between T_1 and S_0 states;
- 2) a minor temperature-dependent radiative pathway, with kinetic rate constant $k_r(T)$, associated with the thermal population of the upper-lying triplet substates of T_1 (e.g., $T_{1\alpha}$, $T_{1\beta}$, and $T_{1\gamma}$) having their own radiative decay rates;
- 3) a strong temperature-dependent non-radiative pathway, with kinetic rate $k_{nr2}(T)$, involving the thermal population of upper-lying non-radiative excited states (i.e., ${}^3\text{MC}$ states), frequently associated with an activation energy barrier.

Following this model, an experimental estimation of the energy gap (ΔE) between the emissive T_1 and the ${}^3\text{MC}$ excited states can be obtained correlating the dependence of k_{in} with temperature, using the Arrhenius-type Equation (3).

$$k_{\text{in}} = k_0 + \sum_i A_i \exp\left[-\frac{\Delta E_i}{RT}\right] \quad (3)$$

Where, k_0 is a low-temperature limiting value and A_i is the pre-exponential frequency factor of the i -th deactivation process. This pre-exponential constant is extremely important to figure out the physical meaning of this model. In fact, once the ${}^3\text{MC}$ state is populated, two limiting kinetic cases can occur:

- 1) a strong coupling between the ${}^3\text{MC}$ state and the S_0 level ($k_2 \gg k_{-1}$, Figure 18b), so that $A_i > 10^{11}$: the ${}^3\text{MC}$ deactivation to the ground state is extremely fast and often leads to dissociative photodegradation of the complex. In this case, ΔE corresponds to the activation energy barrier between the T_1 emitting level and the ${}^3\text{MC}$ state;
- 2) a thermal equilibrium between ${}^3\text{MC}$ and T_1 ($k_{-1} \gg k_2$, Figure 18c), so that $A_i < 10^9$: the ${}^3\text{MC}$ deactivation is slower and the ΔE value corresponds to the difference in energy between the T_1 emitting level and the ${}^3\text{MC}$.

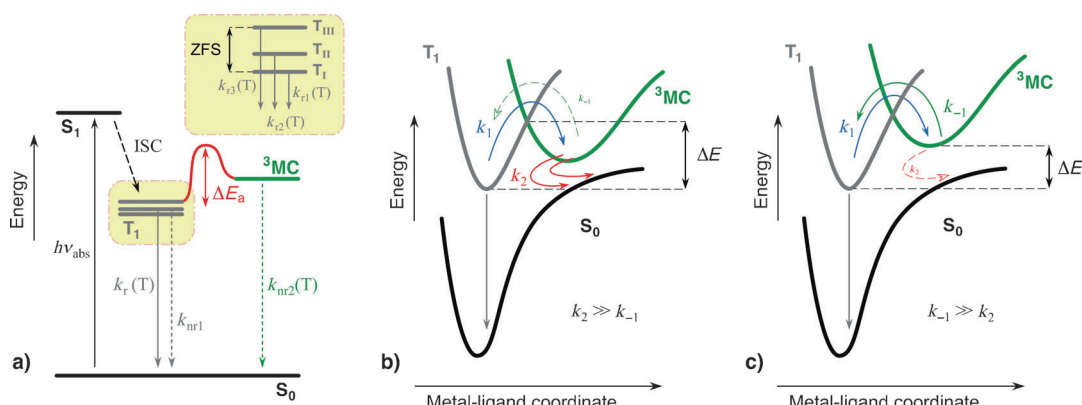


Figure 18. a) Schematic representation of the lowest-energy excited states of Ir^{III} complexes and their deactivation processes. The lowest emitting excited state (T_1) is composed of three levels (T_{1I} , T_{1II} , and T_{1III} , split by zero-field splitting) that undergo thermal equilibration at temperatures above 77 K. b) and c) potential energy curves illustrating the two possible limiting kinetic cases describing the non-radiative deactivation of the emitting T_1 state through thermal population of upper-lying ^3MC levels.

Practically, the k_{in} (i.e., $1/\tau$) values determined in a wide range of temperatures (typically 77–300 K) can be fitted using Equation (3) to obtain all the relevant parameters described above.^[100]

3.2.5. Optimizing Emission Performance in the Solid State

There are many parameters that describe the performance of LECs (see Section 4) and one of them is the external quantum efficiency (EQE, the ratio of photons emerging from the device per injected electron) that is proportional to the fraction of excitons that decay radiatively. Since emission in Ir-iTMCs arises from the triplet state and singlet excitons are efficiently converted into triplets, it has been shown that the EQE should be proportional to the solid-state PLQY measured in thin films.^[102,103] Therefore, a preliminary photo-physical characterization of a given complex in solid-state films can be helpful to predict if it can yield a brightly emitting device. Some main strategies can be used to enhance PLQYs in the solid state and minimize the typical self-quenching effects observed in films:^[29]

- 1) use of inert matrices, such as ionic liquids^[104,105] or polymers^[71,106] to disperse the iTMC; ionic liquids improve both PLQY and LEC properties (e.g., turn-on time, luminance, and efficiency),^[37] but polymers have often a detrimental effect on device efficiency.^[29]
- 2) dispersion of a low-band-gap iTMC in a wider band-gap iTMC, for example, an orange iTMC in a green emitter; this has been successful to increase the device EQE.^[107]
- 3) covalent binding of hydrophobic bulky groups (e.g., *tert*-butyl) to chelating ligands; this improves PLQY as it increases the distance between the emitting complexes in the solid state and therefore can strongly decrease self-quenching, as also found for Ru^{II} complexes.^[108] In addition, hydrophobic bulky groups on iTMCs can also enhance the stability of the complexes because they render the molecule less susceptible to interaction with aggressive nucleophiles.^[109]

Another useful PL parameter to check in solid films is the excited-state lifetime, which can be helpful to evaluate the protecting effect of bulky groups against self-quenching. Practically, shorter lifetimes in neat films (compared to diluted dispersions of inert matrices) indicate interactions between closely packed iTMCs and, hence, additional non-radiative pathways.^[104]

It must be emphasized that, although an accurate photo-physical study of the emitting complex (especially in solid-state film) can be very useful to predict the performance of the active material in LECs, several other parameters that do not usually affect the photoluminescence behavior can strongly affect the device properties, as will be discussed in Section 4.

3.3. Strategies for Tuning the Color of Ir-iTMCs

The key property of Ir-iTMCs to be utilized in LECs is the emission color, which can be tuned by changing or chemically modifying the organic ligand framework around the Ir^{III} metal ion.^[36] A parameter often used to describe the emission color of a given compound is the wavelength of the emission band maximum (λ_{max}). It is a very practical parameter since is directly derived from the photoluminescence (PL) or electroluminescence (EL) spectra corrected for the detector response, but it can only give a rough estimation of the true emission color, which dramatically depends on the specific bandwidth. Moreover, to fully define a color, the sensitivity of the photoreceptors in the human eye has to be considered. Therefore the appropriate method to define colors requires the use of the Commission Internationale de l'Eclairage (CIE) coordinates, that can be calculated from the luminescence spectrum and give a univocal definition of the emission color according to universally accepted international standards.^[110] CIE coordinates are particularly useful to define white-light sources and, to this purpose, the so-called color-rendering index (CRI) is also provided, which gives a quantitative measure of the ability of an emitting device to

reproduce the colors of various objects faithfully, in comparison with natural sunlight.^[110]

A huge number of cationic iridium(III) complexes have been synthesized and characterized.^[29,36,73,75] In this Review we discuss primarily those used as active materials in LECs together with some examples that illustrate the general strategies used for color-tuning and for achieving highly emissive materials. The photophysical and electrochemical properties of many of them are gathered in Table 1 to allow an easy comparison.

3.3.1. Attaching Substituents to the $[\text{Ir}(\text{ppy})_2(\text{bpy})]^+$ Ion

The spatial distribution of the frontier orbitals in $[\text{Ir}(\text{ppy})_2(\text{bpy})]\text{[PF}_6\text{]}$ (**2**, Figure 16a) allows for an almost independent tuning of the HOMO and LUMO energy levels. Consequently, two different strategies are possible: to attach substituents on the bpy ancillary ligand (LUMO tuning) or/and to substitute the cyclometalating ppy ligands (HOMO tuning).

In the first Ir-iTMC used in a LEC (**4**, Figure 9), two *tert*-butyl groups are attached to the 4 and 4' position of the bpy ancillary ligand.^[76] In acetonitrile solution, no substantial shift is observed in the PL spectrum if compared to **2** ($\lambda_{\text{max}} = 581$ nm vs. 585 nm). However, a more marked hypsochromic shift of 30 nm was found in the EL spectrum ($\lambda_{\text{max}} = 560$ nm

vs. 590 nm) of the LEC, a shift which has been observed in more cases, especially in wide-band-gap iTMCs. The main difference between PL and EL spectra, besides the way of excitation, is the concentration of the iTMC in the solvent or in the device film; in PL it is usually low whereas in EL the iTMCs are usually present at a concentration higher than 70 wt %.

To accomplish emission blue-shift, it is necessary to enlarge the HOMO–LUMO energy gap. This can be achieved by anchoring electron-withdrawing substituents on the cyclo-metallated ligands (to stabilize the HOMO) and/or electron-donating substituents on the neutral ancillary ligands (to destabilize the LUMO). Following this approach, using a 4,4'-dimethylamino-substituted bipyridine ligand, with strong electron-donating groups on the 4,4' positions, a hypsochromic shift of almost 60 nm was obtained.^[111] The corresponding complex $[\text{Ir}(\text{ppy})_2(\text{dma-bpy})]\text{[PF}_6\text{]}$ (**9**) exhibits a strong emission band with maxima at 491 and 520 nm (PLQY = 80 %, in deaerated solution). A further blue shift could be obtained by stabilizing the HOMO using difluoro-substituted 2-phenyl-pyridines (dfppy) as the cyclometalating ligands. While the sole effect of the dfppy ligand leads to a blue–green emission around 512 nm in the case of complex $[\text{Ir}(\text{dfppy})_2(\text{dtb-bpy})]\text{[PF}_6\text{]}$ (**10**), the synergetic effects of both the electron-withdrawing substituents on the dfppy ligands and the electron-donating amino substituents on the bpy-based ligand are able

Table 1: Photophysical and electrochemical properties of Ir^{III} complexes utilized in LEC devices.

Complex	Absorption λ_{max} [nm] (ϵ [$\times 10^4 \text{ M}^{-1} \text{ cm}^{-1}$])	Photophysics ^[a]			Electrochemistry ^[b]	
		λ_{max} [nm]	Emission τ [\mu s]	Φ	Oxidation E_{ox} [V]	Reduction E_{red} [V]
2	257 (4.8), 269 (4.7), 309 (2.2, sh), 281 (6.9), 467 (0.83) ^[c]	585	0.43	0.14	0.84	−1.77, −2.60
4	–	581	0.557	0.23	0.83	−1.88, −2.87
7	253 (5.51), 358 (0.53), 411 (0.30)	475, 503 (sh)	1.56	0.23	0.88	−2.19
8	341 (0.75)	453, 485, 509 (sh)	32	0.52	1.23	−2.38
9	268 (5.62), 290 (3.49), 355 (0.95), 472 (0.19)	491, 520	2.43	0.80	0.72	−2.17, −2.61
10	–	512	1.4	0.70	–	–
11	266 (8.27), 316 (2.89), 345 (2.20), 444 (0.14)	463, 493	4.11	0.85	1.00	−2.13, −2.49
12	Approx. 275, 290, 375	687	0.069	0.02	–	–
13	254 (11.9), 266 (11.1), 297 (10.6), 344 (10.3), 415 (0.9), 465 (0.2)	623	0.575	0.17	–	–
14	250 (7.50), 360 (0.78), 387 (0.36)	452, 480 (sh)	1.62	0.20	1.20	−2.15
15	248 (5.13), 302 (2.14,sh), 362 (5.50) ^[c]	453, 483 ^[c]	0.68 ^[c]	0.21 ^[c]	1.22	−2.18, −2.59
16	249, 366 ^[c]	454, 485 ^[c]			1.14	−1.92
17	252 (44.9), 308 (20.1), 412 (0.1), 440 (0.06) ^[c]	444, 468 ^[c]	6.2 ^[d]	0.16 ^[d]	>1.40	−2.19
18	326 (1.2)	447	40	0.55	1.37	−2.43
19	–	451, 482 ^[c]	0.015 ^[c]	0.073 ^[c]	–	–
20	–	445, 474 ^[c]	0.17 ^[c]	0.079 ^[c]	–	–
21	Approx. 250 (3.9), 310 (1.7), 360 (0.6) ^[c]	452, 482 ^[c]	2.08 ^[c]	0.20 ^[c]	0.99	−2.32, −2.67
22	251 (4.7), 266 (4.4), 306 (1.8, sh), 375 (0.51), 459 (0.01)	471	0.065	0.009	0.86	−2.43

[a] Where not specified, the reported data have been obtained at room-temperature in acetonitrile, air-equilibrated (absorption) or oxygen-free (emission) solutions. [b] Relative to Fc^+/Fc , in acetonitrile ($\text{Fc}=[(\text{C}_5\text{H}_5)_2\text{Fe}]$). [c] In dichloromethane. [d] In 2-MeTHF. sh=Shoulder

to shift the emission band of the complex $[\text{Ir}(\text{dfppy})_2(\text{ddma-bpy})][\text{PF}_6]$ (**11**) to the blue with emission maxima at 463 and 493 nm.^[112]

Using the same rationale as above, emission red-shift can be achieved by LUMO stabilization. To this end, there are essentially two methods: 1) adding electron-withdrawing groups to the N⁺N ancillary ligand or 2) increasing the delocalization of its π system. Following the first approach, a deep-red LEC device was obtained using complex $[\text{Ir}(\text{tpy})_2(\text{e-bpy})][\text{PF}_6]$ (**12**): the red-shifted emission (PL emission peak in solution at 687 nm) is due to LUMO stabilization by the electron-withdrawing effect of the ester groups.^[113] The second approach was used with $[\text{Ir}(\text{ppy})_2(\text{pdp-bpy})][\text{PF}_6]$ (**13**), having a 5,5'-diphenyl-substituted-bpy as N⁺N ligand and exhibiting a red PL emission centered around 620 nm.^[114]

3.3.2. Designing Ligands beyond Prototypical bpy and ppy

Using differently substituted bpy-type ancillary ligands, it is very difficult to push the emission of Ir-iTMCs toward the blue because of the intrinsically limited energy gap.^[115] Therefore it is more convenient to replace the bpy-based ancillary ligand with other diimine ligands containing stronger electron-donating nitrogen atoms, such as 2-(1*H*-pyrazol-1-yl)pyridine (pzpy, Figure 12).^[115] For example, in acetonitrile solution, $[\text{Ir}(\text{ppy})_2(\text{pzpy})][\text{PF}_6]$ (**7**) emits blue-green light ($\lambda_{\text{max}} = 475$ nm), which is hypsochromically shifted by more than 100 nm with respect to the bpy analogue **2**, Figure 15. $[\text{Ir}(\text{dfppy})_2(\text{pzpy})][\text{PF}_6]$ (**14**, Figure 19) with fluorine-substituted cyclometalated ligands shows even further blue-shifted light emission ($\lambda_{\text{max}} = 451$ nm).

Compared to pzpy, triazole-pyridine ancillary ligands (Figure 12) have an even stronger electron-donating capability owing to the σ -donor properties of the triazole ring, that make them suitable for preparing sky-blue light-emitting Ir-iTMCs. Indeed, recent examples by De Cola and co-workers show that, by using Ir-iTMCs with 1,2,3-triazole-pyridine as ancillary ligands, PL peaks are in the range 460–490 nm and LECs exhibiting true-blue emission are obtainable;^[116] one of these compounds (**15**) is depicted in Figure 19. Following a similar approach, Chen et al.^[117] used the isomeric 1,2,4-triazole-pyridine with different substituents in the 4 and 5 position of the triazole ring as the ancillary ligand to make an Ir-iTMC (**16**) displaying an EL band further shifted to the blue (457–486 nm).

Tamayo et al. reported the first series of Ir-iTMCs used for LECs without 2-phenylpyridine (ppy) cyclometalating ligands.^[118] The ppy motif was replaced by the higher energy 1-phenylpyrazole (ppz), as exemplified by the green-blue and red-emitting complexes depicted in Figure 20. Ladouceur et al., described a new series of Ir-iTMCs using aryl-triazoles as the cyclometalating ligands, that lead to blue- and green-emitting complexes.^[119] Their use in LECs has not been described yet.

3.3.3. Ir-iTMCs Based on Strong-Field Ancillary Ligands

Deep-blue emissions from Ir-iTMCs can be obtained also by introducing strong ligand-field-stabilizing ligands (e.g.,

CO, isocyanides, or carbenes), so that the HOMO→LUMO transition involves mainly the cyclometalated C⁺N system without participation of the ancillary counterpart. In these cases, the HOMO orbital is predominantly located on the Ir–C bonds on the phenyl moieties of the C⁺N ligands, while the LUMO is mostly found on the pyridine rings of the same cyclometalating ligand. The first two examples of this class of complexes were reported by Thompson et al. in 2005, using isocyanides as strong-field neutral ligands. In 2-methyl-THF solution, $[\text{Ir}(\text{ppy})_2(\text{CN}t\text{Bu})_2][\text{CF}_3\text{SO}_3]$ (**8**) and $[\text{Ir}(\text{dfppy})_2(\text{CN}t\text{Bu})_2][\text{CF}_3\text{SO}_3]$ (**17**) emit with $\lambda_{\text{max}} = 458$ and 444 nm, respectively, and the isocyanide ancillary ligands have a negligible effect in dictating the HOMO–LUMO gap.^[92] Recently, $[\text{Ir}(t\text{Bu}-\text{ppy})_2(\text{CN}t\text{Bu})_2][\text{CF}_3\text{SO}_3]$ (**18**, Figure 19) has turned out to be first example of an Ir^{III} isocyanide complex whose strong blue phosphorescence is unaffected by passing from solution to the solid state, thanks to the presence of the *tert*-butyl groups on the ppy ligand that are particularly effective in preventing self-aggregation.^[93]

In 2007, Chin et al.^[120] synthesized a series of cationic iridium complexes equipped with even stronger-field ligands, such as CO. Complexes $[\text{Ir}(\text{ppy})_2(\text{CO})_2][\text{PF}_6]$ (**19**) and $[\text{Ir}(\text{dfmet-ppy})_2(\text{CO})_2][\text{PF}_6]$ (**20**, Figure 19) emit at 451–482 nm and 441–443 nm, respectively. Following an analogous approach, Yang et al.^[85] have recently reported the first LECs based on N-heterocyclic carbene ligands displaying the bluest emission ever reported for a LEC device (456–488 nm). This class of complexes displays true-blue emission both in solution and in neat film, although exhibit a strong PLQY decrease in the solid state because of self-quenching. Also in this case, the carbene ancillary ligand appears to contribute only with a small electron density to both the HOMO and the LUMO. In Figure 19, one of these complexes (**21**) is reported as an example. Similar results have been recently reported by Kessler et al., who synthesized a series of Ir-iTMCs emitting from near-UV to red using a neutral pyridine-carbene ancillary ligand and different cyclometalating ligands (e.g., **22**, Figure 19).^[121] The low PLQYs observed for these complexes were ascribed to non-radiative process through the population of ³MC states. Nevertheless, LECs with emission from the bluish-green to orange region of the visible spectrum were fabricated.

4. iTMCs-Based LECs

4.1. Fabrication and Architectures

LECs are prepared by solution-based processes with benign solvents. Most devices reported to date consist of one or two active layers sandwiched in between one transparent and one reflecting electrode (Figure 21a). Materials most commonly used for electrodes are ITO (transparent anode) and Au, Al, and Ag (air-stable reflecting cathode). Double-layer LECs, besides the film of the light-emitting iTMC, entail a hole injection layer, generally composed of PEDOT:PSS [poly(3,4-ethylenedioxythiophene):polystyrenesulfonate]. Such a layer is deposited to smoothen the ITO surface and, as a result, increases the yield of device preparation. An inert

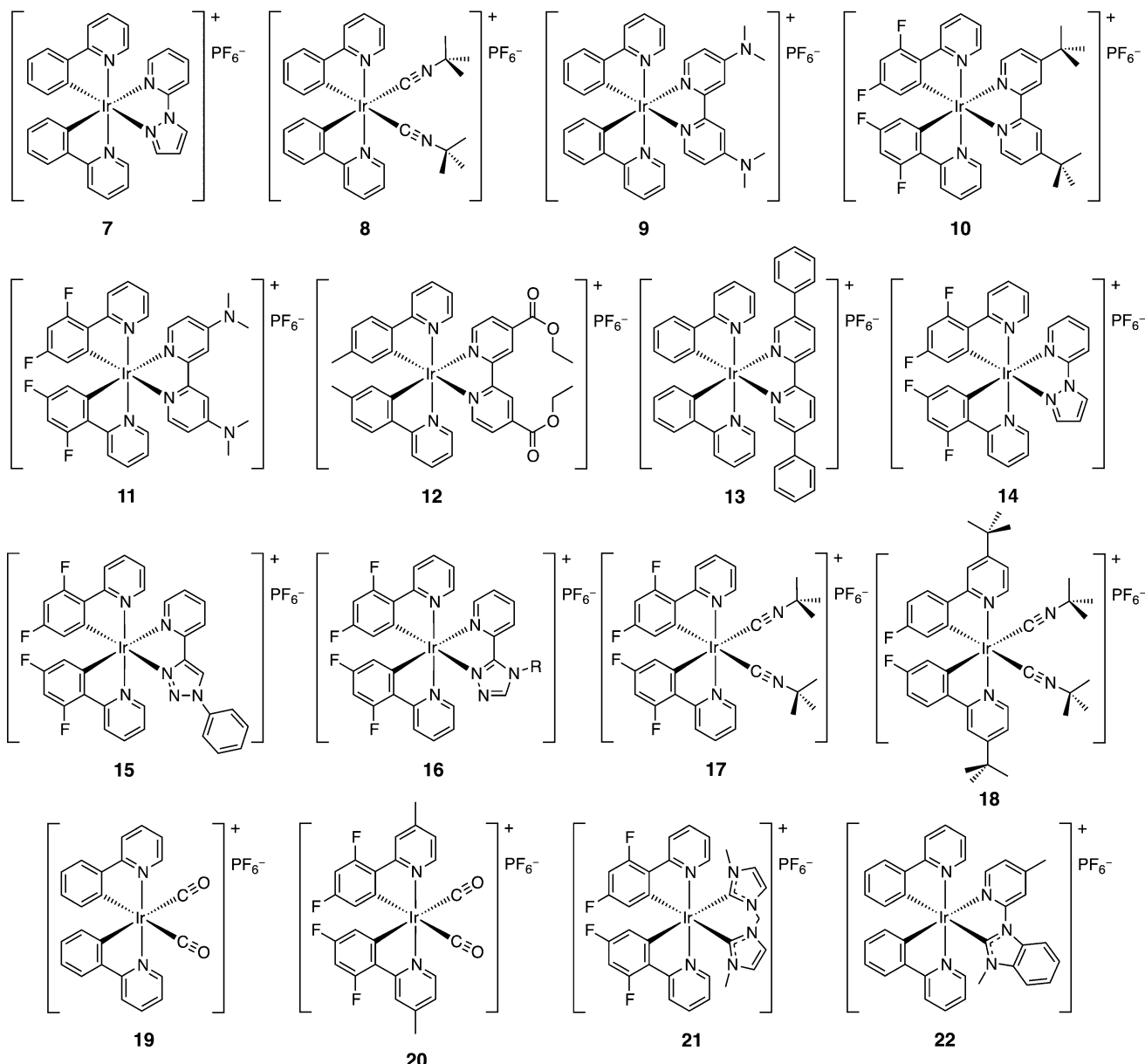


Figure 19. Selected examples of Ir-iTMCs with substituted ppy as cyclometalating ligands.

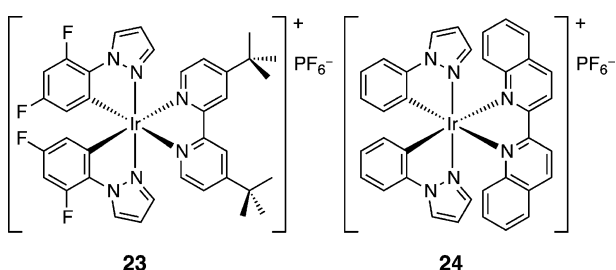


Figure 20. Two examples of complexes with phenylpyrazoles as $C\equiv N$ cyclometalating units: $[Ir(dfppz)_2(dtbbpy)][PF_6]$ (23), $\lambda_{max}=492\text{ nm}$; $[Ir(ppz)_2(biq)][PF_6]$ (24), $\lambda_{max}=616\text{ nm}$.

polymer or an ionic liquid is frequently added to the iTMC core component to facilitate the formation of the film and to enhance the device performances. In most cases, the top metal contact is thermally evaporated; there are few examples in which it was prepared by soft contact lamination;^[38] liquid top contacts are also reported.^[122]

Bernards et al.^[39] and Slinker et al.^[40] have made LEC arrays powered directly by a standard US outlet (120 V, 60 Hz), without the use of transformers. These lighting panels consist of several LECs (16, 24, and 36) that were placed in series in such a way that the anode of a given device acts also as cathode for the next one (Figure 21b). Bernards et al. showed that iTMC-LECs with ITO anodes and laminated Au cathodes (Figure 21c) exhibit comparable performance to

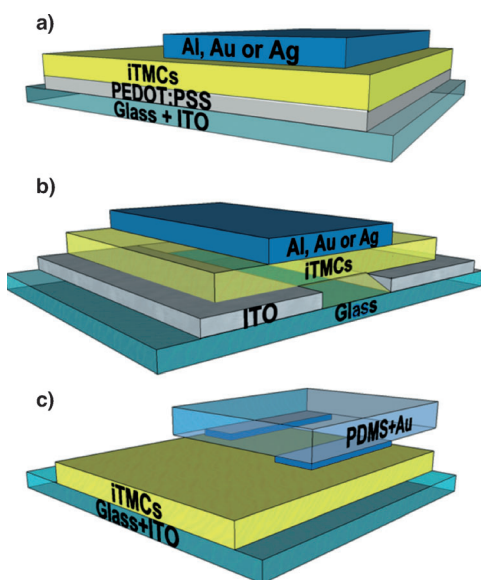


Figure 21. Schematic layout of a sandwiched (a), cascaded (b), and laminated LEC (c).

those fabricated with evaporated top contacts.^[38] These devices were made by evaporating the Au electrode onto a polydimethylsiloxane (PDMS) stamp, followed by soft-contact lamination onto an iTMC-layer deposited on a patterned ITO substrate. Light emission output is uniform over the whole device area, indicating a high-quality mechanical and electrical contact.

4.2. Figures of Merit in LECs

The most important figures of merit used to characterize the performance of LECs are:

- **Luminance (L):** Flux of light emitted by the device, measured in candela per surface unit (cd m^{-2}), red curve in Figure 22.
- **Current density (J):** Flux of current through the device, measured in ampere per surface unit (A m^{-2}), black curve in Figure 22.
- **Turn-on time (t_{on}):** Time needed to reach the maximum luminance; in Figure 22 $t_{\text{on}} = 0.74 \text{ h}$. A parameter often used in literature is t_{100} , which is the time to reach $L = 100 \text{ cd m}^{-2}$.
- **Lifetime ($t_{1/2}$):** Time to reach half of the maximum luminance; in Figure 22, $t_{1/2} = 7.1 \text{ h}$. Sometimes, it is also used $t_{1/5}$, namely the time to reach one fifth of the maximum luminance.
- **Total emitted energy (E_{tot}):** It is calculated by integrating the radiant flux of the device vs. time from $t=0$ (application of bias) to $t=t_{1/2}$.^[123] If this value is divided by the electrode area, it yields the total emitted energy density U_{tot} , which allows devices having electrodes of different shapes to be compared. Herein, all the values are determined using an area of 3 mm^2 , hence only the E_{tot} parameter will be used.

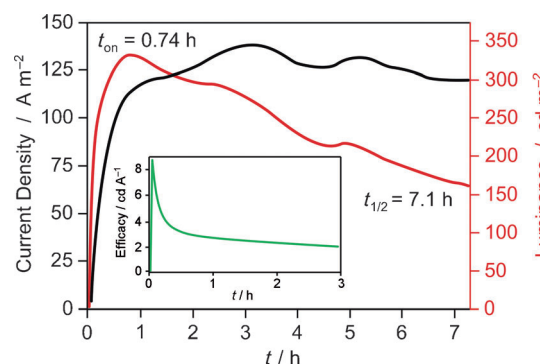


Figure 22. Typical trend of the current density (black), luminance (red), and efficacy (green, inset) over time of a standard LEC at applied constant voltage.

- **Efficacy (or current efficiency):** Emitted light per electric flux, measured in candela per ampere (cd A^{-1}). The value of efficacy reported for a given device is the maximum observed. The evolution of the efficacy over time is displayed in Figure 22 (inset).
- **Power efficiency:** Flux of light per electric input, measured in lm W^{-1} . The value of power efficiency reported for a given device is the maximum observed.
- **External quantum efficiency (EQE):** The ratio of photons emerging from the device per injected electrons. EQE is also defined through the equation $\text{EQE} = b\phi/2n^2$, where b is the recombination efficiency (equal to unity for two ohmic contacts^[124]), ϕ is the fraction of excitons that decay radiatively, and n is the refractive index of the glass substrate and is equal to 1.5 (the factor $1/2n^2$ accounts for the light outcoupling of the device).

The stability of a LEC device is measured by using either the lifetime ($t_{1/2}$) or the total emitted energy (E_{tot}), and this can generate confusion in making comparisons among data from different research groups. E_{tot} is more accurate for comparing the stability of different LECs since $t_{1/2}$ strongly depends on the maximum luminance level reached, which can be rather different; devices running at higher luminance levels typically exhibit lower lifetimes. E_{tot} takes into account the absolute magnitude of the radiant flux as well as the total device lifetime, and does not rely on the shape of the curve of radiant flux versus time.

4.3. Early Studies on LECs

Two excellent Reviews by Slinker et al. cover the development of iTMC-LECs during the first 10 years.^[28,29] The vast majority of reports reviewed in these articles concerns LECs based on ruthenium(II) and osmium(II) complexes, with $[\text{Ru}(\text{bpy})_3]^{2+}$ as the most utilized cationic compound (e.g., complex **3** in Figure 9).^[27–29,31–34,38–40,54,58,66,71,106,108,122,123,125–147] These LECs showed emission in the red and orange-red spectral windows, with stabilities of few hours and low external quantum efficiencies. Other copper(I)- and rhe-

nium(I)-based complexes were also tested in LECs but only few examples were initially described (see Section 4.5).^[148–155]

Herein, only the most significant reports from early times will be summarized. More generally, we will illustrate the latest advances obtained in iTMCs-LECs in terms of turn-on time, stability, efficiency, and color.

4.4. LECs Based on Ir-iTMCs: Recent Advances

In 2004, Slinker et al. pioneered the use of Ir-iTMCs in LECs.^[76] As discussed in Section 3, there are several reasons that justify their selection over Ru^{II} complexes: 1) high PLQY,^[19,86,98,156] 2) easily tunable HOMO-LUMO energy gap by independent chemical modifications of the ligands;^[29,37,75,81,82,85,91,99,103,105,111,113,116,118,157–160] 3) high stability against degradation processes owing to higher ligand-field splitting.^[19,86,97,98,156,161–164] Over the last eight years, the use of Ir-iTMCs has brought very significant advances in LEC performances, that is, color, efficiency, stability, and turn-on times. Notably, Ir^{III} complexes (in most cases neutral) have been extensively used also in OLED technology, and several Reviews covering this vast topic have been published over the years.^[75,165] Shin et al. have also demonstrated that devices based on a combination of neutral Ir^{III} complexes with tetra-*n*-butylammonium tetrafluoroborate in the emitting layer behave similarly to iTMC-based LECs,^[166] obtaining luminances of about 300 cd m⁻² and *t*_{on} shorter than one second. Such devices can be considered borderline cases between iTMC-LECs and PLECs using an ionic liquid.^[167]

4.4.1. Turn-On Time

As discussed in Section 2.2, the movement of ions is essential to promote electronic charge injection in LECs. However, since the ionic conductivity in the solid state is low, it takes time for iTMC-LECs to become operative, therefore the so-called turn-on time (*t*_{on}, see above) generally ranges from a few minutes to several days. This is clearly a formidable obstacle for most practical applications, which require instantaneous response.^[31,32] In the first ten years of activity on LECs, only few reports targeted the improvement of *t*_{on},^[31,32] which were typically achieved by applying higher driving voltages.^[27,33,108] These voltages are provided continuously or, alternatively, initial sequences of high-voltage pulses followed by constant lower bias, once sufficient luminance is reached, are applied.^[33] Higher voltages lead to 1) faster movement of ions towards the electrode interfaces and 2) lower electron/hole injection barriers; both effects reduce the turn-on time.^[33,111,149,168] Notably, the approach entailing a few short higher voltage pulses can lead to both an improvement of *t*_{on} and device stability (see also Section 4.4.2).^[168] Environmental effects during device preparation and operation may also influence *t*_{on}. For instance, devices running in air exhibit shorter turn-on times than those in a nitrogen environment;^[112] this is due to the presence of residual moisture and/or solvent in the iTMC layer, which increases the ionic mobility.^[123,141,146] The use of complexes with counteranions smaller than [PF₆⁻], such as [BF₄⁻] or

[ClO₄⁻], is also beneficial for turn-on times,^[71,122] likewise the addition of salts in the form of electrolytes or ionic liquids.^[37,82,104,105,126,169,170] All these approaches enhance ionic conductivities, thereby causing a faster build-up of the electrical double layer which induces a faster device *t*_{on} but, on the other hand, also a quicker propagation of the doped zones leading to more extensive exciton quenching and decrease of the luminance (see Section 2).

In the last few years, several reports have appeared showing improvements in the turn-on time of LECs by increasing the density of small ions or by adding ionic liquids (see Section 4.4.1.2).

4.4.1.1. Chemical Modifications of Ir-iTMCs

To increase the ionic concentration in the device, extra charged groups were attached at the periphery of the Ir-iTMCs (Figure 23). Zysman-Colman et al.^[171] made a family of novel ruthenium(II) and iridium(III) complexes (e.g., **25**, Figure 23) with triethylammonium hexafluorophosphate groups attached to the 5-position of the bpy ligands through alkyl chains made of four, six, and eight carbon atoms. The turn-on time was strongly reduced for all Ir-iTMCs, down to about 30 min. The EQE values were improved by increasing the length of the carbon chain, reaching a maximum for *n* = 6. With longer chains, the EQE drops as a result of a decrease of electron transport, attributed to a non-optimal spacing of the iTMCs in the film.

Su et al.^[172] reported a significant decrease of *t*_{on} by tethering imidazolium moieties onto a cationic Ir-iTMC (**26**, Figure 23).^[172] The imidazolium groups do not affect the photophysical and electrochemical properties of complex **26**, compared to the parent complex **27** which lacks the cationic fragments, and related LECs have similar luminance (80–100 cd m⁻²) and EQE values of 4–6 %. However, the turn-on times of LECs based on complex **26** (200 min) are much shorter than those based on **27** (500 min). This result was

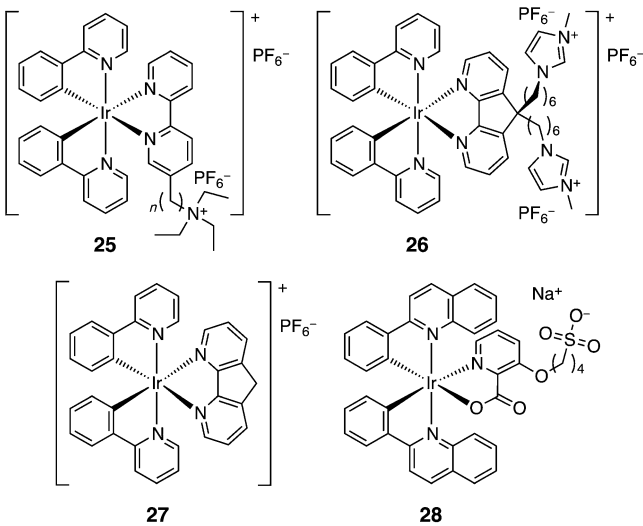


Figure 23. Schematic structures of Ir-iTMCs proposed to reduce the turn-on time in LEC devices.

attributed to the larger number of mobile $[PF_6^-]$ counterions in the neat film.

In a related work, Kwon et al.^[173] modified a neutral Ir-iTMC by attaching an alkyl chain with an anionic sulfonate group to the picolinate ligand (**28**, Figure 23), counterbalanced by a small Na^+ ion. The key idea is to take advantage of the better mobility of small cations in solid films compared to small anions, such as $[PF_6^-]$. Indeed, t_{on} of LECs under reverse bias (-3 V) was reduced compared to those employing similar Ir-iTMCs equipped with $[PF_6^-]$. However, the LEC made with **28** exhibited low efficiency, stability, and luminescence levels.

In a different approach, soft salts of cationic and anionic Ir^{III} complexes were reported; these soft salts do not have small counterions and therefore the related LECs were not made.^[174]

4.4.1.2. Use of Ionic Liquids

In 2005, Malliaras and co-workers proposed for the first time the insertion of an ionic liquid $[BMIM]^+[PF_6^-]$ (3-butyl-1-methylimidazolium hexafluorophosphate) into Ir-iTMC-based LECs (Figure 24, top).^[105,169] Indeed, small amounts of this compound significantly reduced the t_{on} of LECs from 4 h to 25 min, while also increasing luminance levels. These results were attributed to an improvement of ionic conductivity inside the light-emitting layer, because of the higher density of mobile ions. Su et al. studied the effect of $[BMIM]^+[PF_6^-]$ on the film morphology of two different Ir-iTMCs, by means of atomic force microscopy (AFM) measurements. Uniform spin-coated thin films were obtained, with no evidence of aggregation or phase separation. They also examined the effect of the $[BMIM]^+[PF_6^-]$ on the PL properties of films, observing an increase of PLQY upon addition of the ionic liquid (IL).^[104] Using a Ru^{II} complex and an ionic liquid, a LEC operating at 60 Hz (standard US

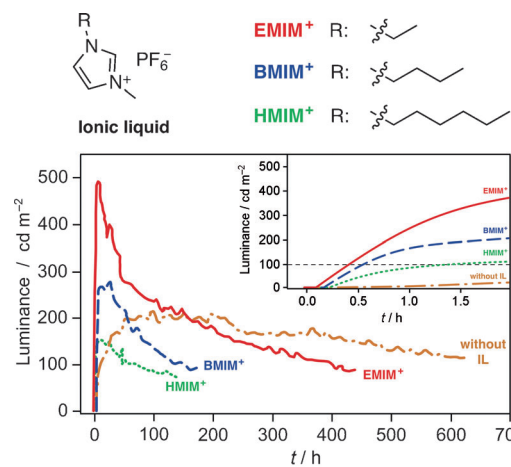


Figure 24. Top: Structural formula of ionic liquids used in LEC devices. Bottom: Luminance versus time plots for ITO/PEDOT:PSS/[Ir(ppy)₂(bpy)][PF₆]:IL/Al LEC devices under a constant voltage of 3 V and a [Ir(ppy)₂(bpy)][PF₆]:IL molar ratio of 4:1. The trend within the first two hours of operation is shown in the inset. For comparison, data for the device without IL are also shown.

outlet) was prepared, which exhibited a response time of about 4 ms.^[40] Similar results were also obtained in LECs using the simple $[\text{Ir}(\text{ppy})_2(\text{bpy})][\text{PF}_6]$ (**2**, Figure 3) and different amounts of $[\text{BMIM}]^+[\text{PF}_6]^-$, significantly reducing the turn-on time from 70 h (pristine device) to 0.7 h (Ir-iTMC: $[\text{BMIM}]^+[\text{PF}_6]^-$, molar ratio of 1:1) and increasing the PLQY in thin films. In all the above examples, device stability decreased upon addition of the ionic liquid, showing that it seems to exist a trade-off between turn-on time and stability.

Surprisingly, although there are hundreds of ionic liquids on the market, all reports on LECs with ionic liquids had utilized $[\text{BMIM}]^+[\text{PF}_6]^-$. Recently, Costa et al. studied the effect of some different ILs, with similar chemical structures but different ionic conductivities, on the performance of LECs based on **2**.^[170] They tested $[\text{HMIM}]^+[\text{PF}_6]^-$ and $[\text{EMIM}]^+[\text{PF}_6]^-$, which exhibit lower and higher ionic conductivities, respectively (Figure 24). Compared to the LEC employing $[\text{BMIM}]^+[\text{PF}_6]^-$, addition of $[\text{HMIM}]^+[\text{PF}_6]^-$ leads to an increase of the turn-on time and a decrease of the maximum luminance, whilst the LEC with $[\text{EMIM}]^+[\text{PF}_6]^-$ has a higher luminance level and turns on faster. Although $t_{1/2}$ is much shorter than that observed for the pristine LEC without any additional IL, the total emitted energy of the device with $[\text{EMIM}]^+[\text{PF}_6]^-$ is larger, thanks to the higher luminance level. Therefore, by adding a carefully optimized amount of ionic liquid with high conductivity (molar ratio Ir-iTMC: $[\text{EMIM}]^+[\text{PF}_6]^-$ 4:1), it is possible to improve the turn-on time without sacrificing the stability of the device thanks to a higher luminance.

4.4.1.3. Operation Mode. Pulsed Driving

Rudman et al. reported the benefits of pulsed driving for a ruthenium-based iTMC in a LEC.^[106] In another report they applied DC current driving, showing that a fixed current density implies the initial application of a high voltage that was rapidly decreased as the injection barriers are reduced by the displacement of the ions in the film.^[71] Using this approach, it takes 0.5 s to reach 50 cd m^{-2} , which required a starting voltage of 7 V, lowered to 3.5 V within the first 10 seconds. Recently, a further advance was reported by using a combined current and pulsed driving approach, that yielded sub-second turn-on times to reach luminances of 150 cd m^{-2} .^[175] This method also slows down the growth of the doped zones, stabilizing the LEC (which will be commented upon in the next Section).

4.4.2. Stability

Stability is an essential figure of merit in electroluminescent devices, but while OLEDs may exhibit lifetimes of thousands of hours, those of most LECs range from a few hours to a few days. The stability of the device can be described by either the lifetime ($t_{1/2}$) or the total emitted energy (E_{tot}).^[123]

LECs using complex $[\text{Ru}(\text{bpy})_3][\text{PF}_6]_2$ (**3**, Figure 9) in polymethylmethacrylate (PMMA) yielded $t_{1/2}$ as high as 1000 h with a luminance of 50 cd m^{-2} .^[71,106] At higher luminance values of 200 cd m^{-2} , the highest E_{tot} reported for

ruthenium-based LECs is around 1 J .^[29] In general, as mentioned previously, device stability is related to the mobility of the ions in the thin film, but the intrinsic robustness of the specific iTMC is also of great relevance. The most detailed studies addressing the degradation of the active luminescent material in LECs were focused on devices using **3**. Based on earlier works about the degradation mechanism of this iTMC in solution,^[161,162,164] Kalyuzhny et al.^[123] postulated that the low stability of LECs involves the formation of a photoluminescence quencher in small quantities (ca. 1 wt %). One possible quencher was complex $[\text{Ru}(\text{bpy})_2(\text{H}_2\text{O})_2]^{2+}$ (**29**), whose formation is facilitated in the excited state. This hypothesis is supported by Pile et al., who observed that humidity significantly reduces the $t_{1/2}$ of LEC devices of $[\text{Ru}(\text{bpy})_3][\text{ClO}_4]_2$ (**30**),^[141] probably as a result of the formation of **29**.^[123] Zhao et al. investigated the effects of residual water and acetonitrile on thin films and devices of complex **30**.^[146] Subsequently, evidence was obtained for the formation of an oxo-bridged dimer $[\{\text{Ru}(\text{bpy})_2(\text{H}_2\text{O})_2\}_2\text{O}]^{+}[\text{PF}_6]^{-}$ as a quencher in devices based on **3**,^[143,144] which probably results from the condensation of two subunits of **29**. Soltzberg et al. used laser desorption/ionization time-of-flight (MALDI-TOF) mass spectrometry and *in situ* Raman spectroscopy to study the generation of the oxo-bridged dimer during device operation.^[144] They demonstrated that this species is an effective quencher of device luminescence, which can explain the decay of the luminance after having reached its maximum value. In a second study, Slinker et al.^[143] employed real-time *in situ* Raman spectroscopy to identify the sequential formation of oxo-bridged species upon device operation showing that, after operating the device for one hour, a low amount of this species (1 wt %) was detected, a quantity sufficient to effectively quench the luminescence of the device, as revealed by fluorescence microscopy. All the above studies show that the stability of LECs based on Ru-iTMCs is strongly affected by the generation of quenching molecules during device operation.

Most strategies to obtain long-lived LECs based on Ir-iTMCs focus on the design of robust hydrophobic complexes. Bolink et al.^[109,134] demonstrated that the use of bulky substituents on both Ru- and Ir-iTMCs leads to more stable LECs, probably through enhanced hydrophobicity of the complexes that limits the occurrence of water-induced substitution reactions. The same group also showed that LECs with lifetimes of thousands of hours are obtained when using intramolecularly caged iridium(III) complexes (Figure 25 and Table 2).^[99,102,168,176] The cage formation effect occurs through an intramolecular $\pi-\pi$ interaction between a pendant phenyl group attached to the $\text{N}^{\text{A}}\text{N}$ bpy ligand and the phenyl of the $\text{C}^{\text{A}}\text{N}$ cyclometalating ppy moiety. Complex **31** (Figure 25) keeps its rigid cage conformation in the ground and excited states acquiring high stability against reactions with water. LECs based on **31** with a small amount of IL $[\text{BMIM}]^{+}[\text{PF}_6]^{-}$ showed $t_{1/2} = 1290\text{ h}$ and $E_{\text{tot}} = 13.6\text{ J}$ at a luminance value of 100 cd m^{-2} (Table 2).^[99] Notably, this stability can be enhanced using a pre-biasing at high voltages, which leads to efficient (10 lm W^{-1}) and stable ($t_{1/2} = 3000\text{ h}$, $E_{\text{tot}} = 73\text{ J}$) LECs with luminance levels of 200 cd m^{-2} .^[168] LECs made with the reference complex $[\text{Ir}(\text{ppy})_2(\text{bpy})][\text{PF}_6]$ (**2**, Figure 3) lacking

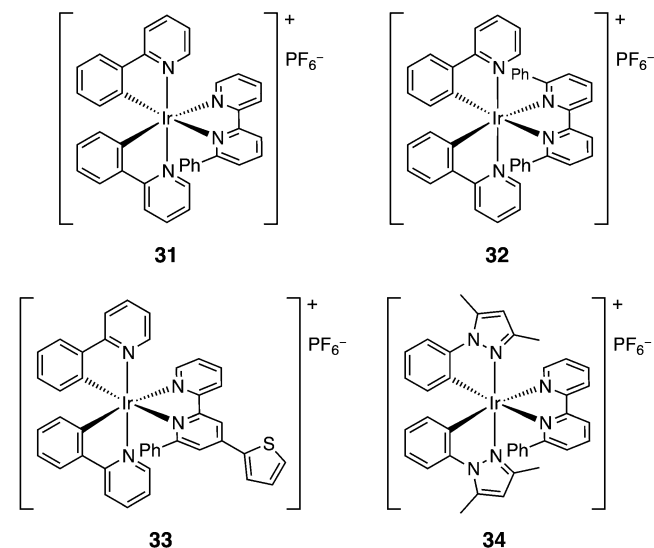


Figure 25. Structural formula of intramolecularly caged Ir-iTMCs proposed to increase the stability of LEC devices.

Table 2: Performance of LECs made with Ir-iTMCs exhibiting the intramolecular caging effect, and that of the reference complex $[\text{Ir}(\text{ppy})_2(\text{bpy})][\text{PF}_6]$ (**2**).^[a]

Value	2	31	32	34
$t_{1/2}\text{ [h]}$	70	1290	1300	2000
$E_{\text{tot}}\text{ [J]}$	2	13.6	6.9	18.7

[a] Light-emitting layer composition is a mixture of Ir-iTMC: $[\text{BMIM}]^{+}[\text{PF}_6]^{-}$ at molar ratio 4:1, measurements at applied constant voltage of 3 V.

the cage effect and having the same amount of IL $[\text{BMIM}]^{+}[\text{PF}_6]^{-}$ exhibit much poorer performance (Table 2), highlighting the relevance of the “locked” structure for device stability.^[37,168] Surprisingly, pristine LECs using **2** but without ionic liquids also had good stability with $t_{1/2} = 670\text{ h}$ and $E_{\text{tot}} = 6.6\text{ J}$ at a luminance of 220 cd m^{-2} .^[37]

Subsequently, the same authors^[99] demonstrated that, by extending the intramolecular $\pi-\pi$ interactions with a second phenyl group to the 6'-position of the ppy ligand (complex **32**, Figure 25) does not strengthen the intramolecular caging effect because the second π -interaction distorts the planarity of the diimine ligand and enables the population of dissociative ${}^3\text{MC}$ states.^[99] Accordingly, **32** yields less-stable LECs (Table 2).

A further step to combine both hydrophobicity and intramolecular caging in one iTMC was accomplished by Gruber et al.^[176] and Costa et al.^[102] In the work by Gruber et al., a thiophene ring was attached to the 4-position of the ppy ligand; the related complex **33** (Figure 25) yields LECs with high luminance levels (2700 cd m^{-2}) upon application of 5 V for 1.5 h, these levels substantially decreased at 3 V (230 cd m^{-2}), with an estimated $t_{1/2}$ of 600 h .^[176] The work by Costa et al is presented in detail in Section 4.4.3.1.

The intramolecular caging strategy has been recently extended to a pyrazole-based Ir-iTMC (**34**, Figure 25),^[177,178]

obtaining LECs with excellent performance (Table 2), thanks to the additional presence of methyl groups above of the octahedral faces that block the entrance of nucleophilic molecules.^[177] In another study, the beneficial effect of a phenyl group on the 1-position of the ancillary ligand (i.e. *phpzpy*, Figure 12) was shown for a LEC with the green-emitting complex **35** (Figure 26).^[178] Also phenyl substitution on the 5,5' positions of bpy affords reduced intermolecular

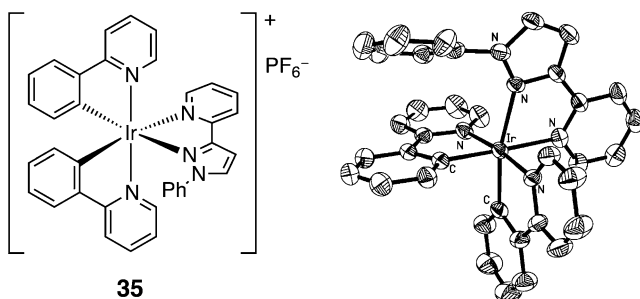


Figure 26. Schematic structure of complex **35** with the related X-ray structure, showing the result of the intramolecular π -stacking.

interactions and, in single-layer LECs, higher stability.^[179] Other bulky groups on the 5 and 5' position of the bpy ligand were also shown to increase the stability of the LECs.^[179] Recently Costa et al. reported an example in which this strategy was extended to phenantroline-based Ir-iTMCs.^[180] They show that, in this particular case, the deactivation to ${}^3\text{MC}$ states is not relevant and thus the enhancement of the device performance is ascribed to an increase of the hydrophobic character.

Although most of the work on the stability issue has been focused on improving the design of the complexes, a few early works also investigated the addition of inactive polymers, the effect of the cathode metal, and the device driving method.^[71,142,181] For both polymer- and iTMC-based LECs, pulsed voltage driving was beneficial for the device stability.^[142,181] Recently, Tordera et al. reported a LEC based on an intrinsically stable iTMC that was driven by pulsed current (square wave, 1000 Hz, and 30% duty cycle). This approach resulted in a $t_{\text{on}} < 1$ s and prevented the propagation of the doped zones, leading to a $t_{1/2}$ of approximately 4000 h with an initial luminance above 600 cd m^{-2} .^[175]

4.4.3. Efficiency

There are three key factors for evaluating the efficiency in LEC devices: 1) the external quantum efficiency (EQE), 2) the power efficiency (lm W^{-1}), and 3) and the efficacy (cd A^{-1} , sometimes also referred as current efficiency).

Initially, single-layer LECs based on Ru-iTMCs had EQE values up to 1.8%.^[33,34,108] Liu et al.^[139,147] discovered that annealing the iTMC layer increased the EQE significantly to values as high as 3.6%. This enhancement is due to partial crystallization of the amorphous film, which enhances the PLQY. As the iTMCs in LECs are responsible not only for the

emission but also for the charge transport, their concentration in films must be high to decrease the inter-site distance. However, high concentrations favor exciton hopping and subsequently emission quenching. Rudmann et al.^[71,106] were capable of increasing the PLQY by reducing the concentration-quenching of excitons by blending the Ru-iTMC with an inert polymer, such as PMMA or PC (polycarbonate). The EQE values of these LECs reached a maximum value of 5.5% at a luminance level in a range of $10\text{--}50 \text{ cd m}^{-2}$.^[71] The limitation of this strategy is the decrease of electron and hole mobility that leads to higher driving voltages and a reduction of the power efficiency. Ultimately, the device efficiency is limited by the PLQY of the iTMC-based film,^[102,103] this is why an alternative to Ru^{II} complexes has been pursued. In this sense, Ir^{III} complexes have emerged as optimal materials for LECs. Indeed, several strategies have been proposed to increase the PLQY of these materials in film, which has led to a significant improvement of the device performance. These new approaches can be placed in two groups, the use of bulky groups and the host-guest approach.

4.4.3.1. Using Bulky Groups

The first Ir-iTMCs that were used in LECs (**4** in Figure 9 and **23** in Figure 20) had *tert*-butyl groups attached to the N^N ligand and afforded LECs with EQE values of 5.0% and 4.6%, respectively.^[76,118] Su et al. systematically showed the importance of the bulky groups using ligand 4,5-diaza-9,9'-spirobifluorene (sb, Figure 12) in two different Ir-iTMCs, **36** and **37** (Figure 27).^[104] They exhibit high PLQYs and long excited-state lifetimes; for instance, the PLQY of a neat film of **36** (31.6%) is ten-times higher than that of **2** (3%).^[37] This situation suggests that sb prevents non-radiative pathways associated with concentration quenching effects. Devices that used single-layer neat films of **36** and **37** achieve high peak external quantum efficiencies and power efficiencies of 7.1% and 22.6 lm W^{-1} at 2.5 V, and 7.1% and 26.2 lm W^{-1} at 2.8 V, respectively.

Following this strategy, complex **10**, which contains the 4,4'-di-*tert*-butyl-2,2'-bipyridine ligand, and is also equipped with a difluorophenylpyridine instead of the conventional ppy cyclometallating ligand (Figure 19), was subsequently proposed.^[103] This compound shows a PLQY value of 72% in thin film, when diluted with the photophysically innocent ionic liquid [BMIM]⁺[PF₆]⁻ at a molar ratio 1:1 (Table 3). The same film composition was used in the LEC device, where the high amount of IL results in a lower turn-on time and higher luminance values (power efficiency 38 lm W^{-1} , EQE = 14.9%). This EQE is close to the value predicted by assuming a light outcoupling efficiency of 20%, suggesting that high external efficiencies are only possible if almost quantitative internal electron-to-photon conversion occurs. This result corroborates the idea that the limiting factor for the efficiency of this kind of LECs is the PLQY of the light-emitting layer.

A series of [Ir(ppy)₂(N^N)][PF₆] complexes that presents several bulky groups attached to the bpy and phen N^N ligands (e.g., ligand hf₂-phen in Figure 12) were reported by the groups of Bryce and Monkman (e.g., complex **38** in Figure 27 and Table 3).^[182,183] The addition of bulky groups

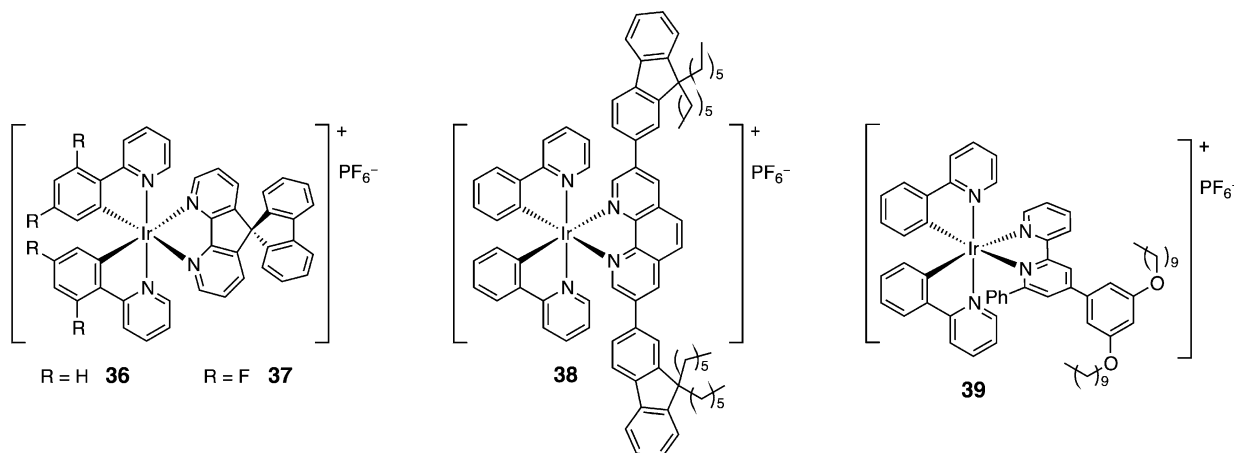


Figure 27. Structural formula of complexes $[\text{Ir}(\text{ppy})_2(\text{sb})]\text{[PF}_6\text{]}^-$ (**36**), $[\text{Ir}(\text{dfppy})_2(\text{sb})]\text{[PF}_6\text{]}^-$ (**37**), $[\text{Ir}(\text{ppy})_2(\text{hf}_2\text{-phen})]\text{[PF}_6\text{]}^-$ (**38**), and $[\text{Ir}(\text{ppy})_2(\text{C}_{10}\text{ppbppy})]\text{[PF}_6\text{]}^-$ (**39**) having bulky ancillary ligands.

Table 3: Photoluminescence and electroluminescence properties of selected Ir-iTMCs with appended bulky groups.

Value	36	10	38	39
PLQY in film	31.6% ^[a]	72% ^[b]	36% ^[a]	34% ^[c]
EQE	7.1% (2.5 V)	14.9% (3 V)	–	6.1% (3 V)

[a] Neat films. [b] Film with a iTMC:[BMIM]⁺[PF₆]⁻ molar ratio of 1:1.

[c] Film with a iTMC:[BMIM]⁺[PF₆]⁻ molar ratio of 4:1.

has little effect on the intrinsic electronic properties of the complex, which exhibited enhanced steric hindrance and reduced self-quenching in thin films. This series of Ir-iTMCs showed high PLQY values (34–44 %) and long excited-state lifetimes (0.15–0.25 μ s) in concentrated thin films. Accordingly, the related LECs yielded efficacies as high as 7 cd A⁻¹ and high luminances (1000 cd m⁻² at 3 V). Notably, there are limits in the use of large substituents because driving voltages tend to increase as a consequence of larger intermolecular separation. In a related work, similar carbazole substituents were used in combination with dimesitylboryl groups,^[184] where high PLQY of the complexes (52 %, PMMA matrix) was obtained, but the related LECs showed poor EQE values.

A new series of $[\text{Ir}(\text{ppy})_2(\text{N}^{\wedge}\text{N})]\text{[PF}_6\text{]}$ complexes that use phenolic ether groups to increase the inter-site distance and the 6-phenyl group on the bpy ligand to allow for intra-complex π – π interactions was recently described (e.g., complex **39** in Figure 27 and Table 3).^[102] By increasing the size of the bulky side groups, the PLQY in the light-emitting layer of LECs (Ir-iTMC/[BMIM]⁺[PF₆]⁻, 4:1) increases from 24 to 38 %. The photophysical, electrochemical, and theoretical studies showed that addition of the bulky groups does not affect the emitting excited state, in agreement with other reports.^[182,183] LECs using these complexes exhibit a roughly sixfold increase in the EQE when compared with the archetype complex without phenyl and phenolic ether groups. Additionally, other important device parameters, such as turn-on time, luminance, and stability improved upon increasing the size of the bulky groups. However, also in this case it was demonstrated that there is a limit to the size of

the bulky groups that can be used before the device driving voltage starts to increase.^[102]

Control over distance between Ir-iTMCs was also attempted using dinuclear complexes equipped with an oligophenyleneethynylene spacer.^[185] However, the spacer introduced efficient non-radiative pathways through its low-lying triplet level, as demonstrated by photophysical, electrochemical, and theoretical studies. The related EQE values (up to 0.16 %) were in line with what was expected taking into account the low PLQYs, suggesting that the introduction of a molecular spacer could be a useful strategy to minimize the self-quenching in the operating device.

4.4.3.2. Diluting an iTMC into an Ionic Matrix: The Host–Guest Approach

To effectively confine excitons, an emitting iTMC can be dispersed in an ionic matrix that has a wider band gap and higher excited-state energy. This approach is analogous to what is frequently carried out in OLEDs, in which iridium complexes are dispersed in matrix materials. Herein, we will not extensively comment on the numerous reports on ionic iridium complexes dispersed in neutral matrix materials; we will focus on ionic matrix materials and refer to a particular paper by He et al.^[186] as well as to recent Reviews for the work related to neutral matrix materials.^[75,165]

In chronological order, Hosseini et al. were the first to propose the doping of a thin film of $[\text{Ru}(\text{bpy})_3]\text{[PF}_6\text{]}_2$ (**3**, host) with small amounts of $[\text{Os}(\text{phen})_3]\text{[PF}_6\text{]}^-$ (**40**, guest),^[138] demonstrating that LECs containing 5 wt % of the Os^{II} complex emit from the guest compound with a higher EQE than the device using pure **40**, thanks to the dilution of the Os-iTMC that decreases self-quenching. They further demonstrated that the electroluminescence spectrum can be tuned by the concentration of the guest and that the doped devices are more stable than those based on the host complex alone.

Subsequently, Su et al. applied this concept to Ir-iTMCs and presented highly efficient LECs consisting of the green-emitting **37** as host and the orange-emitting **36** as guest (Figure 27).^[107] Photophysical studies in thin films showed

that, at an optimized guest concentration of 25 wt %, high PLQYs and long excited-state lifetimes were observed, highlighting a relevant decrease of self-quenching. Notably, the addition of the ionic liquid $[\text{BMIM}]^+[\text{PF}_6]^-$ (19 wt %) further increases the PLQY and the excited-state lifetime. LECs based on this host–guest system exhibit the highest EQEs (10.4 %) and power efficiencies (36.8 lm W^{-1}) observed applying this concept. Soon after this result, the same authors used this approach to prepare the first white LEC, which is described in Section 4.4.4.5.^[159] Recently, they utilized complex **37** (Figure 27) as the host for a fluorescent cationic dye (Rhodamine 6G) achieving high EQE and power efficiency values of 5.5 % and 21.3 lm W^{-1} respectively, using a low dye doping (0.10 wt %).^[187]

Recently, the same group investigated the electroluminescence properties of a cationic terfluorene derivative (Figure 28), obtaining a deep-blue-emitting LEC.^[188] Eventually, they used the host–guest concept by dispersing a red iTMC (**41**) in the same cationic derivative (Figure 28).^[189] The

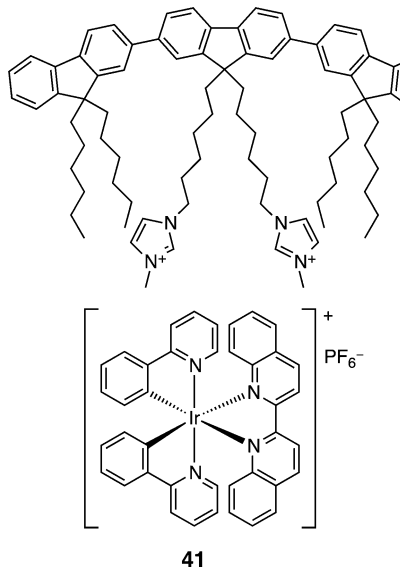


Figure 28. Schematic structures of the host molecule, a cationic terfluorene derivative (top), and the $[\text{Ir}(\text{ppy})_2(\text{biq})][\text{PF}_6]$ guest (**41**, bottom).

main advantage of this approach is the strong reduction in the amount of iridium-based material used, that results in a significant decrease of the material cost. By tuning the concentration of the red iTMC, optimization of the carrier mobilities was achieved leading to relatively high EQE (3.6 %) and power efficiency (7.36 lm W^{-1}). Considering the rather low PLQY of the host–guest film (20 %), an almost perfect charge carrier balance is probably achieved.

In a different approach, Chen et al. prepared an Ir-iTMC in which was integrated a charge-transporting molecule (the neutral ligand bis(diphenylamino)-9,9'-spirobifluorene), with the aim of having a three-in-one system. The LEC prepared using this complex showed very low efficiency as a result of the quenching of the charge-transporting neutral ligand used.^[190]

4.4.4. Color

Most ruthenium-based LECs emit in the orange spectral region.^[28,29] The strategies used to modify the emission color of Ir-iTMCs have been discussed in Section 3. Herein, we focus on LECs emitting across the whole visible spectrum, including white. Their performance is compared with the LEC based on $[\text{Ir}(\text{ppy})_2(\text{bpy})][\text{PF}_6]$ (**2**), the archetypal Ir-iTMC used as reference (Figure 3),^[37] that emits orange light ($\lambda_{\max} = 590 \text{ nm}$, CIE coordinates $x = 0.5078$; $y = 0.4859$).

4.4.4.1. Red LECs

Ancillary N^NN ligands with low-energy LUMO levels have been used to design red Ir-iTMCs. Tamayo et al. proposed the use of various N^NN and C^NN ligands,^[118] presenting LECs with the red-emitting complex **42** (Figure 29; $\lambda_{\max} = 635 \text{ nm}$; CIE coordinates $x = 0.67$; $y = 0.32$; EQE of 7.4 %). Following this result, He et al.^[81] prepared red LECs using complex **43** emitting at about 650 nm (CIE coordinates $x = 0.66$; $y = 0.33$; EQE of 2.6 %); complex **43** has also been used as dopant in the fabrication of white LECs.^[159] Modification of the archetype complex **2** by the attachment of electron-withdrawing groups to the 4,4'-positions of the bpy ligand was also made. Complex **44** (Figure 29) affords LECs with the electroluminescence peaked at 630 nm (CIE: $x = 0.710$; $y = 0.283$).^[113] The EL spectrum is significantly red-shifted compared to the reference LEC with **2**, which was attributed to the stabilization of the LUMO by the introduction of the ester groups. Su et al. used a fluorescent dye in an Ir-iTMC to generate efficient red electroluminescence reaching 19 cd A^{-1} and 21.3 lm W^{-1} .^[187] In a similar approach, Costa et al.^[191,192] showed the beneficial effect of anchoring a perylenediimide (PDI) red fluorescent emitter to an ionic iridium(III) complex (**45**, Figure 29).^[192] The EL spectrum of the LEC incorporating **45** is attributable to the PDI moiety ($\lambda_{\max} = 634 \text{ nm}$, CIE coordinates $x = 0.654$; $y = 0.344$). They also showed in a separate study that triplet radiationless pathways occur through the PDI moiety^[191] but, surprisingly, LECs using such an Ir-iTMC-PDI complex showed external quantum efficiencies as high as 3.3 %. This efficiency was attributed to the high fluorescence quantum yield (55 %) of PDI and short lifetime (3 ns) of the generated exciton, which decreases its diffusion. Thereby, the chance to suffer deactivation by impurities or grain defects in the film is reduced.

4.4.4.2. Near-Infrared-Emitting LECs

Near-infrared (NIR) light-emitting sources are typically expensive and LECs could serve as low-cost alternatives in areas where NIR luminescence is of key importance, such as telecommunications and bioimaging.^[193] Few studies concerning solid-state NIR LECs, that is, having the EL peak wavelength longer than 700 nm, have been reported and most of them concern ruthenium iTMCs. Typically they exhibit $\text{EQE} < 0.1 \%$ ^[133,135,138,194,195] mainly because of the energy gap law that disfavors radiative transition at lower emission energies,^[118] but also owing to self-quenching

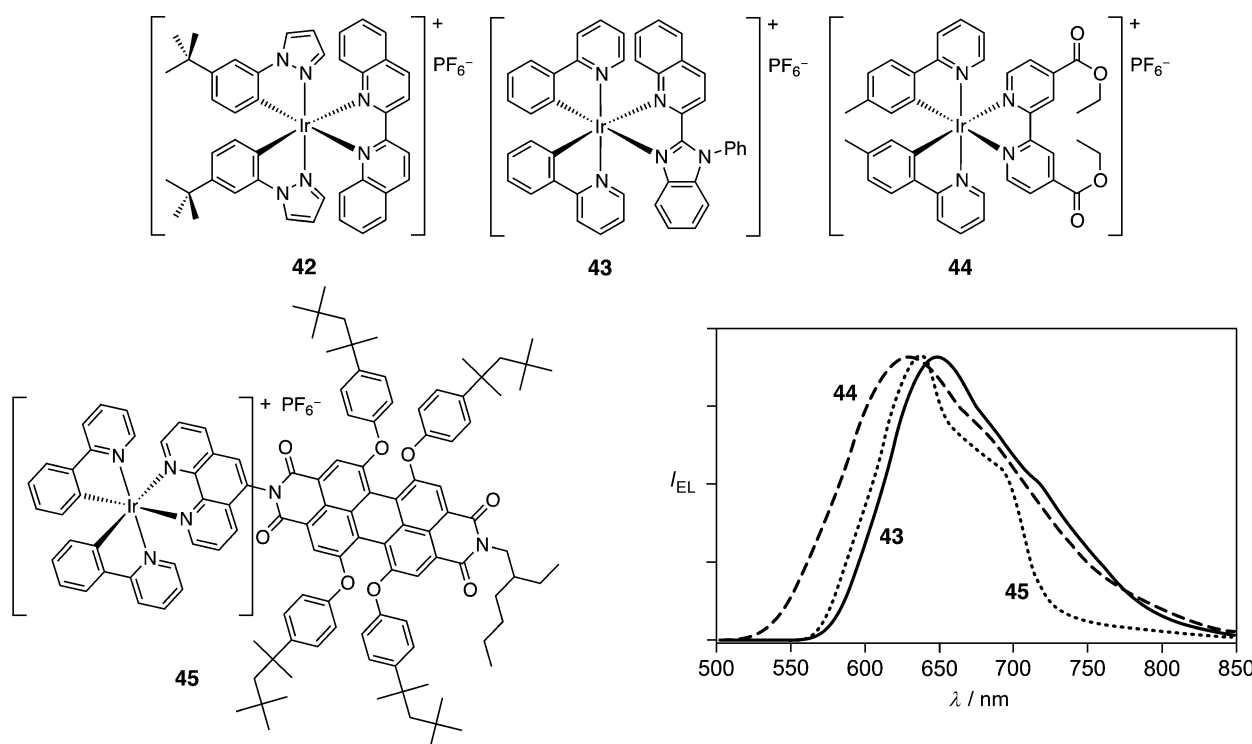


Figure 29. Structural formula of red-emitting Ir-iTMCs: $[\text{Ir}(\text{tb-ppz})_2(\text{biq})]\text{[PF}_6\text{]} \quad \mathbf{42}$, $[\text{Ir}(\text{ppy})_2(\text{qlbi})]\text{[PF}_6\text{]} \quad \mathbf{43}$, $[\text{Ir}(\text{mppy})_2(\text{e-bpy})]\text{[PF}_6\text{]} \quad \mathbf{44}$, and $[\text{Ir}(\text{ppy})_2(\text{phen-PDI})]\text{[PF}_6\text{]} \quad \mathbf{45}$. Bottom-right: EL spectra of LECs based on **43** (solid line), **44** (dashed), and **45** (dotted).

induced by the high density of iTMC in the emitting layer. Recently, Ho et al. reported a more efficient NIR iTMC-based LEC reaching EQEs of 1.2%,^[196] that used the orange-emitting Ir-iTMC **36** (Figure 27) as host and different fluorescent ionic NIR laser dyes as guest. Maximum EQE values (power efficiencies) of 0.8% (5.6 mW W^{-1}) and 1.2% (7.8 mW W^{-1}) were measured, respectively.

4.4.4.3. Yellow and Green LECs

As described in Section 3, the attachment of electron-donating groups on the 4,4'-positions of the bpy ligand increases the HOMO–LUMO gap. Slinker et al. used this strategy for the first time^[76] showing that LECs with complex **4** (Figure 9) exhibit a slightly blue-shifted EL spectrum ($\lambda_{\text{max}} = 560 \text{ nm}$) at 3 V, when compared to that obtained with the reference compound **2** ($\lambda_{\text{max}} = 590 \text{ nm}$). A further blue-shift at λ_{max} of 520 nm was observed for the LEC with complex **9** (Figure 19), which contains two dimethylamino groups.^[111] The luminance level (200 cd m^{-2}) and, more importantly, the efficiency (EQE = 0.2%) of this LEC was significantly reduced compared to reference complexes **2** and **4**.

Costa et al. recently reported a series of Ir^{III} complexes and showed that addition of methyl groups in the 6,6'-positions of the bpy ligand progressively shifts the EL spectrum to the greenish region compared to **2**.^[197] For example, LECs using complex **46** (Figure 30) showed EL maxima at $\lambda = 555 \text{ nm}$ with CIE coordinates $x = 0.436$; $y = 0.549$. In contrast, substitution of these positions by one or

two phenyl groups as for example in complexes **31** and **32** (Figure 25) does not cause any spectral change.^[99,168]

Green LECs were also achieved by using Ir-iTMCs with electron-withdrawing groups attached to the phenyl ring of the C^NN ligands, which stabilize the HOMO level of the complex.^[105,118,157,160] Slinker et al.^[105] made a LEC using complex **47** (Figure 30) with a blue-shifted EL spectrum ($\lambda_{\text{max}} = 542 \text{ nm}$, CIE coordinates $x = 0.368$; $y = 0.577$) compared to non-fluorinated **4** ($\lambda_{\text{max}} = 560 \text{ nm}$). The pristine device showed an EL spectrum that was independent of the bias direction and electrodes used. However, addition of an ionic liquid ($[\text{BMIM}]^+\text{[PF}_6\text{]}^-$) to the light-emitting layer, which improves the turn-on time as discussed in Section 4.4.1.2, introduced a bias-dependent shift in the EL spectrum ($\lambda_{\text{max}} = 531 \text{ nm}$ at +3 V, $\lambda_{\text{max}} = 558 \text{ nm}$ at -3 V). This shift was also observed in LECs involving other Ir-iTMCs combined with $[\text{BMIM}]^+\text{[PF}_6\text{]}^-$.^[82] Following this result, Su et al. proposed a similar strategy involving the use of N^NN ligands with high-energy LUMO levels.^[104,107] They proposed complex **37** (Figure 27), which afforded green LECs ($\lambda_{\text{max}} = 535 \text{ nm}$) with a high EQE (7.1%). A similar emission color ($\lambda_{\text{max}} = 525 \text{ nm}$; CIE coordinates $x = 0.299$; $y = 0.451$) was observed for a LEC with complex **10** (Figure 19).^[103]

Lowry et al.^[91] proposed complex **48**, an Ir-iTMC equipped with two multifluorinated cyclometalating ppy-based ligands (Figure 30). This complex yielded LECs with blue-green emission ($\lambda_{\text{max}} = 500 \text{ nm}$; CIE coordinates $x = 0.198$; $y = 0.512$). Interestingly, these devices also showed a slight blue-shift in the EL peak from $\lambda_{\text{max}} = 520 \text{ nm}$ to 500 nm in going from positive to negative voltages.

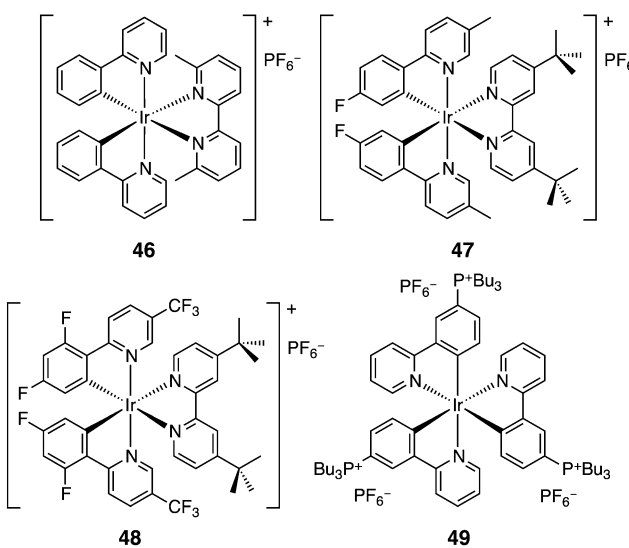


Figure 30. Structural formula of yellow- and green-emitting Ir-iTMCs: $[\text{Ir}(\text{ppy})_2(\text{m}_2\text{bpy})]\text{[PF}_6\text{]}^-$ (**46**), $[\text{Ir}(\text{fmppy})_2(\text{dtb-bpy})]\text{[PF}_6\text{]}^-$ (**47**), $[\text{Ir}\{\text{df-(CF}_3\text{)}\text{ppy}\}_2(\text{dtb-bpy})]\text{[PF}_6\text{]}^-$ (**48**), and $[\text{Ir}(\text{bu}_3\text{P-ppy})_3]\text{[PF}_6\text{]}_3$ (**49**).

Tamayo et al.^[118] demonstrated that the use of Ir-iTMCs with C^NN ligands other than ppy, such as ppz, also blue shifts the emission because of HOMO stabilization. They obtained green LECs ($\lambda_{\max} = 542 \text{ nm}$; CIE coordinates $x = 0.37$; $y = 0.59$) using complex **24** that show a remarkable EQE value of 6.9 %.

To obtain blue-green emission, Bolink et al.^[198] modified a neutral Ir^{III} complex with charged tributylphosphonium side groups at the periphery of the cyclometalating ligands. Blue-green LECs ($\lambda_{\max} = 487 \text{ nm}$) were obtained by blending complex **49** (Figure 30) with 20 % of PMMA, with a spectral shift to $\lambda_{\max} = 570 \text{ nm}$ after 100 s of operation at 4 V. The blue-shifted emission compared to **2** was attributed to the electron-withdrawing nature of the tributylphosphonium group.

4.4.4.4. Blue LECs

The first blue LEC was obtained by attaching electron-withdrawing groups to the Hppz ligand (Figure 11).^[118] LECs using complex **23** (Figure 20) exhibit electroluminescence at $\lambda_{\max} = 492 \text{ nm}$ (CIE coordinates $x = 0.20$; $y = 0.41$) and re-

markable EQE of 4.6 %. Blue LECs have also been obtained by using Ir^{III} complexes based on derivatives of Hppz and devised N^NN ligands. He et al.^[82] utilized N^NN ligands involving electron-donating nitrogen atoms and prepared two blue-emitting Ir-iTMCs, **50** and **14** (Figure 31), using the novel pzpy ligand to make blue LECs with λ_{\max} in the range 450–475 nm, which is shifted by more than 100 nm compared to the EL spectrum of the LEC with the reference complex **2** ($\lambda_{\max} = 590 \text{ nm}$). Single-component LECs (i.e., the active layer is based on only the Ir-iTMC) showed blue-green emission: $\lambda_{\max} = 486 \text{ nm}$ (**50**) and $\lambda_{\max} = 460 \text{ nm}$ (**14**) with CIE coordinates of $x = 0.27$; $y = 0.50$ and $x = 0.20$; $y = 0.28$, respectively. The EQE values of both LECs are in the range 0.3–0.4 %. Addition of the [BMIM]⁺[PF₆]⁻ ionic liquid shifted the EL spectrum of devices using **14** to the green region ($\lambda_{\max} = 526 \text{ nm}$; CIE coordinates $x = 0.33$; $y = 0.45$); however, it did not affect the EL spectrum of LECs made with **50**. The same group presented another example (**54**, Figure 32) with the presence of bulky groups (4-tritylphenyl) to improve the PLQY and, thereby the efficiency of the device. Indeed, LECs based on this complex show remarkably efficient blue-green electroluminescence with peak current efficiency, external quantum efficiency, and power efficiency of 18.3 cd A^{-1} , 7.6 %, and 18.0 lm W^{-1} , respectively.^[199]

Mydlak et al.^[116] proposed the use of several derivatives of the pyridine-1,2,3-triazol ligand together with the dfppyH (Figure 11) cyclometalating ligand. LECs based on complex **15** (Figure 19) show blue EL spectra with two peaks (460 and 480 nm) similar to the results obtained in solution and in thin films. These devices present short turn-on times of a few minutes at 5 V; however, luminance ($10\text{--}20 \text{ cd m}^{-2}$) and stability ($t_{1/2}$ of a few minutes) were moderate. Following this work, Chen et al. proposed a similar family of complexes with triazole pyridine as the ancillary ligand (**16**, Figure 19) which led to LECs with sky-blue ($\lambda_{\max} \approx 458 \text{ nm}$) and blue-green ($\lambda_{\max} \approx 484 \text{ nm}$) emissions and moderate EQE values (ca. 3 %). They also claimed that the addition of cyano groups at the end of the alkyl substituents is responsible of the enhancement of the efficiency.^[117]

A new approach, based on the use of carbene-type ligands, was recently introduced by Yang et al.^[85] They demonstrated that the combination of methyl- or *n*-butyl-substituted bisimidazolium carbene-type ligands together with the dfppyH cyclometalating ligand yields blue LECs

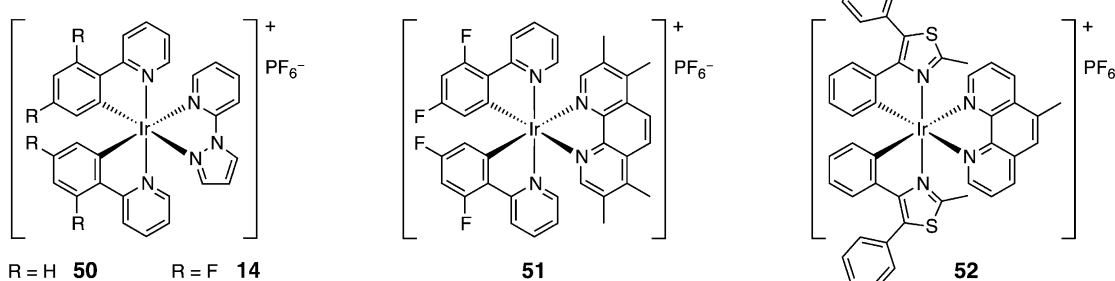


Figure 31. Structural formula of blue-emitting Ir-iTMCs: $[\text{Ir}(\text{ppy})_2(\text{pzpy})]\text{[PF}_6\text{]}^-$ (**50**), $[\text{Ir}(\text{dfppy})_2(\text{pzpy})]\text{[PF}_6\text{]}^-$ (**14**), $[\text{Ir}(\text{dfppy})_2(\text{Me}_4\text{phen})]\text{[PF}_6\text{]}^-$ (**51**), and $[\text{Ir}(\text{dpmt})_2\text{Mephen}]\text{[PF}_6\text{]}^-$ (**52**); dpmt = 4,5-diphenyl-2-methylthiazolo and Mephen = 5-methyl-1,10-phenanthroline.

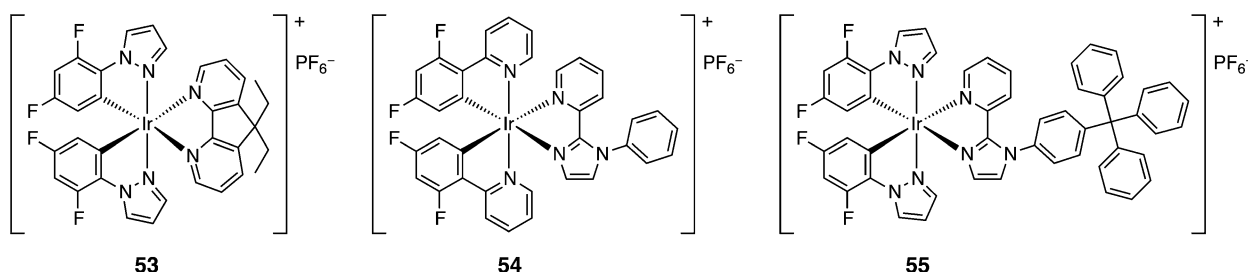


Figure 32. Structural formula of blue–green-emitting Ir-iTMCs used for obtaining white-emitting LECs: $[\text{Ir}(\text{dfppz})_2(\text{dedaf})]\text{[PF}_6\text{]}^-$ (**53**), $[\text{Ir}(\text{dfppz})_2(\text{pyim})]\text{[PF}_6\text{]}^-$ (**54**) and $[\text{Ir}(\text{dfppz})_2(\text{tp-pyim})]\text{[PF}_6\text{]}^-$ (**55**).

with EL maxima in the region 450–490 nm. These devices exhibit luminance and efficiency values lower than 25 cd m^{-2} and 1 cd A^{-1} at 5.5 V. In the same direction, Kessler et al. proposed a family of Ir-iTMCs using a neutral pyridine carbene ancillary ligand (**22**, Figure 19) to cover the whole visible spectrum.^[121] For instance, devices with complex **22** and its fluorinated version (i.e., complex with fluoro groups in the cyclometalating ligand) show blue–green emissions at 544 and 512 nm, respectively. However, high voltages (6 V) are needed to obtain moderate luminance values (20 cd m^{-2}).

Bolink et al.^[158] used **51** as a blue emitter (Figure 31), which exhibits $\lambda_{\text{max}} = 476 \text{ nm}$ in solution and in diluted film but undergoes a substantial shift of 84 nm in EL, emitting green light ($\lambda_{\text{max}} = 560 \text{ nm}$; CIE coordinates $x = 0.417$; $y = 0.533$). This large spectral shift in the LEC does not stem from the different excitation mode or from the presence of large concentrations of ions, but is related to the concentration of the Ir-iTMC in the thin film. In fact, in concentrated films, emission is due to deactivation of metal-to-ligand charge transfer ($^3\text{MLCT}$) states, whereas in diluted samples ligand-centered ($^3\text{LC } \pi-\pi^*$) emission occurs. Using quantum chemical calculations, it was demonstrated that three low-energy triplet states, with associated emission wavelengths differing by as much as 60 nm from each other are present. Notably, the occurrence of excimer formation was ruled out because the excited-state lifetime in concentrated films was found shorter than in diluted samples. In contrast to this finding, Margapoti et al.^[200] showed the formation of excimers by photoluminescence excited-state lifetime measurements in LECs based on complex **52** (Figure 31) at voltages larger than 7 V. Formation of excimers is induced by the applied electric field and is responsible for the different emission maxima observed in photoluminescence and electroluminescence spectra.

Dumur et al. also observed a shift in the emission wavelength over time for a green LEC, they attributed this emission shift to degradation or a temperature-induced modification of the molecular packing.^[174]

In a study by Liao et al., it was shown that the efficiency of a blue-emitting LEC was improved by adding a NIR dye, as a carrier trapper, to the iTMC-emitter blend. This LEC exhibited a 1.4-times higher efficiency than the pristine device leading to an EQE of 12.75% and a power efficiency of 28.7 lm W^{-1} .^[201]

4.4.4.5. White LECs

Su et al.^[25,159] reported the first white LEC based on the host–guest strategy (see Section 3 and 4.4.3.2). They demonstrated that white-light emission (CIE coordinates from $x = 0.45/y = 0.40$ to $x = 0.35/y = 0.39$ at 2.9 and 3.3 V, respectively) with EQE values in the range of 3–4 % are easily achieved by mixing two Ir-iTMCs, namely the blue–green complex **53** (host, 80.5 wt %; Figure 32) and the red complex **41** (guest, 0.4 wt %; Figure 28) in a single-layer, along with the ionic liquid $[\text{BMIM}]^+\text{[PF}_6\text{]}^-$ (19.1 wt %). Although efficient LECs were made, the luminance level reached was low (43 cd m^{-2} at 3.3 V).

He et al.^[81,199] introduced a new series of Ir-iTMCs based on imidazole-type $\text{N}^{\text{+}}\text{N}^{\text{-}}$ ligands with which nearly the whole visible spectral region could be covered.^[81] LECs using complex **54** (Figure 32) showed blue emission ($\lambda_{\text{max}} = 497 \text{ nm}$; CIE coordinates $x = 0.25$; $y = 0.46$; EQE = 3.4 %); by adding the red-emitting complex **43** (Figure 29), warm white host–guest LECs were prepared (CIE coordinates $x = 0.40$; $y = 0.45$). The composition of the light-emitting layer was **54**/ $[\text{BMIM}]^+\text{[PF}_6\text{]}^-$ /**43** at a molar ratio of 1:0.35:0.002. High EQE values of 4.4 % at a luminance value of 115 cd m^{-2} were obtained at 4 V, which are the best performances reported to date for white LECs (Table 4). Recently, the same group synthesized the blue-emitting complex **55** by attaching a bulky tritylphenyl group to the pristine pyim ligand (Figure 12).^[199] The related blue LEC has more than double

Table 4: The best performances reached in white LECs.

Devices	Volt- age [V]	Turn-on time [min]	Luminance [cd m ⁻²]	Lifetime [min]	EQE [%]
53 / $[\text{BMIM}]^+\text{[PF}_6\text{]}^-$ / 41 (80.5/19.1/0.4) ^[a]	2.9	240	2.5	ca. 540	4.0
54 / $[\text{BMIM}]^+\text{[PF}_6\text{]}^-$ / 43 (1:0.35:0.002) ^[b]	4	90	115	ca. 800	4.4
55 / $[\text{BMIM}]^+\text{[PF}_6\text{]}^-$ / 43 (1:1:0.008) ^[c]	3.2	22.5	7.9	ca. 80	5.6
23 / 41 / 36 / $[\text{BMIM}]^+\text{[PF}_6\text{]}^-$ (79.85:0.05:0.1:20) ^[d]	3.1	60	11.5	120	7.4

[a] From Ref. [159], the numbers refer to the composition of the active layer wt %. [b] From Ref. [81], the numbers refer to molar ratios. [c] From Ref. [199], the numbers refers to molar ratios. [d] From Ref. [187]; the numbers refers to wt %.

the EQE value (7.6 %) of LECs with **54** (3.4 %). Again, using the red complex **43** as dopant, they also prepared white LECs (CIE coordinates $x = 0.37$; $y = 0.41$), but the performance was poorer than that reported in their first work: EQE was slightly enhanced (5.6 %) but the luminance level was under 10 cd m^{-2} . Best performances for a white LEC were reached by Su et al., who doped the blue-emitting Ir-iTMC [$\text{Ir}(\text{dfppz})_2(\text{dtb-bpy})\text{PF}_6$] (**23**), with a red, [$\text{Ir}(\text{ppy})_2(\text{biq})\text{PF}_6$] (**41**), and an orange, [$\text{Ir}(\text{ppy})_2(\text{dash})\text{PF}_6$] (**36**), emitting complex. In this way, an EQE of 7.4 % and a power efficiency of 15 lm W^{-1} were obtained.^[187]

Recently, He et al. presented efficient and color-stable white LECs which combine single-layered blue-emitting LECs (complex **23**) with a red-emitting color-conversion layer on the bottom side of the glass substrate. Spectral overlap between the absorption spectrum of the red emitter and the emission spectrum of the blue-emitting material results in efficient energy transfer and down-conversion at low doping concentrations of the red fluorophore. Peak external quantum efficiency and power efficiency of the white LEC reach 5.93 % and 15.34 lm W^{-1} , respectively.^[202]

4.5. LECs based on Metal Complexes other than Iridium(III)

As discussed in the previous Sections, the most widely employed luminophores in LECs are cationic iridium(III) complexes. This is attested by a large body of literature describing a variety Ir^{III} compounds covering the whole

visible spectral window and even showing white emission.^[73] However, the first examples of LEC devices with transition-metal complexes as light-emitting materials were based on ruthenium(II) compounds and reported in 1996.^[27,125] Subsequently, other ruthenium(II)-based complexes, which were discussed in previous Reviews, have been investigated.^[29] However, in recent years, other complexes mainly based on Ru^{II} and Cu^I metals have been reported. Herein, we present some selected examples.

4.5.1. Ruthenium(II)-Based LECs

The mononuclear heteroleptic terpyridine-based Ru^{II} complex **56** (Figure 33) exhibits deep-red emission ($\lambda_{\text{max}} = 750 \text{ nm}$) and was used to make a LEC device with an external quantum efficiency of about 0.005 %.^[135] Ru^{II} complexes involving bipyridine derivatives (complex **57**, Figure 33)^[203] have been also investigated and show enhanced luminescence compared to the parent complex $[\text{Ru}(\text{bpy})_3]\text{PF}_6$ (**3**).^[71] Within this family, Zysman-Colman et al. found that the addition of pendant triethylammonium groups on the bipyridine units (**58**, Figure 33) leads to a device turn-on time as short as 4 s to be compared with 1 min for **3**.^[171] Dinuclear Ru^{II} complexes have been also tested as active materials in devices. For instance, the device made with complex **59** (Figure 33), in the presence of a mixture of Li salt and crown ether as a solid electrolyte, exhibits a particularly low threshold operating voltage of 2.5 V.^[204] Finally, Jia et al. fabricated red electroluminescent devices based on polynuc-

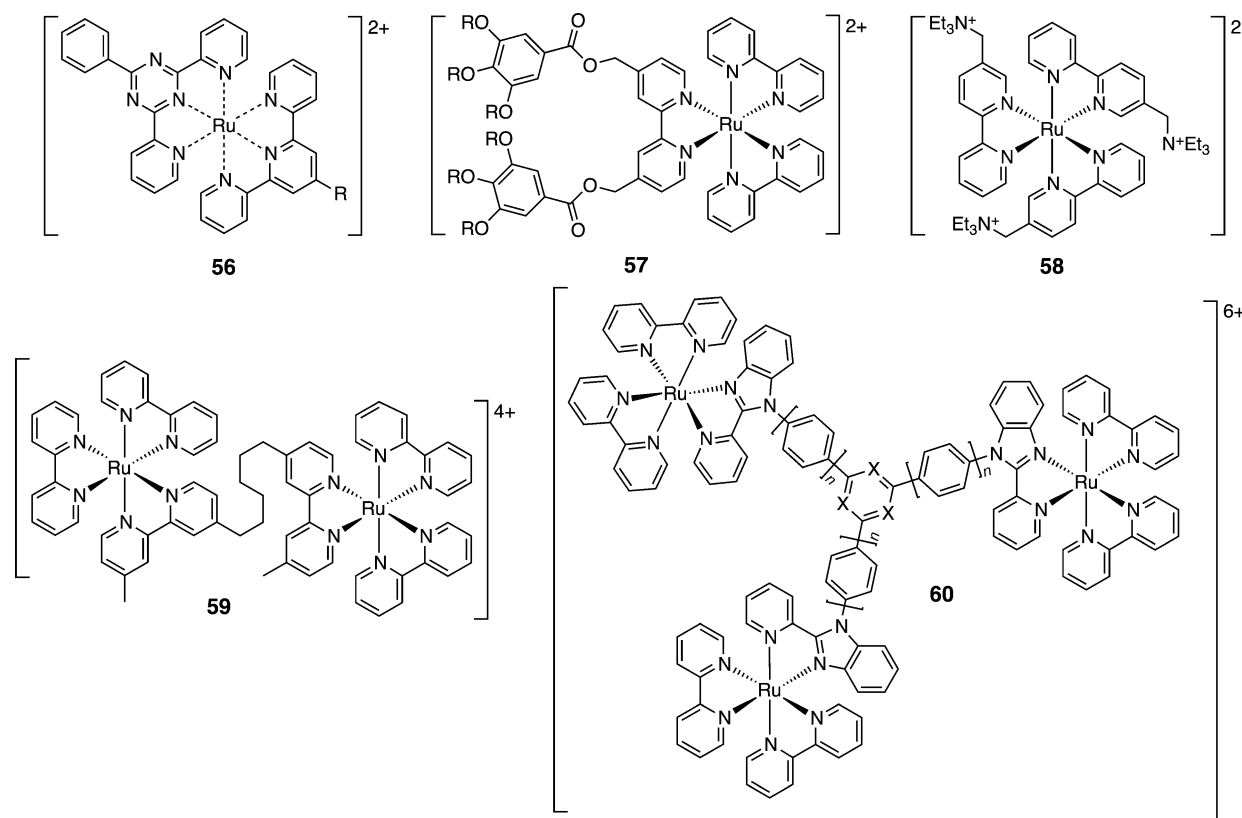


Figure 33. Structural formula of some Ru^{II} complexes used as light-emitting materials in LECs.

lear Ru^{II} complexes (**60**, Figure 33) and involving pyridyl benzimidazolyl derivatives as bridging ligands; they exhibit red emission centered at around 650 nm and perform better than devices based on standard **3**.^[205]

4.5.2. Copper(I)-Based LECs

The limited list of transition-metal ions used to make complexes for LEC devices includes Cu^I. The advantages of using this metal are related to its abundance, low cost compared to platinum-group elements, and low toxicity.^[206,207] The photophysics of Cu^I complexes has been extensively reviewed and the luminescence properties of several classes of Cu^I compounds studied.^[206–208] The most investigated ones include the N^{^N}-type (where N^{^N} indicates a chelating diimine ligand, typically 1,10-phenanthroline) and the P^{^P}-type (where P^{^P} denotes a bisphosphine ligand) giving rise to both homoleptic [Cu(N^{^N})₂]⁺ and heteroleptic [Cu(N^{^N})-(P^{^P})]⁺ motifs.^[22] These tetrahedral cuprous complexes always undergo a significant geometry change going from the ground to excited state because of intra- and intermolecular π-stacking interactions, which cause considerable displacement from D_{2d} symmetry and lead to an increase of nonradiative pathways. Compared to the classical [Cu(N^{^N})₂]⁺ systems, those involving bulky phosphines [Cu(N^{^N})(P^{^P})]⁺ have improved emission properties because the electron-withdrawing effect of the P^{^P} unit on the metal center tends to disfavor the Cu^I→N^{^N} electron donation, leading to a blue-shift of the MLCT transitions. This, according to the energy gap law,^[87] brings about a substantial emission enhancement,^[206] that has greatly increased the interest toward this class of heteroleptic compounds.^[209] Herein, we only report on copper(I) compounds used as light-emitting materials in LEC devices.

The first LEC based on Cu^I complexes involved the heteroleptic system **61** (Figure 34)^[149] that shows excellent green emission at $\lambda_{\text{max}}=550$ nm (PLQY 28% in CH₂Cl₂ solution). The LEC performance was moderate (efficacy at 1 mA cm⁻² between 0.5 and 1 cd A⁻¹), but comparable to that of devices involving green-emitting Ru^{II} complexes at $\lambda_{\text{max}}=540$ nm.

In 2007, Moudam et al.^[150] reported homo- and heteroleptic copper(I) complexes involving chelating phosphine ligands (**62** and **63**, Figure 34), which were also used for the preparation of LECs. The broad electroluminescence band, centered at 580 nm, causes an almost white-light output, and

the devices exhibited a turn-on voltage of 15 V and a brightness up to 490 cd m⁻² at 20 V. Zhang et al. reported LECs made from the heteroleptic [Cu(N^{^N})(P^{^P})]⁺ complex **64** (Figure 34),^[154] which showed green-light emission peaked at $\lambda_{\text{max}}=523$ nm. It was shown that the turn-on time of the devices was strongly affected by the driving voltage, the counterions, and the thickness of the film. The replacement of Al with Ca (a lower work-function metal) significantly enhanced the brightness of the device.

The last example of Cu-iTMC-based LECs was recently reported by Costa et al.^[155] They compared the performance in LECs based on two families of Cu^I complexes with bpy and phen as N^{^N} ligands and pop and pdpb as P^{^P} ligands (Figure 35). They demonstrated that LECs fabricated with those complexes and the ionic liquid [EMIM]⁺[PF₆]⁻ (Figure 24, top) at a molar ratio of 1:1 show comparable performances at low voltages (3–5 V) to those obtained for most LEC devices based on ruthenium(II) and iridium(III) complexes, that is, luminance and efficacy values up to 60 cd m⁻² and 4.5 cd A⁻¹, respectively. This fact highlights the prospect of Cu^I complexes in LECs.

5. Conclusion and Outlook

In the last few years, some technologies have undergone a radical change, particularly in the area of telecommunications, so that nowadays we can easily access a virtually unlimited amount of information at amazingly affordable prices. Similar astounding achievements have not occurred in other sectors; in fact, there are some pervasive technologies that are still far from being massively replaced, a notable example being internal combustion engines for transportation.^[6] In between these extreme cases, some technological sectors are experiencing a progressive transformation that will lead to epochal transitions within the next ten years or so. A notable example is artificial illumination in which, also thanks to the phase-out of traditional filament lamps, the innovative concept of cold lighting has opened the way to new point light sources and flat light sources (LEDs, OLEDs) which are increasingly relevant players in the lighting market, particularly for screen backlighting.^[10]

In the field of innovative flat light sources, OLEDs are presently the most advanced in terms of efficiency, color quality, and operation lifetime, but the still complex and expensive manufacturing routes have stimulated the search

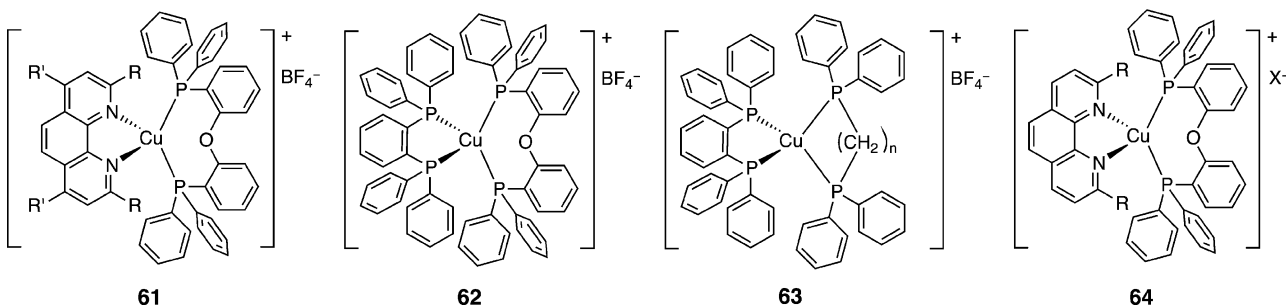


Figure 34. Structural formula of some Cu^I complexes used as light-emitting materials in LECs.

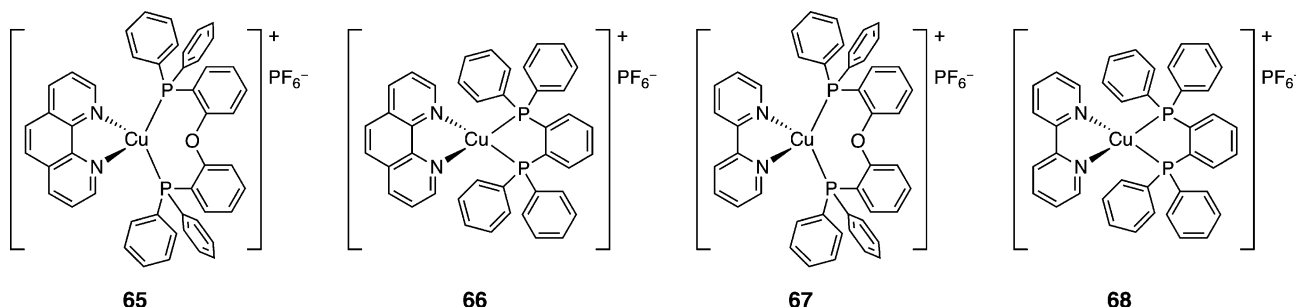


Figure 35. Schematic structures of the most recent examples of Cu^I complexes used in LECs. Complexes **65** and **67** have bis(2-(diphenylphosphino)phenyl ether (pop) as the P^P ligand, complexes **66** and **68** have (1,2-bis(diphenylphosphino)benzene) (pdpb).

for alternative concepts, such as LECs. The basic advantages of LECs over OLEDs are 1) the substantially wider availability of charged transition-metal complexes compared to neutral ones, which widens the spectrum of exploitable phosphorescent emitters and 2) the smaller number and lower chemical reactivity of the layers and the electrodes to assemble, which considerably facilitate the manufacturing of the device.

We have provided herein an overview on the state-of-the art of the performance of LECs, which have achieved respectable efficiency across all the visible spectral region, from blue to deep red, with white LECs having CRI values as high as 80.^[159] This progress has been made possible by the design and synthesis of an enormous number of transition-metal complexes, most of them based on Ir^{III}. This massive synthetic work was driven by a deeper understanding of the factors than govern ground- and excited-state photophysical properties, an understanding which was achieved through a great deal of theoretical modeling and spectroscopic studies. The “historic” drawbacks of LECs, long turn-on times and moderate lifetimes,^[28] have been substantially improved through the use of ionic liquids and by modifying the driving method. However, the best figures of merit of LECs have been met in separate devices and much research will be needed before combining high efficiency, white color, fast turn-on, and long stability in a single device. This calls for further efforts to 1) unravel the intrinsic mechanism of operation of the device, 2) understand the processes of chemical degradation of the luminophores under operating conditions, 3) synthesize new robust electroluminescent materials, 4) design alternative device architectures.

The encouraging progress made in recent years in the improvement of performance,^[24] combined with the two fundamental aforementioned advantages of LECs when compared to OLEDs, makes them promising candidates for low-cost, versatile, and energy-efficient flat light sources. Given the increasing importance of life-cycle sustainability and resource efficiency in the design and fabrication of new products,^[210] particularly those containing rare elements,^[211] the simple structure of LECs may provide a relevant advantage in terms of disassembling and recycling, further enhancing their prospects for successful market applications in the mid-long term.

We thank the European Commission to financially supporting our research through FP7 projects CELLO, STRP 248043, <https://www.cello-project.eu/>, and ITN-FINELUMEN, PITN-GA-2008-215399. We are also grateful to the Spanish Ministry of Economy and Competitiveness (MINECO: MAT2011-24594, CTQ2009-08970 and Consolider-Ingenio CSD2007-00010), the Generalitat Valenciana (Prometeo/2012/053), the Italian MIUR (FIRB Futuro in Ricerca, “SUPRACARBON” n.RBFR10DAK6), and the Italian National Research Council (CNR, MACOL, PM.P04.010). R.D.C. acknowledges the support of a FPU grant by the Spanish Ministry of Science and Innovation (MICINN).

Received: February 22, 2012

-
- [1] V. Smil, *Creating the Twentieth Century: Technical Innovations of 1867–1914 and Their Lasting Impact*, Oxford University Press, Oxford, **2005**.
 - [2] J. Brox, *Brilliant: The Evolution of Artificial Light*, Houghton Mifflin Harcourt, New York, **2010**.
 - [3] L. S. Brown, *Plan B. Mobilizing to Save the Civilization*, W. W. Norton & Company, New York, **2009**.
 - [4] International Energy Agency, *Light’s Labour’s Lost—Policies for Energy-Efficient Lighting*, <http://www.iea.org/>, **2006**.
 - [5] N. Armaroli, V. Balzani, *Energy for a Sustainable World. From the Oil Age to a Sun Powered Future*, Wiley-VCH, Weinheim, **2011**.
 - [6] N. Armaroli, V. Balzani, *Energy Environ. Sci.* **2011**, *4*, 3193–3222.
 - [7] E. Mills, *Science* **2005**, *308*, 1263–1264.
 - [8] W. J. Martin, R. I. Glass, J. M. Balbus, F. S. Collins, *Science* **2011**, *334*, 180–181.
 - [9] G. Zissis, S. Kitsinelis, *J. Phys. D* **2009**, *42*, 173001.
 - [10] C. J. Humphreys, *MRS Bull.* **2008**, *33*, 459–470.
 - [11] M. H. Crawford, *IEEE J. Sel. Top. Quantum Electron.* **2009**, *15*, 1028–1040.
 - [12] C. W. Tang, S. A. Vanslyke, *Appl. Phys. Lett.* **1987**, *51*, 913–915.
 - [13] J. H. Burroughes, D. D. C. Bradley, A. R. Brown, R. N. Marks, K. Mackay, R. H. Friend, P. L. Burns, A. B. Holmes, *Nature* **1990**, *347*, 539–541.
 - [14] *Organic Light Emitting Devices: Synthesis Properties, and Applications* (Eds.: K. Müllen, U. Scherf), Wiley-VCH, Weinheim, **2006**.
 - [15] T. Jüstel in *Luminescence* (Eds.: C. Ronda), Wiley-VCH, Weinheim, **2008**, pp. 179–190.
 - [16] Z. Li, H. Meng, *Organic Light-Emitting Materials and Devices*, CRC, Boca Raton, FL, **2007**.

- [17] *Highly Efficient Oleds with Phosphorescent Materials* (Ed.: H. Yersin), Wiley-VCH, Weinheim, **2008**.
- [18] S. Reineke, F. Lindner, G. Schwartz, N. Seidler, K. Walzer, B. Lussem, K. Leo, *Nature* **2009**, *459*, 234–238.
- [19] “Transition Metal and Rare Earth Compounds Excited States, Transitions, Interactions III”: H. Yersin, *Topics in Current Chemistry*, Vol 241, Springer, Berlin, **2004**.
- [20] “Photochemistry and Photophysics of Coordination Compounds I and II”: V. Balzani, S. Campagna, *Topics in Current Chemistry*, Vol 280–281, Springer, Berlin, **2007**.
- [21] R. C. Evans, P. Douglas, C. J. Winscom, *Coord. Chem. Rev.* **2006**, *250*, 2093–2126.
- [22] A. Barbieri, G. Accorsi, N. Armaroli, *Chem. Commun.* **2008**, 2185–2193.
- [23] M. Sessolo, H. J. Bolink, *Adv. Mater.* **2011**, *23*, 1829–1845.
- [24] T. Hu, L. He, L. Duan, Y. Qiu, *J. Mater. Chem.* **2012**, *22*, 4206–4215.
- [25] H.-C. Su, K.-T. Wong, C.-C. Wu in *WOLEDs and Organic Photovoltaics—Recent Advances and Applications* (Hrsg.: V. W. W. Yam), Springer, Berlin, **2010**.
- [26] Q. Pei, G. Yu, C. Zhang, Y. Yang, A. J. Heeger, *Science* **1995**, *269*, 1086–1088.
- [27] K. M. Maness, R. H. Terrill, T. J. Meyer, R. W. Murray, R. M. Wightman, *J. Am. Chem. Soc.* **1996**, *118*, 10609–10616.
- [28] J. Slinker, D. Bernards, P. L. Houston, H. D. Abruña, S. Bernhard, G. G. Malliaras, *Chem. Commun.* **2003**, 2392–2399.
- [29] J. D. Slinker, J. Rivnay, J. S. Moskowitz, J. B. Parker, S. Bernhard, H. D. Abruña, G. G. Malliaras, *J. Mater. Chem.* **2007**, *17*, 2976–2988.
- [30] Q. J. Sun, Y. F. Li, Q. B. Pei, *J. Disp. Technol.* **2007**, *3*, 211–224.
- [31] J.-K. Lee, D. Yoo, M. F. Rubner, *Chem. Mater.* **1997**, *9*, 1710–1712.
- [32] K. M. Maness, H. Masui, R. M. Wightman, R. W. Murray, *J. Am. Chem. Soc.* **1997**, *119*, 3987–3993.
- [33] E. S. Handy, A. J. Pal, M. F. Rubner, *J. Am. Chem. Soc.* **1999**, *121*, 3525–3528.
- [34] F. G. Gao, A. J. Bard, *J. Am. Chem. Soc.* **2000**, *122*, 7426–7427.
- [35] Q. B. Pei, Y. Yang, G. Yu, C. Zhang, A. J. Heeger, *J. Am. Chem. Soc.* **1996**, *118*, 3922–3929.
- [36] M. S. Lowry, S. Bernhard, *Chem. Eur. J.* **2006**, *12*, 7970–7977.
- [37] R. D. Costa, E. Ortí, H. J. Bolink, S. Gruber, S. Schaffner, M. Neuburger, C. E. Housecroft, E. C. Constable, *Adv. Funct. Mater.* **2009**, *19*, 3456–3463.
- [38] D. A. Bernards, T. Biegala, Z. A. Samuels, J. D. Slinker, G. G. Malliaras, S. Flores-Torres, H. D. Abruña, J. A. Rogers, *Appl. Phys. Lett.* **2004**, *84*, 3675–3677.
- [39] D. A. Bernards, J. D. Slinker, G. G. Malliaras, S. Flores-Torres, H. D. Abruña, *Appl. Phys. Lett.* **2004**, *84*, 4980–4982.
- [40] J. D. Slinker, J. Rivnay, J. A. DeFranco, D. A. Bernards, A. A. Gorodetsky, S. T. Parker, M. P. Cox, R. Rohl, G. G. Malliaras, S. Flores-Torres, H. D. Abruña, *J. Appl. Phys.* **2006**, *99*, 074502.
- [41] J. C. deMello, N. Tessler, S. C. Graham, R. H. Friend, *Phys. Rev. B* **1998**, *57*, 12951.
- [42] J. C. deMello, *Phys. Rev. B* **2002**, *66*, 235210.
- [43] G. G. Malliaras, J. D. Slinker, J. A. DeFranco, M. J. Jaquith, W. R. Silveira, Y. W. Zhong, J. M. Moran-Mirabal, H. G. Craighead, H. D. Abruna, J. A. Marohn, *Nat. Mater.* **2008**, *7*, 168–168.
- [44] D. L. Smith, *J. Appl. Phys.* **1997**, *81*, 2869–2880.
- [45] I. Riess, *Phys. Rev. B* **1987**, *35*, 5740–5743.
- [46] M. J. M. de Jong, P. W. M. Blom in *Proceedings of the 23rd International Conference on the Physics of Semiconductors, Berlin*, Vol 4 (Eds.: M. Scheffler, R. Zimmermann), World Scientific, Singapore, **1996**, pp. 3351–3354.
- [47] S. van Reenen, R. A. J. Janssen, M. Kemerink, *Org. Electron.* **2011**, *12*, 1746–1753.
- [48] V. Bychkov, P. Matyba, V. Akkerman, M. Modestov, D. Valiev, G. Brodin, C. K. Law, M. Marklund, L. Edman, *Phys. Rev. Lett.* **2011**, *107*, 016103.
- [49] J. Gao, J. Dane, *Appl. Phys. Lett.* **2004**, *84*, 2778–2780.
- [50] J. H. Shin, L. Edman, *J. Am. Chem. Soc.* **2006**, *128*, 15568–15569.
- [51] S. van Reenen, P. Matyba, A. Dzwilewski, R. A. J. Janssen, L. Edman, M. Kemerink, *J. Am. Chem. Soc.* **2010**, *132*, 13776–13781.
- [52] J. H. Shin, P. Matyba, N. D. Robinson, L. Edman, *Electrochim. Acta* **2007**, *52*, 6456–6462.
- [53] L. S. C. Pingree, D. B. Rodovsky, D. C. Coffey, G. P. Bartholomew, D. S. Ginger, *J. Am. Chem. Soc.* **2007**, *129*, 15903–15910.
- [54] J. D. Slinker, J. A. DeFranco, M. J. Jaquith, W. R. Silveira, Y. W. Zhong, J. M. Moran-Mirabal, H. G. Craighead, H. D. Abruña, J. A. Marohn, G. G. Malliaras, *Nat. Mater.* **2007**, *6*, 894–899.
- [55] P. Matyba, K. Maturova, M. Kemerink, N. D. Robinson, L. Edman, *Nat. Mater.* **2009**, *8*, 672–676.
- [56] D. B. Rodovsky, O. G. Reid, L. S. C. Pingree, D. S. Ginger, *ACS Nano* **2010**, *4*, 2673–2680.
- [57] Y. F. Li, J. Gao, G. Yu, Y. Cao, A. J. Heeger, *Chem. Phys. Lett.* **1998**, *287*, 83–88.
- [58] H. Rudmann, S. Shimada, M. F. Rubner, *J. Appl. Phys.* **2003**, *94*, 115–122.
- [59] Y. Shao, X. Gong, A. J. Heeger, M. Liu, A. K. Y. Jen, *Adv. Mater.* **2009**, *21*, 1972–1975.
- [60] J. Gao, Y. F. Li, G. Yu, A. J. Heeger, *J. Appl. Phys.* **1999**, *86*, 4594–4599.
- [61] J. M. Leger, D. B. Rodovsky, G. R. Bartholomew, *Adv. Mater.* **2006**, *18*, 3130–3134.
- [62] C. V. Hoven, H. P. Wang, M. Elbing, L. Garner, D. Winkelhaus, G. C. Bazan, *Nat. Mater.* **2010**, *9*, 249–252.
- [63] M. Lenes, G. Garcia-Belmonte, D. Tordera, A. Pertegas, J. Bisquert, H. J. Bolink, *Adv. Funct. Mater.* **2011**, *21*, 1581–1586.
- [64] *Current Injection in Solids* (Eds.: M. A. Lampert, P. Mark), Academic Press, New York, **1970**.
- [65] V. D. Mihailescu, P. W. M. Blom, J. C. Hummelen, M. T. Rispens, *J. Appl. Phys.* **2003**, *94*, 6849–6854.
- [66] K. W. Lee, J. D. Slinker, A. A. Gorodetsky, S. Flores-Torres, H. D. Abruña, P. L. Houston, G. G. Malliaras, *Phys. Chem. Chem. Phys.* **2003**, *5*, 2706–2709.
- [67] P. Pachler, F. P. Wenzl, U. Scherf, G. Leising, *J. Phys. Chem. B* **2005**, *109*, 6020–6024.
- [68] O. Inganäs, *Chem. Soc. Rev.* **2010**, *39*, 2633–2642.
- [69] R. H. Friend, R. W. Gymer, A. B. Holmes, J. H. Burroughes, R. N. Marks, C. Taliani, D. D. C. Bradley, D. A. Dos Santos, J. L. Bredas, M. Logdlund, W. R. Salaneck, *Nature* **1999**, *397*, 121–128.
- [70] M. A. Baldo, D. F. O’Brien, Y. You, A. Shoustikov, S. Sibley, M. E. Thompson, S. R. Forrest, *Nature* **1998**, *395*, 151–154.
- [71] H. Rudmann, S. Shimada, M. F. Rubner, *J. Am. Chem. Soc.* **2002**, *124*, 4918–4921.
- [72] C. M. Elliott, F. Pichot, C. J. Bloom, L. S. Rider, *J. Am. Chem. Soc.* **1998**, *120*, 6781–6784.
- [73] L. Flamigni, A. Barbieri, C. Sabatini, B. Ventura, F. Barigelli, *Top. Curr. Chem.* **2007**, *281*, 143–203.
- [74] A. Juris, V. Balzani, F. Barigelli, S. Campagna, P. Belser, A. Von Zelewsky, *Coord. Chem. Rev.* **1988**, *84*, 85–277.
- [75] C. Ulbricht, B. Beyer, C. Fribe, A. Winter, U. S. Schubert, *Adv. Mater.* **2009**, *21*, 4418–4441.
- [76] J. D. Slinker, A. A. Gorodetsky, M. S. Lowry, J. J. Wang, S. Parker, R. Rohl, S. Bernhard, G. G. Malliaras, *J. Am. Chem. Soc.* **2004**, *126*, 2763–2767.
- [77] M. Nonoyama, *Bull. Chem. Soc. Jpn.* **1974**, *47*, 767–768.
- [78] M. Nonoyama, *J. Organomet. Chem.* **1975**, *86*, 263–267.
- [79] K. Dedeian, P. I. Djurovich, F. O. Garces, G. Carlson, R. J. Watts, *Inorg. Chem.* **1991**, *30*, 1685–1687.

- [80] K. A. King, P. J. Spellane, R. J. Watts, *J. Am. Chem. Soc.* **1985**, *107*, 1431–1432.
- [81] L. He, J. Qiao, L. Duan, G. F. Dong, D. Q. Zhang, L. D. Wang, Y. Qiu, *Adv. Funct. Mater.* **2009**, *19*, 2950–2960.
- [82] L. He, L. Duan, J. Qiao, R. J. Wang, P. Wei, L. D. Wang, Y. Qiu, *Adv. Funct. Mater.* **2008**, *18*, 2123–2131.
- [83] B. Schmid, F. O. Garces, R. J. Watts, *Inorg. Chem.* **1994**, *33*, 9–14.
- [84] J. Li, P. I. Djurovich, B. D. Alleyne, I. Tsyba, N. N. Ho, R. Bau, M. E. Thompson, *Polyhedron* **2004**, *23*, 419–428.
- [85] C. H. Yang, J. Beltran, V. Lemaur, J. Cornil, D. Hartmann, W. Sarfert, R. Frohlich, C. Bizzarri, L. De Cola, *Inorg. Chem.* **2010**, *49*, 9891–9901.
- [86] V. Balzani, G. Bergamini, S. Campagna, F. Puntoriero, *Top. Curr. Chem.* **2007**, *280*, 1–36.
- [87] R. Englman, J. Jortner, *Mol. Phys.* **1970**, *18*, 145–164.
- [88] E. M. Kober, J. V. Caspar, B. P. Sullivan, T. J. Meyer, *Inorg. Chem.* **1988**, *27*, 4587–4598.
- [89] D. Kumaresan, K. Shankar, S. Vaidya, R. H. Schmehl, *Top. Curr. Chem.* **2007**, *281*, 101–142.
- [90] M. Montalti, A. Credi, L. Prodi, M. T. Gandolfi, *Handbook of Photochemistry*, 3rd ed., Taylor and Francis, Boca Raton, FL, **2006**.
- [91] M. S. Lowry, J. I. Goldsmith, J. D. Slinker, R. Rohl, R. A. Pascal, G. G. Malliaras, S. Bernhard, *Chem. Mater.* **2005**, *17*, 5712–5719.
- [92] J. Li, P. I. Djurovich, B. D. Alleyne, M. Yousufuddin, N. N. Ho, J. C. Thomas, J. C. Peters, R. Bau, M. E. Thompson, *Inorg. Chem.* **2005**, *44*, 1713–1727.
- [93] N. M. Shavaleev, F. Monti, R. D. Costa, R. Scopelliti, H. J. Bolink, E. Ortí, G. Accorsi, N. Armaroli, E. Baranoff, M. Grätzel, M. K. Nazeeruddin, *Inorg. Chem.* **2012**, *51*, 2263–2271.
- [94] M. A. L. Marques, E. K. U. Gross, *Annu. Rev. Phys. Chem.* **2004**, *55*, 427–455.
- [95] M. E. Casida, M. Huix-Rotllant, *Annu. Rev. Phys. Chem.* **2012**, *63*, 287–323..
- [96] F. Alary, M. Boggio-Pasqua, J. L. Heully, C. J. Marsden, P. Vicendo, *Inorg. Chem.* **2008**, *47*, 5259–5266.
- [97] F. Alary, J. L. Heully, L. Bijeire, P. Vicendo, *Inorg. Chem.* **2007**, *46*, 3154–3165.
- [98] S. Campagna, F. Puntoriero, F. Nastasi, G. Bergamini, V. Balzani, *Top. Curr. Chem.* **2007**, *280*, 117–214.
- [99] R. D. Costa, E. Ortí, H. J. Bolink, S. Gruber, C. E. Housecroft, M. Neuburger, S. Schaffner, E. C. Constable, *Chem. Commun.* **2009**, 2029–2031.
- [100] R. D. Costa, F. Monti, G. Accorsi, A. Barbieri, H. J. Bolink, E. Ortí, N. Armaroli, *Inorg. Chem.* **2011**, *50*, 7229–7238.
- [101] T. Sajoto, P. I. Djurovich, A. B. Tamayo, J. Oxgaard, W. A. Goddard, M. E. Thompson, *J. Am. Chem. Soc.* **2009**, *131*, 9813–9822.
- [102] R. D. Costa, E. Ortí, H. J. Bolink, S. Gruber, C. E. Housecroft, E. C. Constable, *Adv. Funct. Mater.* **2010**, *20*, 1511–1520.
- [103] H. J. Bolink, E. Coronado, R. D. Costa, N. Lardies, E. Ortí, *Inorg. Chem.* **2008**, *47*, 9149–9151.
- [104] H. C. Su, F. C. Fang, T. Y. Hwu, H. H. Hsieh, H. F. Chen, G. H. Lee, S. M. Peng, K. T. Wong, C. C. Wu, *Adv. Funct. Mater.* **2007**, *17*, 1019–1027.
- [105] J. D. Slinker, C. Y. Koh, G. G. Malliaras, M. S. Lowry, S. Bernhard, *Appl. Phys. Lett.* **2005**, *86*, 173506.
- [106] H. Rudmann, M. F. Rubner, *J. Appl. Phys.* **2001**, *90*, 4338–4345.
- [107] H.-C. Su, C.-C. Wu, F.-C. Fang, K.-T. Wong, *Appl. Phys. Lett.* **2006**, *89*, 261118.
- [108] S. Bernhard, J. A. Barron, P. L. Houston, H. D. Abruna, J. L. Ruglovsky, X. C. Gao, G. G. Malliaras, *J. Am. Chem. Soc.* **2002**, *124*, 13624–13628.
- [109] H. J. Bolink, L. Cappelli, E. Coronado, M. Grätzel, E. Ortí, R. D. Costa, P. M. Viruela, M. K. Nazeeruddin, *J. Am. Chem. Soc.* **2006**, *128*, 14786–14787.
- [110] *Colorimetry—Understanding the CIE System* (Ed.: J. Schanda), Wiley, Hoboken, NJ, **2007**.
- [111] M. K. Nazeeruddin, R. T. Wegh, Z. Zhou, C. Klein, Q. Wang, F. De Angelis, S. Fantacci, M. Grätzel, *Inorg. Chem.* **2006**, *45*, 9245–9250.
- [112] F. De Angelis, S. Fantacci, N. Evans, C. Klein, S. M. Zakeeruddin, J. E. Moser, K. Kalyanasundaram, H. J. Bolink, M. Grätzel, M. K. Nazeeruddin, *Inorg. Chem.* **2007**, *46*, 5989–6001.
- [113] J. L. Rodríguez-Redondo, R. D. Costa, E. Ortí, A. Sastre-Santos, H. J. Bolink, F. Fernández-Lázaro, *Dalton Trans.* **2009**, 9787–9793.
- [114] S. Ladouceur, D. Fortin, E. Zysman-Colman, *Inorg. Chem.* **2010**, *49*, 5625–5641.
- [115] S. Lamansky, P. Djurovich, D. Murphy, F. Abdel-Razzaq, R. Kwong, I. Tsyba, M. Bortz, B. Mui, R. Bau, M. E. Thompson, *Inorg. Chem.* **2001**, *40*, 1704–1711.
- [116] M. Mydlak, C. Bizzarri, D. Hartmann, W. Sarfert, G. Schmid, L. De Cola, *Adv. Funct. Mater.* **2010**, *20*, 1812–1820.
- [117] B. Chen, Y. H. Li, W. Yang, W. Luo, H. B. Wu, *Org. Electron.* **2011**, *12*, 766–773.
- [118] A. B. Tamayo, S. Garon, T. Sajoto, P. I. Djurovich, I. M. Tsyba, R. Bau, M. E. Thompson, *Inorg. Chem.* **2005**, *44*, 8723–8732.
- [119] S. Ladouceur, D. Fortin, E. Zysman-Colman, *Inorg. Chem.* **2011**, *50*, 11514–11526.
- [120] C. S. Chin, M. S. Eum, S. Y. Kim, C. Kim, S. K. Kang, *Eur. J. Inorg. Chem.* **2007**, 372–375.
- [121] F. Kessler, R. D. Costa, D. Di Censo, R. Scopelliti, E. Ortí, H. J. Bolink, S. Meier, W. Sarfert, M. Grätzel, M. K. Nazeeruddin, E. Baranoff, *Dalton Trans.* **2012**, *41*, 180–191.
- [122] M. Buda, G. Kalyuzhny, A. J. Bard, *J. Am. Chem. Soc.* **2002**, *124*, 6090–6098.
- [123] G. Kalyuzhny, M. Buda, J. McNeill, P. Barbara, A. J. Bard, *J. Am. Chem. Soc.* **2003**, *125*, 6272–6283.
- [124] G. G. Malliaras, J. C. Scott, *J. Appl. Phys.* **1998**, *83*, 5399–5403.
- [125] J. K. Lee, D. S. Yoo, E. S. Handy, M. F. Rubner, *Appl. Phys. Lett.* **1996**, *69*, 1686–1688.
- [126] C. H. Lyons, E. D. Abbas, J. K. Lee, M. F. Rubner, *J. Am. Chem. Soc.* **1998**, *120*, 12100–12107.
- [127] A. Wu, J. Lee, M. F. Rubner, *Thin Solid Films* **1998**, 327–329, 663–667.
- [128] A. Wu, D. Yoo, J. K. Lee, M. F. Rubner, *J. Am. Chem. Soc.* **1999**, *121*, 4883–4891.
- [129] J. A. Barron, S. Bernhard, P. L. Houston, H. D. Abruna, J. L. Ruglovsky, G. G. Malliaras, *J. Phys. Chem. A* **2003**, *107*, 8130–8133.
- [130] D. A. Bernards, S. Flores-Torres, H. D. Abruna, G. G. Malliaras, *Science* **2006**, *313*, 1416–1419.
- [131] S. Bernhard, X. Gao, G. G. Malliaras, H. D. Abruna, *Adv. Mater.* **2002**, *14*, 433–436.
- [132] D. R. Blasini, J. Rivnay, D.-M. Smilgies, J. D. Slinker, S. Flores-Torres, H. D. Abruna, G. G. Malliaras, *J. Mater. Chem.* **2007**, *17*, 1458–1461.
- [133] H. J. Bolink, L. Cappelli, E. Coronado, P. Gavina, *Inorg. Chem.* **2005**, *44*, 5966–5968.
- [134] H. J. Bolink, L. Cappelli, E. Coronado, M. Grätzel, M. K. Nazeeruddin, *J. Am. Chem. Soc.* **2006**, *128*, 46–47.
- [135] H. J. Bolink, E. Coronado, R. D. Costa, P. Gavina, E. Ortí, S. Tatay, *Inorg. Chem.* **2009**, *48*, 3907–3909.
- [136] F. G. Gao, A. J. Bard, *Chem. Mater.* **2002**, *14*, 3465–3470.
- [137] A. A. Gorodetsky, S. Parker, J. D. Slinker, D. A. Bernards, M. H. Wong, G. G. Malliaras, S. Flores-Torres, H. D. Abruna, *Appl. Phys. Lett.* **2004**, *84*, 807–809.

- [138] A. R. Hosseini, C. Y. Koh, J. D. Slinker, S. Flores-Torres, H. D. Abruña, G. G. Malliaras, *Chem. Mater.* **2005**, *17*, 6114–6116.
- [139] C.-Y. Liu, A. J. Bard, *Appl. Phys. Lett.* **2003**, *83*, 5431–5433.
- [140] C.-Y. Liu, A. J. Bard, *Appl. Phys. Lett.* **2005**, *87*, 061110–061113.
- [141] D. L. Pile, A. J. Bard, *Chem. Mater.* **2005**, *17*, 4212–4217.
- [142] H. Rudmann, S. Shimada, M. F. Rubner, D. W. Oblas, J. E. Whitten, *J. Appl. Phys.* **2002**, *92*, 1576–1581.
- [143] J. D. Slinker, J.-S. Kim, S. Flores-Torres, J. H. Delcamp, H. D. Abruña, R. H. Friend, G. G. Malliaras, *J. Mater. Chem.* **2007**, *17*, 76–81.
- [144] L. J. Soltzberg, J. D. Slinker, S. Flores-Torres, D. A. Bernards, G. G. Malliaras, H. D. Abruña, J.-S. Kim, R. H. Friend, M. D. Kaplan, V. Goldberg, *J. Am. Chem. Soc.* **2006**, *128*, 7761–7764.
- [145] W. Y. Ng, X. Gong, W. K. Chan, *Chem. Mater.* **1999**, *11*, 1165–1170.
- [146] W. Zhao, C. Y. Liu, Q. Wang, J. M. White, A. J. Bard, *Chem. Mater.* **2005**, *17*, 6403–6406.
- [147] C.-Y. Liu, A. J. Bard, *J. Am. Chem. Soc.* **2002**, *124*, 4190–4191.
- [148] X. Gong, P. K. Ng, W. K. Chan, *Adv. Mater.* **1998**, *10*, 1337–1340.
- [149] N. Armaroli, G. Accorsi, M. Holler, O. Moudam, J. F. Nierengarten, Z. Zhou, R. T. Wegh, R. Welter, *Adv. Mater.* **2006**, *18*, 1313–1316.
- [150] O. Moudam, A. Kaeser, B. Delavaux-Nicot, C. Duhamon, M. Holler, G. Accorsi, N. Armaroli, I. Seguy, J. Navarro, P. Destruel, J. F. Nierengarten, *Chem. Commun.* **2007**, 3077–3079.
- [151] P. K. Ng, X. Gong, S. H. Chan, L. S. M. Lam, W. K. Chan, *Chem. Eur. J.* **2001**, *7*, 4358–4367.
- [152] W. K. Chan, P. K. Ng, X. Gong, S. Hou, *Appl. Phys. Lett.* **1999**, *75*, 3920–3922.
- [153] Y.-M. Wang, F. Teng, Y.-B. Hou, Z. Xu, Y.-S. Wang, W.-F. Fu, *Appl. Phys. Lett.* **2005**, *87*, 233512.
- [154] Q. S. Zhang, Q. G. Zhou, Y. X. Cheng, L. X. Wang, D. G. Ma, X. B. Jing, F. S. Wang, *Adv. Funct. Mater.* **2006**, *16*, 1203–1208.
- [155] R. D. Costa, D. Tordera, E. Ortí, H. J. Bolink, J. Schonle, S. Gruber, C. E. Housecroft, E. C. Constable, J. A. Zampese, *J. Mater. Chem.* **2011**, *21*, 16108–16118.
- [156] D. M. Roundhill, *Photochemistry and Photophysics of Metal Complexes*, Plenum Press, New York, **1994**.
- [157] M. S. Lowry, W. R. Hudson, R. A. Pascal, S. Bernhard, *J. Am. Chem. Soc.* **2004**, *126*, 14129–14135.
- [158] H. J. Bolink, L. Cappelli, S. Cheylan, E. Coronado, R. D. Costa, N. Lardies, M. K. Nazeeruddin, E. Ortí, *J. Mater. Chem.* **2007**, *17*, 5032–5041.
- [159] H. C. Su, H. F. Chen, F. C. Fang, C. C. Liu, C. C. Wu, K. T. Wong, Y. H. Liu, S. M. Peng, *J. Am. Chem. Soc.* **2008**, *130*, 3413–3419.
- [160] R. D. Costa, P. M. Viruela, H. J. Bolink, E. Ortí, *J. Mol. Struct.: THEOCHEM* **2009**, *912*, 21–26.
- [161] D. W. Thompson, J. F. Wishart, B. S. Brunschwig, N. Sutin, *J. Phys. Chem. A* **2001**, *105*, 8117–8122.
- [162] J. Van Houten, R. J. Watts, *J. Am. Chem. Soc.* **1976**, *98*, 4853–4858.
- [163] A. W. Adamson, P. D. Fleischauer, *Concepts in Inorganic Photochemistry*, Wiley, New York, **1975**.
- [164] B. Durham, J. V. Caspar, J. K. Nagle, T. J. Meyer, *J. Am. Chem. Soc.* **1982**, *104*, 4803–4810.
- [165] P.-T. Chou, Y. Chi, *Chem. Eur. J.* **2007**, *13*, 380–395.
- [166] I. S. Shin, H. C. Lim, J. W. Oh, J. K. Lee, T. H. Kim, H. Kim, *Electrochim. Commun.* **2011**, *13*, 64–67.
- [167] Y. Shao, G. C. Bazan, A. J. Heeger, *Adv. Mater.* **2007**, *19*, 365–370.
- [168] H. J. Bolink, E. Coronado, R. D. Costa, E. Ortí, M. Sessolo, S. Gruber, K. Doyle, M. Neuburger, C. E. Housecroft, E. C. Constable, *Adv. Mater.* **2008**, *20*, 3910–3913.
- [169] S. T. Parker, J. D. Slinker, M. S. Lowry, M. P. Cox, S. Bernhard, G. G. Malliaras, *Chem. Mater.* **2005**, *17*, 3187–3190.
- [170] R. D. Costa, A. Pertegás, E. Ortí, H. J. Bolink, *Chem. Mater.* **2010**, *22*, 1288–1290.
- [171] E. Zysman-Colman, J. D. Slinker, J. B. Parker, G. G. Malliaras, S. Bernhard, *Chem. Mater.* **2008**, *20*, 388–396.
- [172] H.-C. Su, H.-F. Chen, C.-C. Wu, K.-T. Wong, *Chem. Asian J.* **2008**, *3*, 1922–1928.
- [173] T.-H. Kwon, Y. H. Oh, I.-S. Shin, J.-I. Hong, *Adv. Funct. Mater.* **2009**, *19*, 711–717.
- [174] F. Dumur, G. Nasr, G. Wantz, C. R. Mayer, E. Dumas, A. Guerlin, F. Miomandre, G. Clavier, D. Bertin, D. Gigmes, *Org. Electron.* **2011**, *12*, 1683–1694.
- [175] D. Tordera, S. Meier, M. Lenes, R. D. Costa, E. Ortí, W. Sarfert, H. J. Bolink, *Adv. Mater.* **2012**, *24*, 897–900.
- [176] S. Gruber, K. Doyle, M. Neuburger, C. E. Housecroft, E. C. Constable, R. D. Costa, E. Ortí, D. Repetto, H. J. Bolink, *J. Am. Chem. Soc.* **2008**, *130*, 14944–14945.
- [177] R. D. Costa, E. Ortí, H. J. Bolink, S. Gruber, C. E. Housecroft, E. C. Constable, *J. Am. Chem. Soc.* **2010**, *132*, 5978–5980.
- [178] L. He, L. Duan, J. Qiao, D. Q. Zhang, L. D. Wang, Y. Qiu, *Chem. Commun.* **2011**, *47*, 6467–6469.
- [179] L. F. Sun, A. Galan, S. Ladouceur, J. D. Slinker, E. Zysman-Colman, *J. Mater. Chem.* **2011**, *21*, 18083–18088.
- [180] R. D. Costa, E. Ortí, H. J. Bolink, S. Gruber, C. E. Housecroft, E. C. Constable, *Chem. Commun.* **2011**, *47*, 3207–3209.
- [181] G. Yu, Y. Cao, C. Zhang, Y. F. Li, J. Gao, A. J. Heeger, *Appl. Phys. Lett.* **1998**, *73*, 111–113.
- [182] C. Rothe, C.-J. Chiang, V. Jankus, K. Abdullah, X. Zeng, R. Jitchati, A. S. Batsanov, M. R. Bryce, A. P. Monkman, *Adv. Funct. Mater.* **2009**, *19*, 2038–2044.
- [183] X. Zeng, M. Tavasli, I. F. Perepichka, A. S. Batsanov, M. R. Bryce, C.-J. Chiang, C. Rothe, A. P. Monkman, *Chem. Eur. J.* **2008**, *14*, 933–943.
- [184] W. J. Xu, S. J. Liu, T. C. Ma, Q. Zhao, A. Pertegas, D. Tordera, H. J. Bolink, S. H. Ye, X. M. Liu, S. Sun, W. Huang, *J. Mater. Chem.* **2011**, *21*, 13999–14007.
- [185] R. D. Costa, G. Fernandez, L. Sanchez, N. Martin, E. Ortí, H. J. Bolink, *Chem. Eur. J.* **2010**, *16*, 9855–9863.
- [186] L. He, L. A. Duan, J. A. Qiao, D. Q. Zhang, L. D. Wang, Y. Qiu, *Org. Electron.* **2010**, *11*, 1185–1191.
- [187] H. C. Su, Y. H. Lin, C. H. Chang, H. W. Lin, C. C. Wu, F. C. Fang, H. F. Chen, K. T. Wong, *J. Mater. Chem.* **2010**, *20*, 5521–5526.
- [188] H. F. Chen, C. T. Liao, T. C. Chen, H. C. Su, K. T. Wong, T. F. Guo, *J. Mater. Chem.* **2011**, *21*, 4175–4181.
- [189] C.-T. Liao, H.-F. Chen, H.-C. Su, K.-T. Wong, *Phys. Chem. Chem. Phys.* **2012**, *14*, 1262–1269.
- [190] H.-F. Chen, K.-T. Wong, Y.-H. Liu, Y. Wang, Y.-M. Cheng, M.-W. Chung, P.-T. Chou, H.-C. Su, *J. Mater. Chem.* **2011**, *21*, 768–774.
- [191] R. D. Costa, F. J. Cespedes-Guirao, H. J. Bolink, F. Fernandez-Lazaro, Á. Sastre-Santos, E. Ortí, J. Gierschner, *J. Phys. Chem. C* **2009**, *113*, 19292–19297.
- [192] R. D. Costa, F. J. Cespedes-Guirao, E. Ortí, H. J. Bolink, J. Gierschner, F. Fernandez-Lazaro, Á. Sastre-Santos, *Chem. Commun.* **2009**, 3886–3888.
- [193] J. C. G. Bünzli, S. V. Eliseeva, *J. Rare Earth* **2010**, *28*, 824–842.
- [194] S. Wang, X. Z. Li, S. D. Xun, X. H. Wan, Z. Y. Wang, *Macromolecules* **2006**, *39*, 7502–7507.
- [195] S. D. Xun, J. D. Zhang, X. Z. Li, D. G. Ma, Z. Y. Wang, *Synth. Met.* **2008**, *158*, 484–488.
- [196] C. C. Ho, H. F. Chen, Y. C. Ho, C. T. Liao, H. C. Su, K. T. Wong, *Phys. Chem. Chem. Phys.* **2011**, *13*, 17729–17736.
- [197] R. D. Costa, E. Ortí, D. Tordera, A. Pertegas, H. J. Bolink, S. Gruber, C. E. Housecroft, L. Sachno, M. Neuburger, E. C. Constable, *Adv. Energy Mater.* **2011**, *1*, 282–290.

- [198] H. J. Bolink, L. Cappelli, E. Coronado, A. Parham, P. Stössel, *Chem. Mater.* **2006**, *18*, 2778–2780.
- [199] L. He, L. Duan, J. Qiao, G. Dong, L. Wang, Y. Qiu, *Chem. Mater.* **2010**, *22*, 3535–3542.
- [200] E. Margapoti, V. Shukla, A. Valore, A. Sharma, C. Dragonetti, C. C. Kitts, D. Roberto, M. Murgia, R. Ugo, M. Muccini, *J. Phys. Chem. C* **2009**, *113*, 12517–12522.
- [201] C.-T. Liao, H.-F. Chen, H.-C. Su, K.-T. Wong, *J. Mater. Chem.* **2011**, *21*, 17855–17862.
- [202] H. B. Wu, H. F. Chen, C. T. Liao, H. C. Su, K. T. Wong, *Org. Electron.* **2012**, *13*, 483–490.
- [203] D. Pucci, A. Bellusci, A. Crispini, M. Ghedini, N. Godbert, E. I. Szerb, A. M. Talarico, *J. Mater. Chem.* **2009**, *19*, 7643–7649.
- [204] J. C. Leprêtre, A. Deronzier, O. Stéphan, *Synth. Met.* **2002**, *131*, 175–183.
- [205] W. L. Jia, Y. F. Hu, J. Gao, S. N. Wang, *Dalton Trans.* **2006**, 1721–1728.
- [206] N. Armaroli, G. Accorsi, F. Cardinali, A. Listorti, *Top. Curr. Chem.* **2007**, *280*, 69–115.
- [207] A. Lavie-Cambot, M. Cantuel, Y. Leydet, G. Jonusauskas, D. M. Bassani, N. D. McClenaghan, *Coord. Chem. Rev.* **2008**, *252*, 2572–2584.
- [208] N. Armaroli, *Chem. Soc. Rev.* **2001**, *30*, 113–124.
- [209] K. Saito, T. Arai, N. Takahashi, T. Tsukuda, T. Tsubomura, *Dalton Trans.* **2006**, 4444–4448.
- [210] *A Resource-Efficient Europe—Flagship Initiative of the Europe 2020 Strategy*, see <http://ec.europa.eu/resource-efficient-europe/>.
- [211] United Nations Environment Programme (UNEP), *Recycling Rates of Metals—A Status Report*, see <http://www.unep.org/2011>.